5-2013

Development of sediment budgets at multiple scales

Susannah O'brien Erwin
Utah State University

DEVELOPMENT OF SEDIMENT BUDGETS AT MULTIPLE SCALES: INVESTIGATIONS INTO THE INFLUENCE OF SEDIMENT SUPPLY ON CHANNEL MORPHOLOGY

by

Susannah O. Erwin

A dissertation submitted in partial fulfillment
of the requirements for the degree

of

DOCTOR OF PHILOSOPHY

in

Watershed Science

Approved:

John C. Schmidt Major Professor	Peter R. Wilcock Committee Member
Joel L. Pederson Committee Member	David G. Tarboton Committee Member
Joseph M. Wheaton Committee Member	Mark R. McLellan Vice President for Research and Dean of the School of Graduate Studies

UTAH STATE UNIVERSITY
Logan, Utah

2012

ABSTRACT

Development of Sediment Budgets at Multiple Scales:

Investigations into the Influence of Sediment

Supply on Channel Morphology

by

Susannah O. Erwin, Doctor of Philosophy

Utah State University, 2012

Major Professor: Dr. John C. Schmidt
Department: Watershed Sciences

Channel morphology in alluvial rivers results from the interactions among the flow of water and sediment, the grain size distribution of the material in transport, and the characteristics of the materials making up the channel boundary. Many modern river management problems depend upon the ability to predict channel behavior in response to changes in the delivery of sediment. Sediment budgets provide a framework for explicitly evaluating the links between sediment delivery to and export from a river, and changes in storage. In the work presented here I have developed sediment budgets at three different spatial and temporal scales in an effort to gain insight to channel response to a change in sediment supply.

In Chapter 2, I present a bed load budget for the Snake River in Grand Teton National Park (GTNP), Wyoming. The analysis was designed to evaluate the effects of

50 years of flow regulation on net sediment flux and, thus, sediment storage for the Snake River below Jackson Lake Dam. In Chapter 3 I present a sediment mass balance constructed for a single flood on an aggrading 4-km reach of the middle Provo River, Utah. Sediment accumulation in the Provo River had driven significant point bar growth, and the sediment budget was designed to explicitly link patterns in sediment flux with morphologic change. In Chapter 4, I present the results from a physical experiment designed to further evaluate the effect of changing sediment supply on point bar morphology in a single meander bend. The experiment was conducted in a field-scale flume, the Outdoor StreamLab (OSL), at the University of Minnesota.

In each of the cases I present here, the channel was subject to sediment accumulation due to either an increase in sediment supply (Provo River and OSL) or a decrease in transport capacity (Snake River). The analyses provide insight into processes governing channel response to changes in sediment supply and highlight the inherent challenges and uncertainties associated with sediment budgets, regardless of the scale of the analysis.

(178 pages)

PUBLIC ABSTRACT

Development of Sediment Budgets at Multiple Scales:

Investigations into the Influence of

Sediment Supply on Channel Morphology

Susannah O. Erwin

Channel morphology in alluvial rivers is determined by the flow of water and sediment, and the characteristics of the materials making up the channel boundary. Many modern river management problems depend upon our ability to predict channel behavior in response to changes in the delivery of water or sediment. Sediment delivery to a river may be altered by natural or human-caused changes, such as changes in land use in the watershed, construction and operations of dam, forest fires, or climate change. Understanding and predicting the effects of these alterations is important because changes in sediment supply and transport may alter river characteristics, impact riverine habitat, and affect aquatic organisms.

Sediment budgets – an accounting of the sediment delivered to, transport through, and exported from a river network – are a fundamental tool used to understand how rivers respond to perturbations in sediment supply. Here, I developed sediment budgets at three different spatial and temporal scales in order to investigate the influence of sediment supply on channel form. In this dissertation I present (1) a large-scale field study of systemic change on the Snake River in Grand Teton National Park (GTNP); (2) an intermediate-scale field study on a section of the reconfigured Provo River in Heber Valley, UT, where gravel is actively accumulating; and (3) a small-scale, physical experiment of point bar response to changes in sediment influx. Together, these three studies highlight the inherent challenges and uncertainties encountered when developing sediment budgets. Additionally, the work furthers our understanding of how rivers respond to a change in the delivery of water or sediment.

ACKNOWLEDGMENTS

I would like to thank my friend and mentor Jack Schmidt. Jack taught me how to be a good field scientist, a critical thinker, and to be passionate about what I do. Through Jack I gained the opportunity to work in some of the most spectacular landscapes in the American west. I am also grateful for the mentorship provided by Peter Wilcock. Although I will never embrace his enthusiasm for tubular meat, Peter has inspired me with his contagious enthusiasm for sediment transport. I would especially like to thank my committee members, Drs. Joel Pederson, David Tarboton, and Joe Wheaton – I learned a tremendous amount from each of them.

My research was made possible by numerous partnerships and collaborations. My work on the Snake River would not have happened without the assistance of Sue O'Ney and Sue Consuelo-Murphy of Grand Teton National Park (GTNP). Thanks also to the River Rangers of GTNP, who worked closely with me to ensure that I could safely sample bed-load transport in a high-traffic, high-visibility section of the Snake River. Graham Matthews and Associates were incredibly generous in their willingness to teach me how to do large river, bed-load sampling. My work on the Provo River greatly benefited from the support of Mark Holden of the Utah Reclamation, Mitigation, and Conservation Commission and of Tyler Allred of Allred Restoration. Special thanks go to Daryl Devy, who was exceptionally accommodating in his willingness to modify releases from Jordanelle Dam. My work in the Outdoor StreamLab would not have been possible without the assistance of Anne Lightbody, Christian Braudrick, and numerous staff of Saint Anthony Falls Laboratory, MN.

There have been an astonishing number of friends and technicians who helped in the field and lab to make this work possible. Special thanks go to my friends made throughout the years in the Fluvial Geomorphology Lab, and to my fellow "Barflies." for many good times wandering around gravel bars.

I was fortunate to receive financial assistance from several sources throughout my time as a student at USU. The S.J. and Jessie E. Quinney Foundation provided funding throughout the duration of my Ph.D. program. Additional funding was provided by the National Park Service, the U.S. Geological Survey Northern Rocky Mountain Science Center, the Intermountain Center for River Rehabilitation and Restoration at Utah State University, the Science and Technology Centers Program of the U.S. National Science Foundation via the National Center for Earth-Surface Dynamics, and the Utah Reclamation, Mitigation, and Conservation Commission.

Lastly, words cannot express how appreciative I am of the love and support I've received from my family. Thank you to my parents, Tom and Joanna, for their encouragement and their enthusiasm for all of my pursuits in life. Thank you to my husband, Matt, for his patience and unwavering support, and to Milo and Nellie, for keeping life exciting and making me smile every day.

Susannah O. Erwin

CONTENTS

LIST OF TABLES

LIST OF FIGURES

CHAPTER 1

INTRODUCTION

Sediment budgets are a fundamental tool in geomorphology, used across the discipline in theoretical and applied studies [*Reid and Dunne*, 2003]. A fluvial sediment budget provides insights into the effects of changing land use [*Trimble*, 1983] or river regulation [*Grams and Schmidt*, 2005], or may address more fundamental questions, such as how channels respond to perturbations in the sediment transport regime [*Wathen and Hoey*, 1998]. In fluvial systems, the sediment mass balance, or budget, is

$$I - E = \Delta S \qquad (1)$$

where I is sediment influx, E is sediment efflux, and ΔS is change in sediment storage [*Reid and Dunne*, 2003]. Fully developing and closing a sediment budget involves quantifying each of these terms, such that the difference between the measured influx and efflux is compared to with the measured change in channel storage, which allows assessment of uncertainty in the measured terms. Though simple in concept, selecting the appropriate suite of methods to quantify each term in (1) can be quite challenging. The challenges faced in developing a sediment budget, and the questions that can be addressed, can vary strongly with spatial and temporal scale. This dissertation examines the interplay among scale, sediment budget scope and accuracy, and channel adjustment for three cases in which ΔS is increased, resulting from either an increase in sediment supply (I) or a decrease in transport capacity.

I investigated the linkages between sediment supply and morphodynamic response at three scales: (1) a large-scale, field study of systemic change on the Snake River, Wyoming; (2) an intermediate, reach-scale field study on the reconfigured Provo

River, Utah; and (3) a small-scale, physical experiment in an outdoor flume. In all three settings, the unifying questions guiding the research were: *how does a river channel accommodate sediment accumulation when sediment supply increases or transport capacity decreases?* And, *how does the scale of the investigation limit or influence the scope of the sediment budget and the approach used to develop the budget?*

Chapter 2 presents a 50-year sediment mass balance constructed for a 16-km reach of the Snake River in Grand Teton National Park, Wyoming. At this large spatial and temporal scale, we constructed a sediment budget by estimating sediment inputs from tributaries and mainstem sediment output. Accurately quantifying sediment transport rates remains a fundamental challenge and there are very few examples of large river, bed load sampling programs [*McLean et al.*, 1999; *Major*, 2004; *Vericat and Batalla*, 2006; *Wallick et al.*, 2009]. The difficulty in determining rates of bed load flux in part stems from the fact that bed load transport rates are highly stochastic, exhibiting great spatial and temporal variability even under steady flow conditions [*Davies*, 1987; *Gomez*, 1991; *Ashmore and Church*, 1998; *Hicks and Gomez*, 2003]. This fact, combined with the fluctuating flows and uneven bed topography found in natural channels, makes estimating and measuring bed load transport rates challenging [*Ryan*, 2003]. Thus, we employed an approach where we used a small number of direct measurements to calibrate existing transport formulas [*Wilcock*, 2001; *MacArthur et al.*, 2008]. In an effort to understand multi-decadal patterns of sediment flux, we used the calibrated transport functions to model sediment flux for the period of modern dam management. Because of the scale of the analysis, it was not possible to comprehensively document change in storage. Thus,

the ΔS term of the mass balance could only be estimated as the difference between influx and efflux.

Construction of a sediment budget for the Snake River was motivated by the desire to understand the downstream effects of operations of Jackson Lake Dam on hydrology and channel morphology of the Snake River. Prior research had provided conflicting views of channel response to regulation [*Marston et al.*, 2005; *Nelson*, 2007], yet there had been no previous effort to quantify sediment flux in the study reach. I initially hypothesized that dam operations resulted in sediment surplus conditions through the study area. However, my field work and subsequent analyses revealed a more nuanced response that was not evident in the absence of bed load transport data.

Chapter 3 presents a sediment mass balance constructed for a single flood on a 4-km reach of the middle Provo River, UT. The study area was completely reconfigured in 2004 as part of the Provo River Restoration Project. Qualitative observations suggested that an unanticipated sediment influx to the study reach was driving the point bar formation and bankline migration. The study area provided a field setting in which I could investigate the changes in topography and bar morphology in response to an increase in sediment flux. The smaller scale of the Provo River made it possible to quantify changes in morphology and channel geometry to a degree that was not possible on the Snake River. On the Provo River I sought to explicitly link the morphologic adjustments and point bar evolution to patterns in sediment flux.

On the Provo River I worked in partnership with the U.S Bureau of Reclamation to create a controlled flood release from Jordanelle Dam and we attempted to quantify all terms of the sediment budget for the flood. Typically, all components in a mass balance

are not directly measured. Instead, one or more components of the budget are determined as the residuals of other measured values. In many cases, including the sediment budget presented in Chapter 2, sediment inputs and outputs from a system are measured or modeled, and the change in storage can only be estimated as the difference in flux [*McLean et al.*, 1999; *Singer and Dunne*, 2004; *Vericat and Batalla*, 2006]. Alternatively, a morphological approach may be applied, where the difference between the sediment influx and efflux in a reach is inferred from net measured changes in channel morphology and fluxes are not directly measured [*Lane et al.*, 1995; *Martin and Church*, 1995; *Ashmore and Church*, 1998; *Ham and Church*, 2000; *Surian et al.*, 2009; *Harrison et al.*, 2011]. The controlled flood experiment on the Provo River provided a good opportunity to measure and estimate the uncertainty associated with all terms in a sediment mass balance for a discrete, bed-mobilizing flood.

Chapter 4 documents a physical experiment designed to explore the response of a point bar to an increase in sediment supply, such as observed on the Provo River. To date, the majority of experimental studies on the effects of sediment supply on bar morphology have focused on alternate bars in straight flumes [e.g. *Lisle et al.*, 1993; *Madej et al.*, 2008]. Less well studied are the effects of sediment supply on point bars, yet these features are a fundamental attribute of meandering channels. Point bars are a significant zone of in-channel sediment storage, contribute to flow resistance, provide critical aquatic habitat, and determine channel form and rates of floodplain formation [*Knighton*, 1998; *Hassan et al.*, 2008]. Although flow and sediment transport in steady state meanders have received extensive attention [e.g. *Leopold and Wolman*, 1960; *Engelund*, 1974; *Dietrich and Whiting*, 1989; *Bridge*, 1992; *Seminara*, 2006], the work in

Chapter 4 presents the first detailed observations of point bar response to changes in sediment supply.

The experiment was conducted in a field-scale, outdoor flume – the Outdoor StreamLab at Saint Anthony Falls Laboratory at the University of Minnesota. The objective was to document point bar response to an increase and subsequent decrease in sediment supply. It was possible to measure the evolving topography and flow field in much greater detail than in the field. The high temporal and spatial resolution of the measurements allowed me to investigate the interplay among topography, velocity, shear stress, and grain size distribution as the channel adjusted to a changing sediment load. These observations provided insight into the linked hydraulic and topographic mechanisms governing point bar response to changes in sediment supply that were impossible to document at the large spatial-scale of a natural river.

Chapter 5 summarizes the main findings from each of the preceding chapters. Additionally, the chapter highlights insights gained into the challenges and opportunities that arise from the construction of sediment budgets at different spatial and temporal scales.

References

Ashmore, P. E., and M. A. Church (1998), Sediment transport and river morphology: A paradigm for study, in *Gravel-bed Rivers in the Environment*, edited by P. C. Kingman, et al., pp. 115-148, Water Resources Publications, Highlands Ranch, Colo.

Bridge, J. S. (1992), A revised model for water flow, sediment transport, bed topography and grain size sorting in natural river bends, *Water Resour. Res.*, *28*(4), 999-1013.

Davies, T. R. H. (1987), Problems of bed load transport in braided gravel-bed rivers, in *Sediment Transport in Gravel-bed Rivers*, edited by C. R. Thorne, et al., pp. 793-811, Wiley, Chichester.

Dietrich, W. E., and P. J. Whiting (1989), Boundary shear stress and sediment transport in rivers meanders of sand and gravel, in *River Meandering*, edited by S. Ikeda, et al., pp. 1-50, AGU, Washington, D.C.

Engelund, F. (1974), Flow and bed topography in channel bends, *J. Hydraul. Div.*, *100*(11), 1631-1648.

Gomez, B. (1991), Bedload transport, *Earth-Science Reviews*, *31*(2), 89-132.

Grams, P. E., and J. C. Schmidt (2005), Equilibrium of indeterminate? Where sediment budgets fail: sediment mass balance and adjustment of channel form, Green River downstream from Flaming Gorge Dam, Utah and Colorado, *Geomorphology*, *71*(1-2), 156-181, doi: 10.1016/j.geomorph.2004.10.012.

Ham, D. G., and M. Church (2000), Bed-material transport estimated from channel morphodynamics: Chilliwack River, British Columbia, *Earth Surf. Proc. Landforms*, *25*(10), 1123-1142.

Harrison, L. R., C. J. Legleiter, M. A. Wydzga, and T. Dunne (2011), Channel dynamics and habitat development in a meandering, gravel bed river, *Water Resour. Res.*, *47*(4), W04513, doi: 10.1029/2009WR008926.

Hassan, M. A., B. J. Smith, D. L. Hogan, D. S. Luzi, A. E. Zimmerman, and B. C. Eaton (2008), Sediment storage and transport in coarse bed streams: scale considerations in *Gravel-bed rivers VI: From Process Understanding to River Restoration*, edited by H. Habersack, et al., pp. 473-500, Elsevier, Amsterdam.

Hicks, D. G., and B. Gomez (2003), Sediment transport, in *Tools in Fluvial Geomorphology*, edited by G. M. Kondolf, et al., pp. 425-461, John Wiley and Sons Ltd, Chichester, England.

Knighton, D. (1998), *Fluvial forms and processes: a new perspective*, Hodder Arnold Publications, London.

Lane, S. N., K. S. Richards, and J. H. Chandler (1995), Morphological estimation of the time-integrated bed load transport rate, *Water Resour. Res.*, *31*(3), 761-772.

Leopold, L. B., and M. G. Wolman (1960), River meanders, *Geol. Soc. Am. Bull.*, *71*(6), 769.

Lisle, T. E., F. Iseya, and H. Ikeda (1993), Response of a channel with alternate bars to a decrease in supply of mixed-size bed load: A flume experiment, *Water Resour. Res.*, *29*(11), 3623-3629.

MacArthur, R. C., C. R. Neill, B. R. Hall, V. J. Galay, and A. B. Schvidchenko (2008), Overview of Sedimentation Engineering, in *Sedimentation Engineering: Processes, Measurements, Modeling, and Practice*, edited by M. H. Garcia, pp. 1-20, ASCE, Reston, Va.

Madej, M. A., D. G. Sutherland, T. E. Lisle, and B. Pryor (2008), Channel responses to varying sediment input: A flume experiment modeled after Redwood Creek, California, *Geomorphology*, *103*(4), 507-519.

Major, J. J. (2004), Posteruption suspended sediment transport at Mount St. Helens: Decadal-scale relationships with landscape adjustments and river discharges, *J. Geophysical Research-Earth Surf.*, *109*(F1), -, doi: 10.1029/2002jf000010.

Marston, R. A., J. D. Mills, D. R. Wrazien, B. Bassett, and D. K. Splinter (2005), Effects of Jackson Lake Dam on the Snake River and its floodplain, Grand Teton National Park, Wyoming, USA, *Geomorphology*, *71*(1-2), 79-98.

Martin, Y., and M. Church (1995), Bed-Material Transport Estimated from Channel Surveys - Vedder River, British-Columbia, *Earth Surf. Process. Landforms*, *20*(4), 347-361, doi: 10.1002/esp.3290200405.

McLean, D. G., M. Church, and B. Tassone (1999), Sediment transport along lower Fraser River - 1. Measurements and hydraulic computations, *Water Resour. Res.*, *35*(8), 2533-2548.

Nelson, N. C. (2007), Hydrology and geomorphology of the Snake River in Grand Teton National Park, Wyoming., M.S. thesis, Department of Watershed Sciences, Utah State University, Logan.

Reid, L. M., and T. Dunne (2003), Sediment budgets as an organizing framework in geomorphology, in *Tools in Geomorphology*, edited by G. M. Kondolf, et al., pp. 463-500, John Wiley & Sons Ltd., Chichester, England.

Ryan, S. E. (2003), The use of pressure-difference samplers in measuring bedlad transport in small, coarse-grained alluvial channels, edited by USFS Rocky Mountain Res. Station, U.S. Department of Agriculture, USDA, Laramie, Wyo.

Seminara, G. (2006), Meanders, *J. Fluid Mechanics*, *554*(1), 271-297.

Singer, M. B., and T. Dunne (2004), Modeling decadal bed material sediment flux based on stochastic hydrology, *Water Resour. Res.*, *40*(3), doi: 10.1029/2003WR002723.

Surian, N., L. Mao, M. Giacomin, and L. Ziliani (2009), Morphological effects of different channel-forming discharges in a gravel-bed river, *Earth Surf. Process. Landforms*, *10*, doi: 10.1002/esp.1798.

Trimble, S. W. (1983), A sediment budget for Coon Creek basin in the Driftless Area, Wisconsin, 1853-1977, *Am. J. Science*, *283*(5), 454.

Vericat, D., and R. J. Batalla (2006), Sediment transport in a large impounded river: The lower Ebro, NE Iberian Peninsula, *Geomorphology*, *79*(1-2), 72-92, doi: 10.1016/j.geomorph.2005.09.017.

Wallick, J. R., S. W. Anderson, C. Cannon, and J. E. O'Connor (2009), Channel change and bed-material transport in the lower Chetco River, Oregon, *Rep. 2010-5065*, 83 pp, Scientific Investigations Report, U.S. Geological Survey, Reston, Va.

Wathen, S. J., and T. B. Hoey (1998), Morphological controls on the downstream passage of a sediment wave in a gravel bed stream, *Earth Surf. Process. Landforms*, *23*(8), 715-730.

Wilcock, P. R. (2001), Toward a practical method for estimating sediment-transport rates in gravel-bed rivers, *Earth Surf. Process. Landforms*, *26*, 1395-1408.

CHAPTER 2

DOWNSTREAM EFFECTS OF IMPOUNDING A NATURAL LAKE: THE SNAKE RIVER DOWNSTREAM FROM JACKSON LAKE DAM, WYOMING, USA[1]

Abstract

A sediment mass balance constructed for a 16-km reach of the Snake River downstream from Jackson Lake Dam (JLD) indicates that river regulation has reduced the magnitude of sediment mass balance deficit that would naturally exist in the absence of the dam. The sediment budget was constructed from calibrated bed load transport relations, which were used to model sediment flux into and through the study reach. Calibration of the transport relations was based on bed load transport data collected over a wide range of flows on the Snake River and its two major tributaries within the study area in 2006 and 2007.

Comparison of actual flows with unregulated flows for the period since 1957 shows that operations of JLD have reduced annual peak flows and increased late summer flows. Painted tracer stones placed at five locations during the 2005 spring flood demonstrate that despite the reduction in flood magnitudes, common floods are capable of mobilizing the bed material. The sediment mass balance demonstrates that more sediment exits the study reach than is being supplied by tributaries. However, the volume of sediment exported using estimated unregulated hydrology indicates that the magnitude of the deficit would be greater in the absence of JLD. Our calculations suggest that the Snake River was not in equilibrium prior to construction of JLD, but was naturally in sediment deficit. Our conclusion that impoundment lessened a natural sediment deficit

[1] Coauthored by Susannah O. Erwin, John C. Schmidt, and Nicholas C. Nelson

condition rather than causing sediment surplus could not have been predicted in the absence of sediment transport data, and highlights the value of transport data and calculation of sediment mass balance in informing dam operations.

1. Introduction

Changes in the physical attributes of channels downstream from large dams are described in an extensive, and growing, literature (Williams and Wolman, 1984; Graf, 1999; Brandt, 2000b; Petts and Gurnell, 2005). These adjustments are caused by changes in stream flow and sediment supply that are produced by water and sediment storage upstream. The style and magnitude of downstream channel adjustments depend on the relative change in stream flow and sediment supply that causes the downstream sediment mass balance to be perturbed (Lane, 1955; Brandt, 2000a; Grant et al., 2003; Schmidt and Wilcock, 2008). Calculation of this perturbation depends on accurate computation of main-stem sediment transport and tributary sediment supply rates.

Sediment budgets have been developed from field resurveys of channel morphology at large and small scale and from aerial photograph comparisons that incorporate the concept of sediment travel distance (Goff and Ashmore, 1994; Lane et al., 1995; Martin and Church, 1995; Ashmore and Church, 1998; McLean and Church, 1999; Ham and Church, 2000; Eaton and Lapointe, 2001; Sutherland et al., 2002; Gaeuman et al., 2003). However, there is insufficient historic bed topographic data on many regulated rivers to develop morphologic budgets.

An alternative strategy for developing sediment budgets is to quantify influx and efflux. Quantitative evaluation of changes in annual bed material transport and construction of associated mass balances provide valuable insight about channel

dynamics and may inform management in the absence of detailed topographic data. Such an approach has been employed on some large rivers with sandy beds or where the suspended load is of interest: the Colorado River in Grand Canyon (Schmidt, 1999; Topping et al., 2000; Hazel et al., 2006), the Sacramento River (Singer and Dunne, 2004), the Toutle River (Major, 2004), and the Ebro River (Vericat and Batalla, 2006).

Whereas sand has a relatively low threshold of entrainment and its transport can be affected by a wide range of discharges, gravel is not typically entrained until flows approach bankfull conditions. Thus, changes in stream flow caused by dam regulation have the potential to greatly change gravel flux if the duration of bed entraining flows is significantly altered, either by decrease in the magnitude of floods or increase in the frequency of moderate flows in some seasons. However, bed load transport rates have been measured at few sites, and there are relatively few examples of bed load mass balance for the purposes of informing river management (Jones and Seitz, 1980; McLean et al., 1999; Vericat and Batalla, 2006; Wallick et al., 2009).

Scientific advances in understanding the linkages between changing boundary conditions and channel response are therefore hindered by the high cost and labor investment of sediment transport measurements and the large uncertainty in application of sediment transport relations (Wilcock, 2001; Singer and Dunne, 2004). A reconnaissance approach to quantifying hydrologic and geomorphic effects of dam operations is the use of metrics to infer changes in sediment regime (Brandt, 2000a; Grant et al., 2003; Schmidt and Wilcock, 2008). In general, these metrics predict the direction of the change in sediment balance but rely on simplified hydrologic and

sediment transport analysis. Interpretation of these metrics to predict post-dam channel change has assumed that the pre-dam mass balance was in equilibrium.

Here, we describe a field campaign involving tracer gravels and field measurement of transport that allowed development of calibrated transport relations and an associated bed load mass balance budget for 16 km of the Snake River in Grand Teton National Park (GTNP) downstream from Jackson Lake Dam (JLD) in northwestern Wyoming (Figure 2.1). We use this budget to understand how dam operations have perturbed the natural sediment mass balance. Our findings are in general agreement with a previous study (Marston et al., 2005), and with a regional analysis of dam-induced perturbations (Schmidt and Wilcock, 2008), indicating that dam operations have reduced the magnitude of annual sediment flux on the Snake River. However, our analysis reveals a subtlety about how JLD affects the downstream channel that had not been detected prior to the direct calculation of a sediment mass balance. Our calculations suggest that the Snake River was not in equilibrium prior to construction of JLD, but was naturally in sediment deficit. Our conclusion that impoundment lessened a natural sediment deficit condition rather than causing sediment surplus could not have been predicted from the reconnaissance metrics used to predict the geomorphic effects of dams (Brandt, 2000a; Grant et al., 2003; Schmidt and Wilcock, 2008). Thus, this analysis demonstrates the important insights that may be gained from measurements of bed load transport, despite the large uncertainty associated with these data, and shows an important way in which predictions made in the absence of transport data may be misleading

2. Study Area

2.1. Jackson Lake Dam

The study area is the Snake River downstream from JLD and is entirely within GTNP (Figure 2.1). A gravel mass balance was calculated for the 16 km of the Snake River between Buffalo Fork and Deadman's Bar. Other data are presented that characterize bed mobilization immediately downstream from the dam and further downstream from Deadman's Bar. JLD is part of the Minidoka Project, one of the earliest integrated projects of the Bureau of Reclamation (BoR), and consists of dams on the Snake River and other headwater tributaries and diversion canals on the Snake River Plain in Idaho. Today, more than 4000 km^2 of the Snake River Plain are irrigated by this project. JLD was the first headwater storage dam of this project and was originally constructed in 1908 at the outlet of naturally-occuring Jackson Lake. The dam was rebuilt in 1916, increasing the level of Jackson Lake by 11.9 m and creating 1.04×10^9 m^3 of storage.

Prior to 1957, the sole purpose of JLD was to provide storage of late spring snowmelt (Marston et al., 2005). In most years, stored water was released in summer when downstream demand for irrigation water was greatest. In 1957, Palisades Dam was completed 160 km downstream from JLD, providing 1.48×10^9 m^3 of additional storage. Reservoir operating rules for JLD were changed to include some flood control, and a guaranteed minimum release was established for environmental purposes. Because Palisades Reservoir is larger than Jackson Lake Reservoir and is located closer to the Snake River Plain, releases from JLD are no longer timed to meet the peak summer irrigation demand.

2.2. Hydrology and Geomorphology

The upper Snake River and its tributaries in GTNP drain the Teton Range, the Absaroka Mountains, and the Yellowstone Plateau. The annual flood in the watershed is caused by spring snowmelt and typically occurs in May or June. Although stream flow of the Snake River immediately downstream from the dam is entirely determined by JLD releases, flow further downstream results from the combined effects of dam releases and natural inflow from Pacific Creek, Buffalo Fork, and Spread Creek. Measurements of JLD releases (Snake River near Moran; station number 13011000) began in September 1903. The largest tributaries, Pacific Creek (station number 13011500) and Buffalo Fork (station numbers 13011900 and 13012000), join the Snake River relatively close to the dam and have drainage areas of 438 km^2 and 979 km^2, respectively. The Pacific Creek gage has been in operation since 1944. On Buffalo Fork, the gage was established at its current location in 1965. From 1944 to 1960, the gage was located 3 km downstream of its present site. Pacific Creek and Buffalo Fork contribute approximately 28% of the mean annual flow at Moose, based on gaging between 1996 and 2008 near Moran and at Moose (station number 130136599). Another 20% of the stream flow at Moose comes from three ungagged, smaller tributaries: Spread Creek (drainage area = 262 km^2), Cottonwood Creek (187 km^2), and Ditch Creek (161 km^2), and from ground-water inflow.

The Snake River in GTNP is a wandering, gravel-bed river, with single-thread and multi-thread reaches. Single-thread reaches occur where the Holocene alluvial valley is narrow, and multi-thread reaches occur where the valley is wide (Figure 2.1). Between JLD and Pacific Creek, the Holocene alluvial valley is narrow and confined by Tertiary

and Upper Cretaceous sedimentary rocks, Holocene landslide debris, and Pleistocene alluvial deposits (Love et al., 2003). Pleistocene outwash terraces flank much of the Snake River downstream from Buffalo Fork (Love et al., 2003) and intermittently confine the valley.

Sediment supply to the Snake River upstream from Pacific Creek comes from eroding hillslopes and terrace banks, and aerial photograph comparisons indicate that this supply is very small (Nelson, 2007). There is no geological evidence that gravel from the headwaters of the Snake River or its tributaries upstream from Jackson Lake by-passed Jackson Lake in the centuries immediately preceding construction of JLD. Jackson Lake was excavated by Pleistocene glaciers, and today, the lake is contained by glacial moraines (Love et al., 2003) and JLD. The delta of the Snake River where it enters Jackson Lake is more than 25 km from JLD. Pilgrim Creek is the closest tributary to JLD, and it enters the lake 2.3 km upstream from the dam outlet. Although the north abutment of JLD is on the Pilgrim Creek alluvial fan, Piety and Randle (1998) determined that Pilgrim Creek has not shifted from its present course during the past 2000 yrs. Downstream from JLD, sediment is supplied from Pacific Creek, Buffalo Fork, smaller tributaries, and eroding hillslopes.

3. Methods

3.1. Hydrology

Most case studies compare pre-dam and post-dam hydrology, but such a comparison is complicated by interannual or decadal climatic patterns that may result in distinct wet and dry periods. Marston et al. (2005) recognized the value of evaluating the effects of dams based on comparing actual dam releases to those estimated to have

occurred in the absence of the dam. We employed this approach, comparing daily mean discharge at JLD to estimates made for the Snake River at the same site as if the dam did not exist. The BoR provides these estimates (http://www.usbr.gov/pn/hydromet/arcread.html) to inform reservoir operations and interstate compact compliance. The flow estimates are based on measurements of daily change in reservoir volume and measured inflow as determined by a gage immediately upstream from the reservoir (Snake River above Jackson Lake at Flagg Ranch WY, station number 13010065). We refer to the gage data at Moran as 'actual' daily mean discharge and the values estimated by the BoR as 'unregulated' daily mean discharge. These data describe flow in the reach between JLD and Pacific Creek. The unregulated values have been reconstructed for all years since 1910. In addition, we compared actual flows with unregulated flows further downstream to evaluate the effects of tributaries on Snake River hydrology and dam operations. To calculate the actual and unregulated hydrology through the majority of the study reach, we added the measured mean daily tributary inflows of Pacific Creek and Buffalo Fork to the actual and unregulated mean daily discharges for the Snake River at JLD.

We used three flow metrics (annual peak flow, mean annual summer flow, and annual number of days exceeding the threshold for bed mobilization) to evaluate the effects of flow regulation on the Snake River since completion of Palisades Dam in 1957. These metrics were computed for the study area as well as for the reach immediately downstream from JLD, for both the actual and estimated unregulated flows. Annual peak discharge was taken as the annual maximum daily mean discharge, because this value could be determined for unregulated and actual conditions at JLD and downstream from

Buffalo Fork. We defined mean summer flow as the mean daily discharge occurring in July and August, the period during which dam releases are unusually high in relation to unregulated conditions. We also computed the annual number of days when flows of the Snake River exceed the threshold for bed mobilization.

3.2. Sediment Transport

At the outset of this study, we recognized that launching a comprehensive program of sediment transport measurement was not feasible. We also recognized that developing a sediment budget based on uncalibrated bed load transport relations was likely to produce estimates with unacceptable levels of uncertainty. This difficulty in part stems from the fact that bed load transport rates are highly stochastic and exhibit great spatial and temporal variability (Ashmore and Church, 1998; Hicks and Gomez, 2003). Even under stable flow conditions, bed load transport rates are highly variable (Davies, 1987; Gomez, 1991; Knighton, 1998). This fact, combined with the fluctuating daily flows that are typical during snowmelt, make estimating and measuring bed load transport challenging (Ryan, 2003).

We used an approach in which estimates of sediment transport are developed by calibrating transport functions using a limited number of field measurements (Andrews, 2000; Wilcock, 2001; Singer and Dunne, 2004; MacArthur et al., 2008). The process of calibration improves the accuracy of sediment transport functions by appropriately scaling the flow to the site-specific, reference shear stress. The reference shear stress may vary by as much as an order of magnitude among sites (Church and Hassan, 2002); thus, determination of reference shear stress is the most site-dependent attribute of sediment

transport estimates, and its empirical determination eliminates much uncertainty associated with estimates of sediment flux.

3.2.1. Painted Tracer Analysis of Bed Mobility

As a precursor to measuring bed load transport rates, we conducted a tracer study to estimate the flows competent to mobilize the channel bed. Additionally, the tracer study allowed us to assess bed mobility at more locations than was possible to sample transport rates.

The entrainment of painted gravel was measured at 5 sites during the 2005 flood season: (1) immediately downstream from JLD, (2) near the confluences of the Snake River with Pacific Creek and with Buffalo Fork, (3) Deadman's Bar, and (4) at two sites further downstream (Figure 2.1). More than 3800 clasts were painted as patches of exposed bars, and 264 painted rocks were placed in the channel. Placed rocks represented the D_{16}, D_{50}, and D_{84} of the local bed material, and painted patches represented the entire range of bed sizes. Repeat photographs and field surveys were used to relocate tracers after recession of two flood pulses. Tracers not found in the vicinity of their original placement were assumed to have moved beyond the area of inspection, because topographic surveys did not indicate that fill had occurred at any sites. The occurrence of two flood peaks in 2005 allowed us to bracket the range of flows that cause bed entrainment. We defined immobility where less than 10% of the bed was entrained and full mobility where more than 90% of the bed moved (Haschenburger and Wilcock, 2003). Intermediate conditions were considered partially mobile.

3.2.2. Field Measurements of Bed Load Transport Rates

In 2006 and 2007, we measured bed load transport at three locations: (1) Pacific Creek near its mouth, (2) Buffalo Fork near its mouth, and (3) Snake River at Deadman's Bar. The measurement site on Pacific Creek was 650 m upstream from the Snake River confluence and adjacent to the USGS gage. The measurement site on Buffalo Fork was 1950 m upstream from the Snake River confluence. Stream flow at the time of each measurement at this site was taken as that measured at the gage approximately 9.5 km upstream (station number 13011900). Discharge contributed to Buffalo Fork from an intervening tributary is insignificant relative to the discharge measured at the gage.

The Deadman's Bar measurement site was 400 m downstream from the Deadman's Bar boat ramp. In order to accurately estimate flow at Deadman's Bar, travel time based on average water velocity was developed to account for the time required for the flow measured at each of the three gaging stations to arrive at Deadman's Bar. We summed the discharges from each upstream gage to compute a discharge for each bed load measurement at Deadman's Bar.

None of the study sites are wadable at discharges when bed material is moving, and a raft-based sampling platform was used to deploy the bed load sampler. We collected samples using a Toutle River Sampler (TR-2), a pressure-difference sampler with a 52 x 305 mm inlet nozzle and 1.4 expansion ratio. We modified the TR-2 by adding a front stayline to the sampler to reduce the scooping tendency associated with many large pressure-difference samplers. The stayline was attached to the mouth of the TR-2, making it possible to rapidly "jerk" the sampler off the bed prior to raising the sampler from the river bottom. We mounted a crane to a 4.9-m long cataraft and used an

E-reel to lower the sampler to the channel bed. The sampling raft was held stationary in the channel at predetermined intervals using roller-towers and a fixed cable. The system allowed us to safely repeat measurements at specified locations over a range of flows. We selected our sampling sites by considering crew safety, simplicity of flow patterns through the cross-section, proximity of tributary sampling sites to the Snake River confluence, and accessibility.

We collected samples using the Equal Width Increment (EWI) method (Edwards and Glysson, 1988). Each complete measurement was comprised of one pass across the channel and consisted of 10 – 12 samples taken at equally spaced intervals across the active bed. The duration of time the sampler remained on the bed at each vertical varied between measurements, from 30 – 240 s, and was held constant for a given sample. The determination of the time interval used for sampling reflects a compromise between the need for a long sampling duration and the capacity of the sampling bag. Prior studies suggest that measurements may be inaccurate if the sampler bag is filled beyond 40% of its capacity (Emmett, 1981; Bunte et al., 2005). Therefore, the length of time the sampler was left on the bed at any single vertical was shorter than the length of time it took the sampler to approach its limiting capacity at the vertical where the most sediment was moving. We regularly reassessed the sampling time interval, because flow and sediment transport conditions changed.

We dried, weighed, and sieved bed load samples to determine the size distribution of the transported load. We sieved the portion of each sample that was greater than 2 mm into ϕ fractions ($\phi = \log_2 D$, were D is grain size diameter) and divided each sample as needed using a splitter.

Transport rates were calculated for grains larger than sand. Analysis of subsurface grain size distributions at the three sampling locations revealed that at each site approximately 80% of the bed is > 2 mm (Figure 2.2). Thus, the majority of the bed material is gravel. Additionally, we evaluated what grain sizes are transported as bed load by calculating the Rouse number (R_o) for a range of flow conditions and grain sizes

$$R_0 = \frac{W_s}{ku^*} \quad (1)$$

where *Ws* is the fall velocity (calculated using the method of Dietrich (1982)), *k* is Von Karman's constant (0.4), and u^* is the shear velocity (Table 2.1). Calculation of R_o demonstrated that particles < 2 mm are predominantly transported in suspension.

Additional parameters measured in the field included water surface slope, surface grain size distribution, and subsurface grain size distribution. Water surface slope was measured over a range of discharges at each sampling site. We used the average value of the water surface slope measurements for sediment transport calculations, because values differed minimally with variations in discharge. Bed surface point counts (n ≥ 100) were conducted on bed facies (Wolman, 1954), and we used a weighted average based on relative facies area to develop reach-average estimates of bed material size. Subsurface material was sampled at two randomly selected locations at each sampling site that were exposed during low flows. When sampling the subsurface, we first removed a surface layer that was approximately equivalent in depth to the diameter of the largest particle. The subsurface material > 11mm was sieved in the field and a sample of the fine material

was returned to the lab for sieving. The largest particle of each subsurface sample did not account for more than 1% of the total weight of the sample.

3.2.3. Estimating Long-term Annual Bed Load Flux

We calibrated bed load transport functions for the 3 measurement sites by adjusting the reference shear stress, τ_r, to best fit measured bed load transport data. For $\tau'/\tau_r > 1$, we used the function of Parker (1979)

$$W^* = 11.2\left(1 - 0.846\frac{\tau_r}{\tau'}\right). \quad (2)$$

For $\tau'/\tau_r < 1$, we used Parker's (1990) transport relation

$$W^* = 0.0025\left(\frac{\tau'}{\tau_r}\right)^{14.2} \quad (3)$$

where τ' is the skin friction and W* is the dimensionless transport rate, defined as

$$W^* = \frac{gq_s(s-1)}{\left(\frac{\tau'}{\rho}\right)^{1.5}} \quad (4)$$

where g is the gravitational acceleration, q_s is the unit transport rate, s is the immersed specific density (assumed to be 2.65), and ρ is the density of water. Wilcock (2001) advocated use of (2) and (3), because each is well suited for predicting transport rates over a different range of excess grain shear stress; (2) and (3) are equal when $\tau'/\tau_r = 1$.

Skin friction was estimated by incorporating a form of the Manning-Strickler flow resistance equation

$$n = \frac{S^{1/2}R^{2/3}}{U} \quad (5)$$

where n is the Manning resistance coefficient, U is mean velocity, R is the hydraulic radius, and S is the slope, into the duBoys equation

$$\tau_o = \rho g R S. \tag{6}$$

Rearrangement and substitution of (5) into (6) yields

$$\tau_o = \rho g (nU)^{1.5} S^{.25}. \tag{7}$$

The Strickler relation

$$n' = 0.013 D^{0.167}, \tag{8}$$

where n' is the resistance due to the grains on the bed, is substituted into (7)

$$\tau' = \rho g (0.013)^{1.5} (SD)^{0.25} U^{1.5} \tag{9}$$

to produce a relation defining the shear stress acting on the grains. Using $2D_{65}$ for D, in mm (Wilcock, 2001), and common values for g and ρ yields

$$\tau' = 17 (SD_{65})^{0.25} U^{1.5} \tag{10}$$

that expresses grain stress as a function of slope, grain size, and mean channel velocity, all of which were measured. We substituted the hydraulic geometry relation

$$U = kQ^m \tag{11}$$

into (10), yielding

$$\tau' = 17 k^{1.5} (SD_{65})^{.25} Q^{1.5m} \tag{12}$$

where Q is discharge.

In order to determine the coefficient k and exponent m for the hydraulic geometry relation for each measurement site, U was computed from

$$U = \frac{Q}{A} \tag{13}$$

where A is cross-section area at the time of each measurement. On Pacific Creek and Buffalo Fork, A was measured during each sample. At Deadman's Bar, we estimated (11) from a one-dimensional HEC-RAS flow model for a 1500-m reach encompassing the measurement cross-section (Nelson, 2007).

The input parameters used to calibrate the transport functions for each of the three measurement sites are presented in Table 2.2. Additionally, Table 2.2 presents the dimensionless reference transport rate, τ_r^*

$$\tau_r^* = \frac{\tau_r}{(s-1)\rho g D_{50}} \quad (14)$$

When adjusting the τ_r to calibrate the transport functions, we focused on how well the curve fit our data, rather than whether the calculated τ_r^* matched a predetermined, expected value. To quantify the uncertainty associated with our calibrated transport relations, we also identified high and low τ_r values, to define an uncertainty envelope for each transport relation.

We used the site-specific values of τ_r and τ' in (2) and (3) to calculate the daily and annual loads between 1958 and 2008, the period of time influenced by the modern rules of dam releases. Mean daily discharge was used for these computations. We compared the magnitude of sediment influx into our study reach delivered from Pacific Creek and Buffalo Fork to the magnitude of the efflux from the downstream boundary of our study area at Deadman's Bar. We used the high and low estimates of τ_r to calculate "low" and "high" estimates, respectively, of annual bed load flux. Additionally, we used the estimated unregulated hydrology at Deadman's Bar to compute sediment flux for estimated flow conditions in the absence of JLD.

4. Results

4.1. Hydrology

Operations of JLD have changed the temporal patterns in discharge in the Snake River: the average peak flow has decreased by 40%, and late summer flows are 99% greater than unregulated flows (Table 2.3; Figure 2.3a). Average peak flow releases, 166.2 m^3s^{-1}, are significantly less than unregulated average peak flows, 283.8 m^3s^{-1} (Figure 2.4a). Reservoir operations dampen the differences between floods in wet and dry periods, but actual summer flows are significantly greater than unregulated summer flows, with mean values of 79.6 m^3s^{-1} and 39.9 m^3s^{-1}, respectively.

Similar trends occur downstream from Buffalo Fork, but Pacific Creek and Buffalo Fork mitigate the effect of dam operations on the flow regime. The actual average peak flow is now 284.4 m^3s^{-1}, significantly less than the estimated unregulated peak flow of 429.9 m^3s^{-1} (Table 2.4; Figure 2.4b). Mean summer flows are now 110.5 m^3s^{-1}, significantly greater than unregulated summer flows of 70.7 m^3s^{-1} (Figure 2.3b). These changes represent a 34% decrease in peak flows and a 56% increase in late summer flows.

4.2. Sediment Transport

4.2.1. Bed Mobility

Tracer movement indicates that the bed is entrained by low magnitude, common floods. All study sites were partially or fully mobile during the 1.2-yr recurrence floods of 2005 (Table 2.5). There were no fully mobile clusters upstream from Pacific Creek, where the dam release flood that occurred between June 15 and 18 reached a magnitude of 117 m^3s^{-1}. Downstream from Pacific Creek, there were two flood events: a natural,

tributary-driven flood on May 21 (~ 92 m^3s^{-1}) and a larger flood during the June peak dam release (~ 133 m^3s^{-1}). In this segment of river, there were several fully mobile clusters during the June flood. Individual grains larger than 100 mm moved at all sites; 100 mm exceeds the D_{84} at all but one location (Nelson, 2007). The proportion of entrained particles and the proportion of particles that moved more than 1 m were greater at sites downstream from Pacific Creek than at the one site upstream from Pacific Creek (Table 2.6).

4.2.2. Bed Load Transport Data

We sampled bed load transport during the 2006 spring runoff season on Pacific Creek and Buffalo Fork and during the 2007 spring runoff season on Snake River at Deadman's Bar (Figure 2.5; see Appendix for complete hydraulic and sediment transport data). Samples were collected over a range of discharges at each sampling site: 26 – 144 $m^3\ s^{-1}$ on Pacific Creek (3 – 200% of the 2-yr flood), 45 – 117 $m^3\ s^{-1}$ on Buffalo Fork (35 – 105% of the 2-yr flood), and 48 - 181 $m^3\ s^{-1}$ on Snake River (20 – 60% of the 2-yr flood). In total, 24 samples were collected on Pacific Creek, 39 on Buffalo Fork and 62 on Snake River (Figure 2.6). Samples collected at the 3 sites ranged in size from a few hundred grams to 136 kg on Pacific Creek during peak flow. We were able to collect samples during flows of at least the magnitude of the 2-yr flood on both tributaries, but the channel was too wide and water velocities too high to collect samples at high flows of the Snake River at Deadman's Bar.

The data exhibit an order of magnitude scatter in transport rates that cannot be attributed to variations in discharge. Similar scatter has been observed elsewhere (McLean et al., 1999; Hassan and Church, 2001). On Buffalo Fork and Pacific Creek, the

transport rates measured at relatively low discharges display substantially less scatter than those measurements from relatively high discharges. On the Snake River, however, there is similar scatter in the transport rates measured at low and high discharges.

At Deadman's Bar, measurements of bed load transport rates ranged from < 1 to 200 g m^{-1} s^{-1} (Figure 2.6c). All measurements at this site were collected on the rising limb of the hydrograph (Figure 2.5c). Time that the sampler remained on the bed of the channel varied from 30 – 240 seconds. Longer sampling intervals were not desirable because of the strong diurnal fluctuation in discharge.

The single largest measured transport rate, 1250 g m^{-1} s^{-1}, was measured on Pacific Creek, on May 23, 2006, during the flood of record. The instantaneous peak discharge, 164 m^3 s^{-1}, occurred at approximately 4:00 a.m., and we collected our first sample at 9:30 a.m. On Pacific Creek, samples were primarily collected on the receding limb of the hydrograph, and measured transport rates were much lower on the day prior to the peak than those collected during the day the peak flow occurred (Figure 2.6a). Some of the variation in transport rates measured at high flow is likely due to the short time that the sampler was on the bed (30 seconds per vertical), but longer sampling times caused the sampling bags to overfill at these high transport rates.

On Buffalo Fork, we sampled transport rates on both the rising and falling limbs of the hydrograph. The measured bed load transport rates ranged from 25 to 180 g m^{-1} s^{-1}. The range of bed load transport rates measured from June 7 to June 9 was comparable to the range of transport rates measured from June 17 to June 21, despite the fact that the magnitude of discharge was half as great during the later period of time (Figure 2.6b).

The grain sizes in transport increased as total load increased (Figure 2.7), providing insight into the mode of transport at each site. On Pacific Creek, there is a high degree of variability in the grain size of the sediment in transport at discharges less than 50 $m^3 s^{-1}$. However, at approximately 50 $m^3 s^{-1}$, the median grain size of the transport was similar in size to the median grain size of the bed material (Figure 2.7a). Similarly, the maximum grain size from each sample approached the size of the largest bed clasts. These trends in grain size distribution of the sediment in transport suggest that bed load becomes fully mobilized on Pacific Creek at discharge greater than 50 $m^3 s^{-1}$. On the Snake River, the size of both the median and the largest clast of the material in transport steadily increased with increasing discharge (Figure 2.7c), but there was no indication that full bed mobilization occurred at the largest discharges that we measured. We collected only one sample where the median grain size of the transport was approximately equal to the median grain size found in the bed (at approximately 160 $m^3 s^{-1}$); thus, most, if not all, of our samples were collected during partial transport conditions at this site.

We calculated the number of days when flows exceed the threshold for mobilization on the mainstem Snake River at Deadman's Bar, approximately 80 $m^3 s^{-1}$. On average, for the 50-year hydrologic record analyzed, the bed would be mobilized 20% of the year under unregulated conditions. In contrast, under regulated conditions, the bed is mobilized 30% of the year on average (Table 2.4). Thus, although peak flows have diminished, the proportion of the time that the bed remains mobilized in a given year has increased due to the elevated summer flows.

4.2.3. Long-term estimates of bed load flux

Calibration of the site-specific transport relations resulted in different values of τ_r for each site: 9.5 Pa at Buffalo Fork, 9.8 Pa at Deadman's Bar, and 14.2 Pa at Pacific Creek (Table 2.2; Figure 2.8). In calibrating relations at Pacific Creek and Buffalo Fork, we placed greater emphasis on the measurements made at low discharge, because it was during these measurements that the sampler remained on the bed for the longest period of time, and therefore when we sampled the greatest proportion of the actual transport occurring at these discharges. Transport measurements from Pacific Creek and Buffalo Fork were more consistent at lower flows and displayed greater scatter at higher flows. For these sites, we identified high and low values of τ_r such that all of the measurements made at low discharge were within the uncertainty envelope created by the high and low τ_r values (Figure 2.8). Transport data collected at the Snake River site displayed similar scatter at both low and high discharge measurements; thus, we adjusted the τ_r to provide the best fit to the entire data set. We selected high and low values of τ_r that produced an uncertainty envelope that bracketed 90% of all measurements.

Figure 2.9 depicts the total annual gravel influx and efflux for the study reach between 1958 and 2007, which was calculated using the calibrated transport relations and mean daily discharge for Pacific Creek, Buffalo Fork, and Snake River. As described above, the magnitude of uncertainty varied substantially among sites due to differences in the range of τ_r used to calculate uncertainty at each site, and the range is especially large for Buffalo Fork (Table 2.2). Thus, there is between ± 100% and ± 200% uncertainty for both the influx and efflux in calculating the annual sediment budgets for the study area. The large uncertainty masks most of the differences between influx and efflux in most

years, and we cannot demonstrate with certainty whether the study area experienced net accumulation or evacuation of sediment in most years. The general trend of the years indicates, however, that the Snake River tended to evacuate sediment during the period 1958 to 2007. Budget calculations indicate that for those years in which the difference between inputs and outputs exceeds the uncertainty associated with those estimates, in all but one case, there was net evacuation of sediment. The years in which we estimated net evacuation with confidence are 1963, 1977, 1980, 1981, 1984, 1985, 1986, 1988, 1992, 1993, 1996, and 2004. The single year in which we estimated net accumulation is 1989.

In many settings downstream from dams, the sediment transport capacity has diminished due to decreases in the magnitude of flood events, but the sediment supply has also been reduced or eliminated. Due to the construction of JLD at the outlet of a natural lake, the sediment supply was unaltered by dam construction. Although the long-term sediment budget suggests net evacuation of sediment between JLD and Deadman's Bar, estimation of sediment flux using estimated unregulated hydrology indicates that evacuation would have been even greater in the absence of JLD. In nearly all years between 1958 and 2007, the magnitude of bed load flux at Deadman's Bar calculated using estimated unregulated hydrology exceeds the magnitude of flux calculated using the actual hydrology (Figure 2.10). Thus, though our results suggest net evacuation of sediment from the study reach under impounded conditions, dam operations diminished the magnitude of the imbalance between sediment influx to and efflux from the reach.

5. Discussion

5.1. Effects of dam operations on hydrology and sediment flux

The hydrological analysis presented here demonstrates that the flow regime of the modern Snake River downstream from JLD is very different than it would be if the current rules of operations were not in place. Because there are no diversions, the actual mean annual flow does not differ from estimated unregulated mean annual flow. However, the seasonal patterns in flows are significantly different than they would be in the absence of JLD. There has been a pronounced reduction in peak flows and a substantial increase in late summer flows.

The effects of these hydrologic changes on sediment flux could not be predicted in the absence of sediment transport data due to the nonlinear relation between sediment flux and hydrology and the local variation in bed entrainment thresholds. Comparison of estimated bed load flux at Deadman's Bar for regulated and estimated unregulated conditions reveals that although there is net evacuation of sediment from the Snake River, the magnitude of sediment deficit would be greater in the absence of JLD. Presumably, the unregulated, "natural" Snake River in Jackson Hole was in sediment deficit, and evacuated more gravel then was supplied by tributaries. The decrease in sediment transport capacity was caused by the decrease in flood flows, despite the fact that in many years elevated summer flows extend the duration of the period when the bed is mobilized. Although modern dam operations are still capable of fully mobilizing the bed, the total sediment load has decreased substantially. Thus, current operations of JLD have served to decrease the long-term natural conditions of sediment deficit that existed before completion of JLD. This implies that the Snake River in GTNP was not in equilibrium

prior to construction of JLD. Indeed, the modern Snake River is inset in thick Pleistocene (Figure 2.11) outwash terraces, providing geologic evidence of the incision that has occurred since the retreat of the most recent glaciers 11,000 years ago (Love et al., 2003). Our findings indicate that incision continues today, but to a lesser degree than would have occurred in the absence of JLD. The apparent paradox of channel incision on a braided river has been observed elsewhere: in a flume (Germanoski and Schumm, 1993) and on the River Feshie (Wheaton et al., Submitted).

In addition to changes in the total annual sediment load, the change in the temporal pattern of sediment transport has potentially important implications for the aquatic ecosystem. In the absence of JLD, flows would be substantially lower during late summer and the channel bed would not be mobilized during this period of the year. Typically, in river systems where the flood hydrology is dominated by spring snowmelt, as is the case for the Snake River, bed load transport occurs during a short window of time during the annual spring runoff. Given the current operations of JLD, bed load transport often persists during late summer, and in some years, this transport accounts for a substantial portion of the total load (Figure 2.12). The tracer data and bed load transport data indicate that the increase in late summer flows creates conditions in which the bed is at least partially mobile during the months of July and August.

5.2. Predicting downstream effects of dams

Prior to measuring bed load transport rates, we were unable to quantitatively evaluate the role of dam releases in determining the Snake River sediment mass balance Indeed, the sediment mass balance presented here presents a nuanced view of sediment transport changes than that concluded by prior research based on the analysis of

hydrologic data and repeat aerial imagery (Marston et al., 2005; Schmidt and Wilcock, 2008). Marston et al. (2005) suggested that the regulated Snake River no longer had the capacity to mobilize tributary-derived bed material, but the analysis did not consider hydrology downstream from Buffalo Fork. Schmidt and Wilcock (2008) suggested that the Snake River had been perturbed into sediment surplus, based on the fact that the magnitude of the 2-yr flood was decreased but sediment influx from the tributaries had not changed.

The predictions of both Marston et al. (2005) and Schmidt and Wilcock (2008) were correct in suggesting that operations of JLD decreased the annual transport capacity of the Snake River. However, the sediment transport data indicate that the Snake River is still capable of mobilizing the channel bed in common, as well as large, floods. The analysis here suggests that the river was not in sediment mass balance equilibrium prior to construction of JLD, and this was not evident prior to quantitative evaluation of sediment transport rates.

This study underlines the importance of considering geologic and watershed context when anticipating downstream effects of a dam. In this case, it is inappropriate to presume that conditions of equilibrium existed prior to regulation or flow alteration. Our results highlight the value of considering both measured changes in hydrology and sediment flux when evaluating the effects of dam operations. Metrics based on changes in hydrologic variables, such as changes in the 2-yr flood, are not sensitive in predicting changes in sediment flux over the full range of the annual flow regime

6. Conclusions

JLD and the increased storage thereby provided in Jackson Lake has allowed the adoption of reservoir management rules that significantly change the flow regime of the Snake River in GTNP. Actual flood flows are significantly less than estimated unregulated flows, and late summer flows are typically greater than estimated unregulated flows. Tracer data and measurements of bed load transport demonstrate that bed load material is readily entrained during these reduced magnitude flood events and during elevated late summer flows. Calibrated transport relations provide insight into long-term trends in sediment flux, demonstrating that, in contrast to previously published studies, the system has not been perturbed into a state of net sediment accumulation. Instead, operations of JLD have diminished the magnitude of the naturally occurring net sediment evacuation. The study highlights the value of sediment transport data and calculation of sediment mass balance in informing dam operations. Additionally, the analysis presented here demonstrates a case in which a reconnaissance approach to estimating downstream effects of dam operations, and the associated assumption of pre-dam equilibrium, resulted in an erroneous prediction regarding channel response to dam operations.

References

Andrews, E.D., 2000. Bed material transport in the Virgin River, Utah. Water Resources Research 36(2): 585-596.

Ashmore, P.E., Church, M.A., 1998. Sediment transport and river morphology: A paradigm for study. In: P.C. Kingman, R.L. Beschta, P.D. Komar and J.B. Bradley (Editors), Gravel-bed Rivers in the Environment. Water Resources Publications, Highlands Ranch, Colo., pp. 115-148.

Brandt, S.A., 2000a. Classification of geomorphological effects downstream of dams. Catena 40(4): 375-401.

Brandt, S.A., 2000b. Prediction of downstream geomorphological changes after dam construction: A stream power approach. International Journal of Water Resources Development 16(3): 343-367.

Bunte, K., Swingle, K.W., Abt, S.R., 2005. Guidelines for using bedload traps in coarse-bedded mountain streams: contruction, installation, operation and sample processing, Stream Systems Techology Center, Rocky Mountain Research Station, Forest Service, U.S. Department of Agriculture, Fort Collins, Colo.

Church, M., Hassan, M.A., 2002. Mobility of bed material in Harris Creek. Water Resources Researcg 38(11).

Davies, T.R.H., 1987. Problems of bed load transport in braided gravel-bed rivers. In: C.R. Thorne, J.C. Bathurst and R.D. Hey (Editors), Sediment Transport in Gravel-bed Rivers. Wiley, Chichester, England; pp. 793-811.

Dietrich, W.E., 1982. Settling Velocity of Natural Particles. Water Resources Research 18(6): 1615-1626.

Eaton, B.C., Lapointe, M.F., 2001. Effects of large floods on sediment transport and reach morphology in the cobble-bed Sainte Marguerite River. Geomorphology 40(3-4): 291-309.

Edwards, T.K., Glysson, G.D., 1988. Field methods for measurement of fluvial sediment, USGS Techniques of Water-Resources Investigations, Reston, Va.

Emmett, W.W., 1981. Measurement of bed load in rivers, Erosion and Sediment Transport Measurements. Proceedings of the Florence Symposium, IAHS Publications, pp. 3-15.

Gaeuman, D.A., Schmidt, J.C., Wilcock, P.R., 2003. Evaluation of in-channel gravel storage with morphology-based gravel budgets developed from planimetric data. J. Geophysical Res.-Earth Surface 108(F1): 6001.

Germanoski, D., Schumm, S.A., 1993. Changes in Braided River Morphology Resulting from Aggradation and Degradation. J. Geology 101: 16.

Goff, J., Ashmore, P.E., 1994. Gravel transfer rates and morphological changes in braided Sunwapta River, Alberta, Canada. Earth Surface Processes Landforms 19: 195-212.

Gomez, B., 1991. Bedload transport. Earth-Science Reviews 31(2): 89-132.

Graf, W.L., 1999. Dam nation: A geographic census of american dams and their large-scale hydrologic impacts. Water Resources Research 35(4): 1305-1311.

Grant, G.E., Schmidt, J.C., Lewis, S.L., 2003. A geological framework for interpreting downstream effects of dams on rivers. In: J.E. O'Connor and G.E. Grant (Editors), A peculiar river: geology, geomorphology, and hydrology of the Deschutes River, Oregon. AGU, Washington, D.C., pp. 203-219.

Ham, D.G., Church, M., 2000. Bed-material transport estimated from channel morphodynamics: Chilliwack River, British Columbia. Earth Surface Processes Landforms 25(10): 1123-1142.

Haschenburger, J.K., Wilcock, P.R., 2003. Partial transport in a natural gravel bed channel. Water Resources Research 39(1): 1020.

Hassan, M.A., Church, M., 2001. Sensitivity of bed load transport in Harris Creek: Seasonal and spatial variation over a cobble-gravel bar. Water Resources Research 37(3): 813-825.

Hazel, J.E., Topping, D.J., Schmidt, J.C., Kaplinski, M., 2006. Influence of a dam on fine-sediment storage in a canyon river. Journal Geophysical Research-Earth Surface 111(F1): -.

Hicks, D.G., Gomez, B., 2003. Sediment transport. In: G.M. Kondolf and H. Piegay (Editors), Tools in Fluvial Geomorphology. John Wiley and Sons Ltd, Chichester, England, pp. 425-461.

Jones, M.L., Seitz, H.R., 1980. Sediment transport in the Snake and Clearwater rivers in the vicinity of Lewiston, Idaho, USGS Open-File Report 80-690, Reston, Va.

Knighton, D. 1998. Fluvial forms and processes: a new perspective. Hodder Arnold Publications, London.

Lane, E.W., 1955. The importance of fluvial morphology in hydraulic engineering. American Soceity of Civil Engineering Proceedings 81: 1 - 17.

Lane, S.N., Richards, K.S., Chandler, J.H., 1995. Within-reach spatial patterns of process and channel adjustment. River Geomorphology: 105-130.

Love, D.J., Reed, J.C., Pierce, K.L. 2003. Creation of the Teton landscape: A geologic chronicle of Jackson Hole and the Teton Range. Grand Teton Natural History Association, Moose, WY, 130 pp.

Macarthur, R.C., Neill, C.R., Hall, B.R., Galay, V.J., Schvidchenko, A.B., 2008. Overview of Sedimentation Engineering. In: M.H. Garcia (Editor), Sedimentation Engineering: Processes, Measurements, Modeling, and Practice. ASCE, Reston, Va, pp. 1-20.

Major, J.J., 2004. Posteruption suspended sediment transport at Mount St. Helens: Decadal-scale relationships with landscape adjustments and river discharges. Joural of Geophysical Research - Earth Surface 109(F1).

Marston, R.A., Mills, J.D., Wrazien, D.R., Bassett, B., Splinter, D.K., 2005. Effects of Jackson Lake Dam on the Snake River and its floodplain, Grand Teton National Park, Wyoming, USA. Geomorphology 71(1-2): 79-98.

Martin, Y., Church, M., 1995. Bed-material transport estimated from channel surveys - Vedder River, British-Columbia. Earth Surface Processed Landforms 20(4): 347-361.

McLean, D.G., Church, M., 1999. Sediment transport along lower Fraser River - 2. Estimates based on the long-term gravel budget. Water Resources Research 35(8): 2549-2559.

McLean, D.G., Church, M., Tassone, B., 1999. Sediment transport along lower Fraser River - 1. Measurements and hydraulic computations. Water Resources Research 35(8): 2533-2548.

Nelson, N.C., 2007. Hydrology and geomorphology of the Snake River in Grand Teton National Park, Wyoming, M.S. thesis, Utah State University, Logan.

Parker, G., 1979. Hydraulic geometry of active gravel rivers. Journal of the Hydraulics Division-Asce 105(9): 1185-1201.

Parker, G., 1990. Surface-based bedload transport relation for gravel rivers. Journal of Hydraulic Research 28(4): 417-436.

Petts, G.E., Gurnell, A.M., 2005. Dams and geomorphology: research progress and future directions. Geomorphology 71(1-2): 27-47.

Piety, L.A., Randle, T.J., 1998. Physical processes of Pilgrim Creek in context with the operations and maintenance history for the Pilgrim Maintenance Program, Jackson Lake Dam, Minidoka Project, Wyoming and Idaho. In: B.o.R. U.S. Department of the Interior (Editor), Denver, pp. 116.

Ryan, S.E., 2003. The use of pressure-difference samplers in measuring bedlad transport in small, coarse-grained alluvial channels. In: F.S.R.M.R.S. U.S. Department of Agriculture (Editor). USDA, Laramie, Wyo.

Schmidt, J.C., 1999. Summary and synthesis of geomorphic studies conducted during the 1996 controlled flood in Grand Canyon. In: R.H. Webb (Editor). The Controlled Flood in Grand Canyon. AGU, Washington, D.C., pp. 329-341.

Schmidt, J.C., Wilcock, P.R., 2008. Metrics for assessing the downstream effects of dams. Water Resources Research 44(4): W04404.

Singer, M.B., Dunne, T., 2004. Modeling decadal bed material sediment flux based on stochastic hydrology. Water Resources Research 40(3).

Sutherland, D.G., Ball, M.H., Hilton, S.J., Lisle, T.E., 2002. Evolution of a landslide-induced sediment wave in the Navarro River, California. Geological Society of America Bulletin 114(8): 1036-1048.

Topping, D.J., Rubin, D.M., Vierra Jr. , L.E., 2000. Colorado River sediment transport 1. Natural sediment supply limitation and the influence of Glen Canyon Dam. Water Resources Research 36(2): 515-542.

Vericat, D., Batalla, R.J., 2006. Sediment transport in a large impounded river: The lower Ebro, NE Iberian Peninsula. Geomorphology 79(1-2): 72-92.

Wallick, J.R., Anderson, S.W., Cannon, C., O'connor, J.E., 2009. Channel change and bed-material transport in the lower Chetco River, Oregon, U.S. Geological Survey, Reston, Va.

Wheaton, J.M., Brasington, J., Darby, S.E., Sear, D.A., Vericat, D., Submitted. Morphodynamic explanation of net degradation in a braided river. JGR Earth Surface.

Wilcock, P.R., 2001. Toward a practical method for estimating sediment-transport rates in gravel-bed rivers. Earth Surface Processes and Landforms 26: 1395-1408.

Williams, G.P., Wolman, M.G., 1984. Downstream effects of dams on alluvial rivers. US Geological Survey Professional Paper 1286(83): 54-74.

Wolman, M.G., 1954. A method of sampling coarse river-bed-material. EOS Transactions 35(6): 951-956.

Table 2.1. Rouse numbers calculated for a range of discharges and grain sizes for the Snake River at Deadman's Bar. Hydraulic radius (*Rh*) associated with each discharge from Nelson [2007]. Shaded region highlights Rouse numbers too large for suspension.

	Q (m3s-1)	**Rh (m)**	**Grain Size (mm)**						
			0.5	0.7	1	1.4	2	2.8	4
2 yr	75	0.39	1.5	2.3	3.3	4.6	6.2	8.1	10.4
5 yr	95	0.41	1.5	2.2	3.2	4.5	6.1	7.9	10.1
10 yr	115	0.43	1.5	2.2	3.2	4.4	6.0	7.8	10.0

Table 2.2. Variables used to calibrate bed load transport functions.

Variable	Pacific Creek	Buffalo Fork	Snake River
Water surface slope, S	0.0035	0.0025	0.0025
D_{65} (mm)	29	29	50
D_{50} (mm)	21	18	34
Active channel width, b (m)	43	45	70
Reference shear stress, t_r (lower, upper)	14.2 (13.2, 14.2)	9.5 (8.5, 12.5)	9.8 (8.3, 11.3)
Dimensionless ref. shear stress, t^*_r (lower, upper)	0.042 (0.039 , 0.045)	0.032 (0.029, 0.043)	0.018 (0.015, 0.021)

Table 2.3. Comparison of estimated unregulated flows and actual flows at Moran.

	Unregulated flow (cms)		**Actual flows (cms)**		
	mean	std. dev.	mean	std dev	% difference
peak annual flow	283.75	77.03	166.16	50.22	-41.44
late summer flow	39.92	20.28	79.63	23.34	99.48

Table 2.4. Comparison of estimated unregulated flows and actual flows downstream from Buffalo Fork.

	Unregulated flow (cms)		**Actual flows (cms)**		
	mean	std. dev.	mean	std. dev.	% difference
peak annual flow	429.86	119.31	284.40	88.80	-33.84
late summer flow	70.76	37.30	110.53	32.60	47.84
Annual % of time bed mobilized at Deadman's Bar	19.99	4.38	30.18	10.12	10.19

Table 2.5. Mobility of tracer clusters in each mobility category during the natural and dam-released floods in 2005. 'DS JLD' = downstream from JLD; 'DS PC' = downstream from Pacific Creek; 'DMB/SCH' = combined results from Deadman's Bar and Schwabachers Landing; and 'MOOSE' = Moose.

	Flood magnitude (m^3s^{-1})	**Tracers placed within active channel**			**Tracers marked in situ**		
		Immobile	Partially Mobile	Fully Mobile	Immobile	Partially Mobile	Fully Mobile
Natural Flood – May 21							
DS JLD	--	--	--	--	--	--	--
DS PC	92	1	0	0	7	0	1
DMB/SCH	170	16	3	0	4	0	0
MOOSE	174	18	0	0	18	0	0
Dam-Released Flood – June 15 - 18							
DS JLD	117	2	4	0	17	13	0
DS PC	133	2	0	0	7	20	2
DMB/SCH	183	15	3	1	0	1	3
MOOSE	192	10	6	2	0	7	11

Table 2.6. Percent of inundated clasts that moved during the peak flows of 2005. 'DS JLD' = downstream from JLD; 'DS PC' = downstream from Pacific Creek.

	Tracers placed within active channel					**Tracers marked in situ**				
		All tracers that moved		Tracers that moved ≥1m			All tracers that moved		Tracers that moved ≥1m	
	Total #	#	%	#	%	Total #	#	%	#	%
DS JLD	90	16	18	0	0	523	75	14	1	0.2
DS PC	105	35	33	5	5	309	9	3	1	.3
DMB/SCH	16	15	94	13	81	1232	90	7	25	2
MOOSE	53	43	81	26	49	1782	268	15	71	4

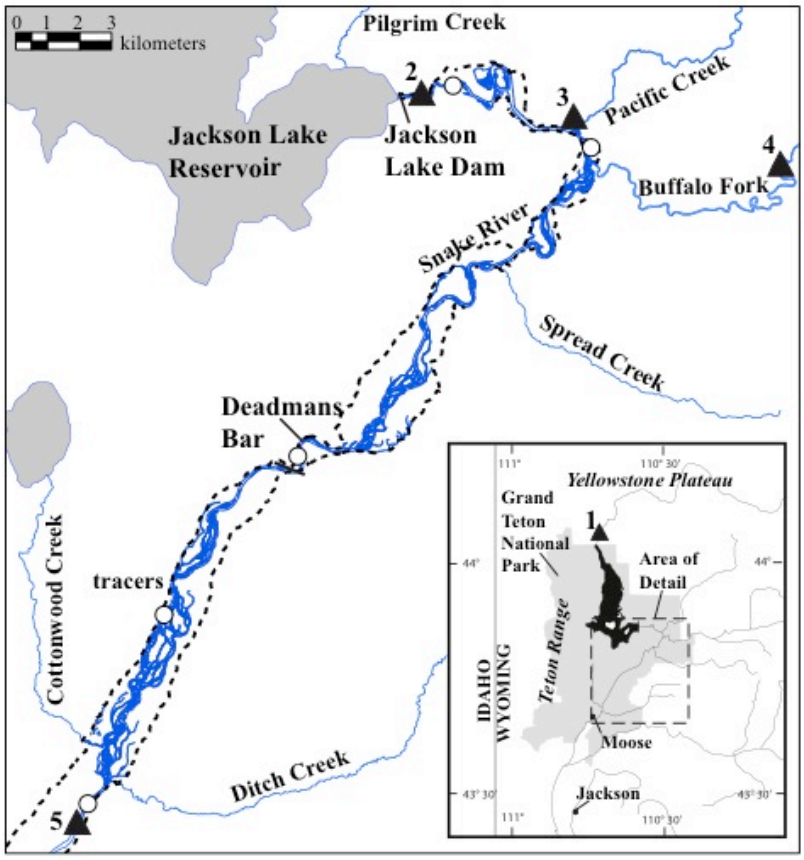

Figure 2.1. The Snake River in Grand Teton National Park, extending from Jackson Lake Dam to Moose; the river channel is that of 2002. The approximate width of the Holocene valley in the study area is marked by the bold, dashed line. The location of gaging stations are indicated by triangles: (1) station 13010065, Snake River above Jackson Lake at Flagg Ranch; (2) station 13011000, Snake River at Moran; (3) station 13011500, Pacific Creek at Moran; (4) station 13011900, Buffalo Fork above Lava Creek near Moran; and (5) station 130136500, Snake River at Moose. Hollow circles are the locations of painted rocks.

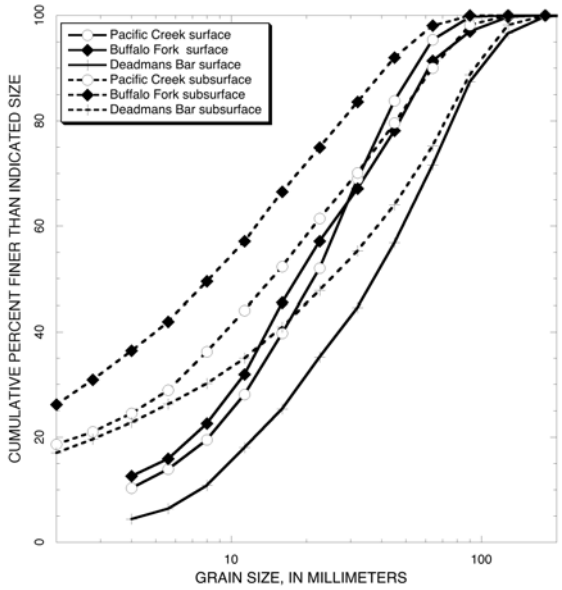

Figure 2.2. Surface and subsurface grain size distribution at the three bed load measurement sites, Pacific Creek, Buffalo Fork, and Deadman's Bar.

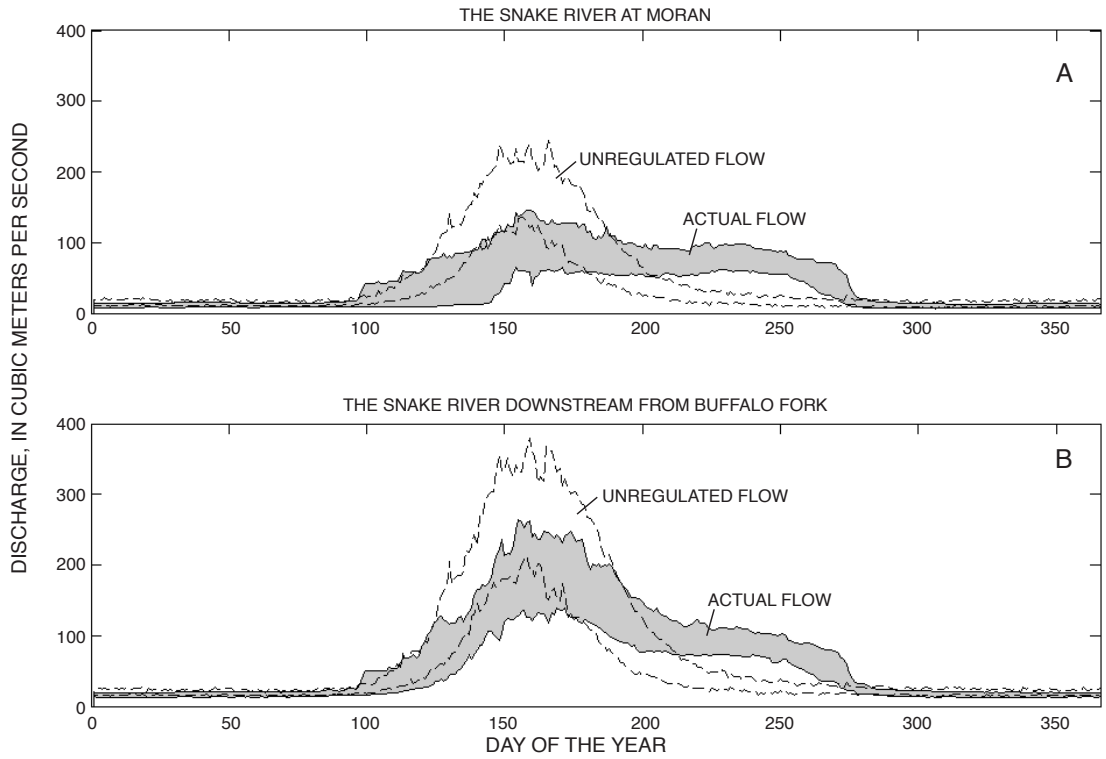

Figure 2.3. The interquartile range of actual and unregulated mean daily flows for (A) Snake River at Moran and (B) Snake River downstream from Deadman's Bar. The shaded area in (A) and (B) represents actual flows and the dashed lines bound the estimated unregulated flows.

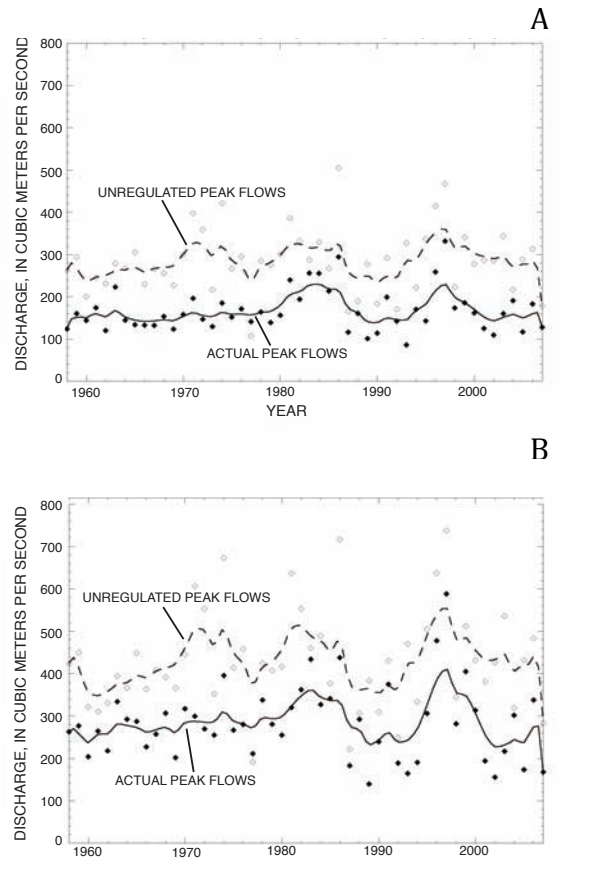

Figure 2.4. Actual and estimated unregulated annual peak flow for (A) Snake River at Moran and (B) Deadman's Bar. Lines represent the weighted average. Open symbols and dashed lines depict estimated unregulated flow; the solid symbols and solid lines depict actual flows.

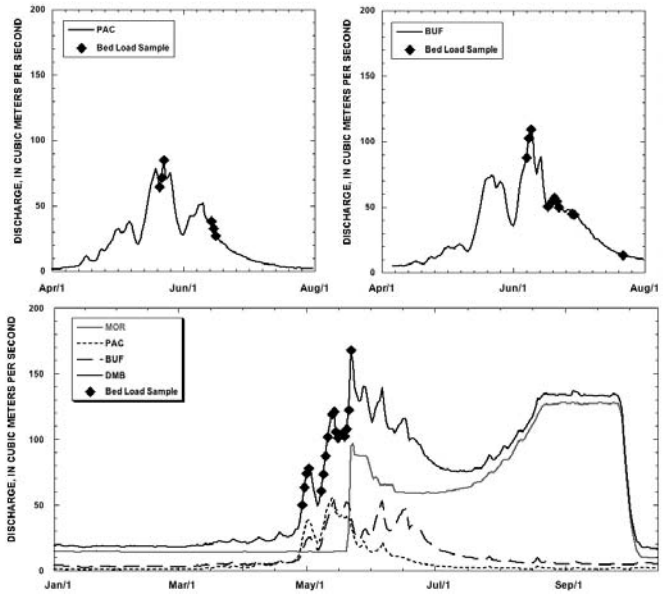

Figure 2.5. Hydrographs of mean daily discharge and dates of bed load transport measurements on Pacific Creek (2006), Buffalo Fork (2006) and Snake River (2007). Plot of Snake River hydrology includes the hydrographs for the Snake River at Moran (MOR), Pacific Creek (PAC), and Buffalo Fork (BUF). Flow at these three locations was summed to compute the Snake River at Deadman's Bar hydrograph (DMB).

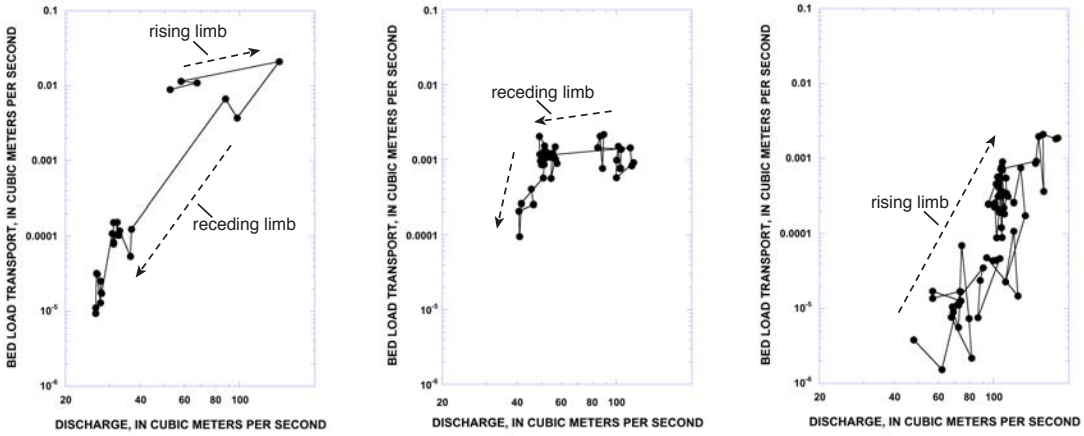

Figure 2.6. Bed load transport data measured on Pacific Creek (A), Buffalo Fork (B) and Snake River (C).

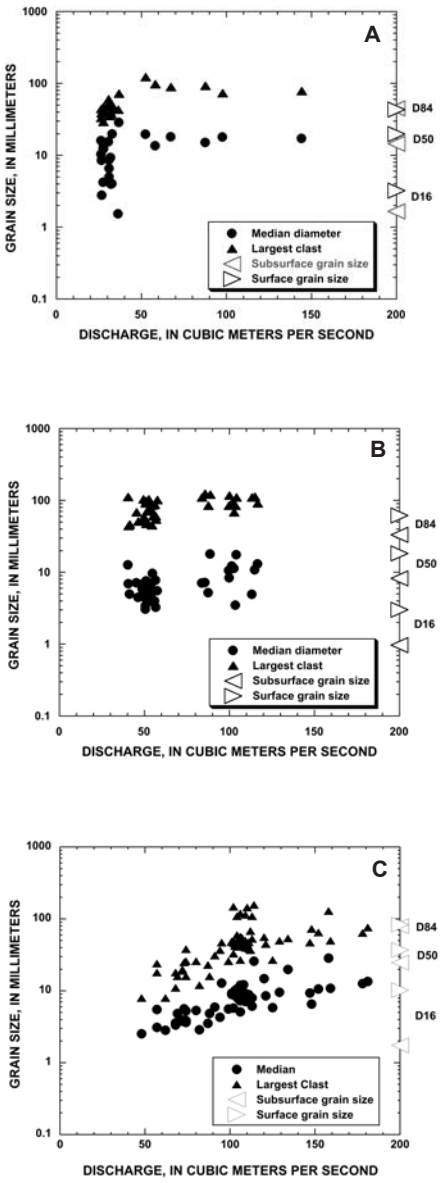

Figure 2.7. Grain size distribution of sediment in transport on Pacific Creek (A), Buffalo Fork (B) and Snake River (C). Surface and subsurface grain size data (D16, D50 and D84) is plotted along the right y-axis.

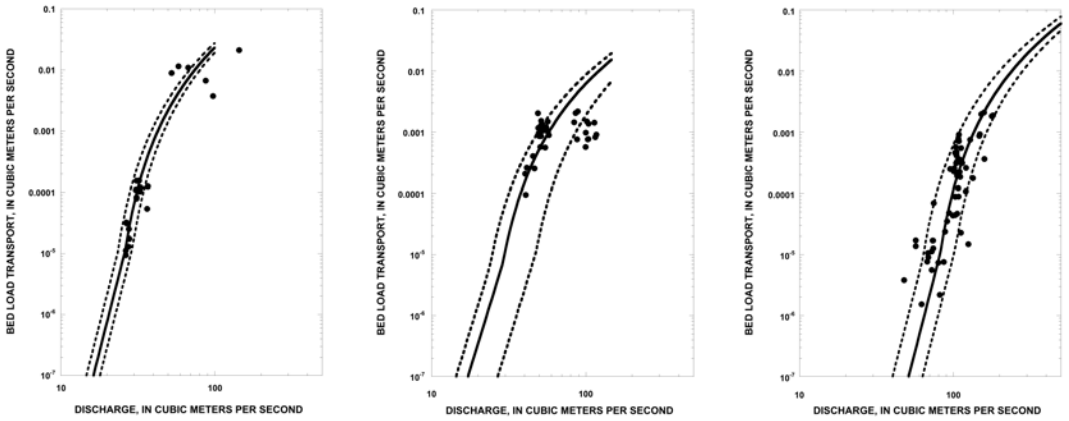

Figure 2.8. Transport data from Pacific Creek (A), Buffalo Fork (B) and Snake River (C) fitted with Parker (1979, 1990) transport functions (solid line). The dashed lines represent the uncertainty envelope used for long-term transport calculations.

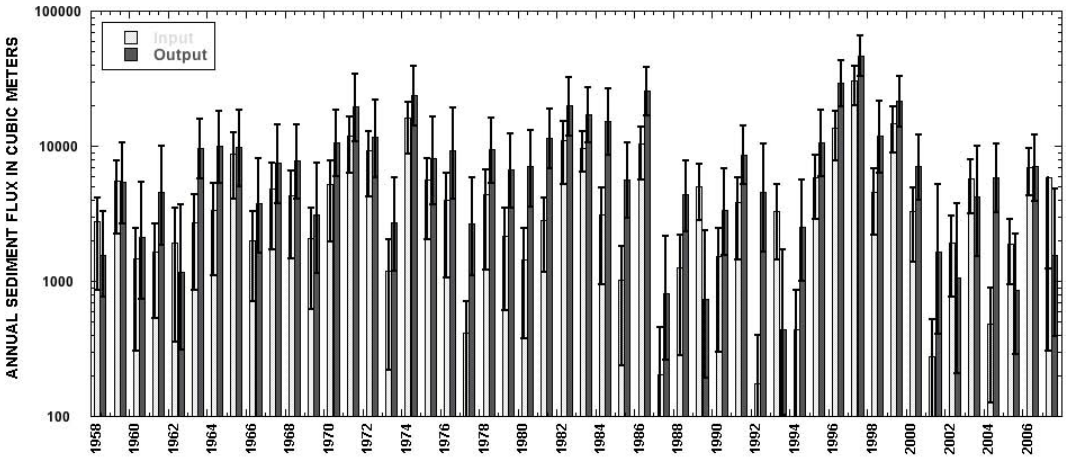

Figure 2.9. Sediment budget for 1958 to 2007 developed using calibrated bed load transport relations and discharge data from USGS gages. The error bars demonstrate that there is still great uncertainty associated with our estimates of sediment flux, and that uncertainty results in a budget that is indeterminate for the majority of years. However, for the years in which the magnitude of the difference between inputs and outputs exceeds the uncertainty associated with those estimates, in all but one case, the budget calculations indicate net evacuation.

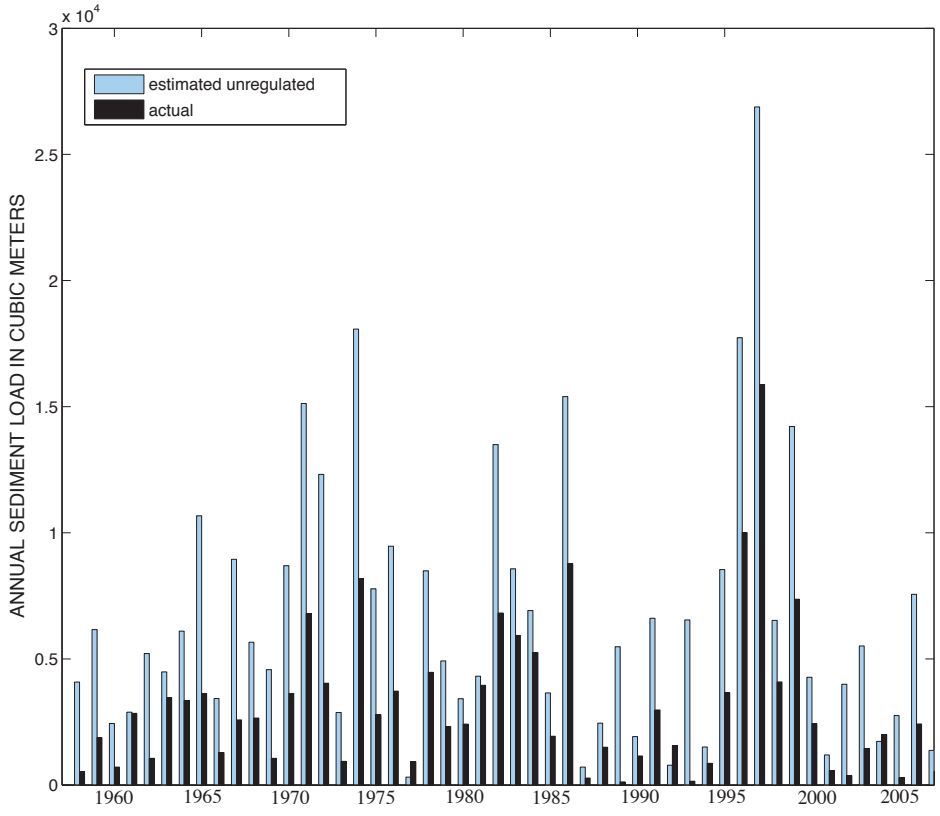

Figure 2.10. Estimated sediment flux at Deadman's Bar using actual mean daily discharge and estimated unregulated mean daily discharge. In almost all of the years, the sediment flux computed using the estimated unregulated flows exceeds the flux computed using the actual flows.

Figure 2.11. Pleistocene terraces along the Snake River at the Deadman's Bar boat launch in Grand Teton National Park. Flow is from bottom to top of the photo, and the Deadman's Bar bed load sampling site is located towards the downstream end (top) of the photo. Note the vehicles on the left of the photo for scale.

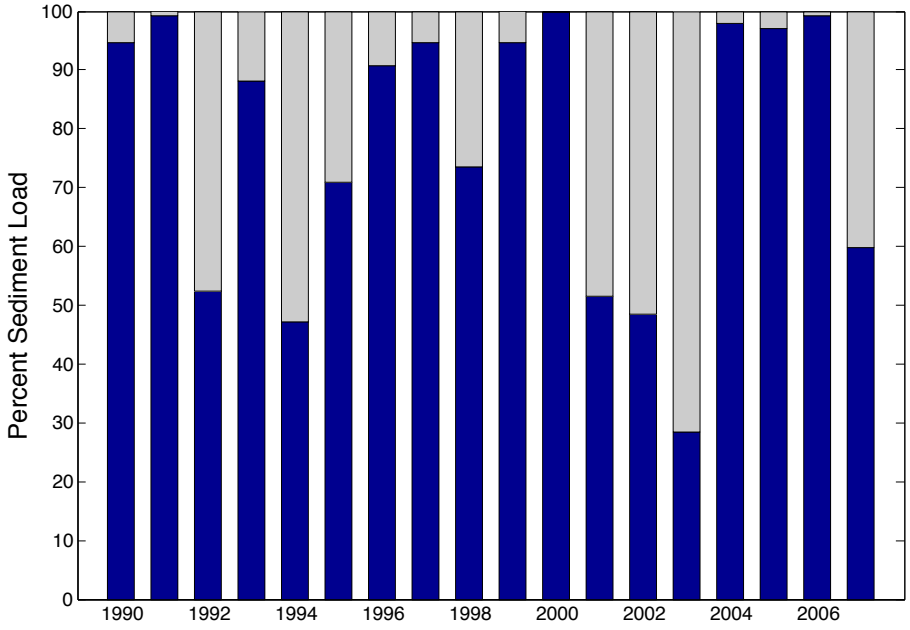

Figure 2.12. Estimated percent of the annual sediment load that is transported in May/June (dark shading) and July/August (light shading) for the Snake River at Deadman's Bar. Although the percent of the annual load that is transported during May/June, the period when flood releases occur, accounts for the majority of the annual load, in some years, a substantial portion of the load is transported by late summer flows due to the artificially high flows.

CHAPTER 3

CLOSING A SEDIMENT BUDGET FOR A RECONFIGURED REACH OF THE PROVO RIVER, UTAH

Abstract

We quantified all components of a fluvial sediment budget for a discrete flood on an aggrading gravel bed river. Bed load transport rates were measured at the upstream and downstream ends of a 4-km study area on the Provo River, Utah, during a dam-controlled flood. We also collected high-resolution measurements of channel topography before and after the controlled flood for the entire reach. Topographic uncertainty in the digital elevation models (DEM) were characterized using a spatially-variable approach. Sediment input to the reach (286 m^3) exceeded output (29 m^3), producing a net accumulation of approximately 260 m^3. The net sediment flux provided unambiguous indication of storage. The difference between the scour and fill was also positive (470 m^3), but uncertainty in the topographic differencing was larger than the observed net storage. Although topographic differencing was not sufficiently accurate to indicate net storage, it was able to demonstrate that internal erosion was a larger sediment source than the net sediment flux. The magnitude of total erosion (1454 m^3) and deposition (1926 m^3) was considerably larger than the sediment flux terms. Thus, internal sources and sinks were the dominant driver of channel change.

1. Introduction

Sediment budgets are a fundamental tool in geomorphology, used across the discipline in theoretical and applied studies [*Reid and Dunne*, 2003]. A fluvial sediment budget provides the context needed to evaluate channel response to changes in flow or sediment supply [e.g. *Trimble*, 1983; *Wathen and Hoey*, 1998; *Grams and Schmidt*, 2005]. A sediment budget balances sediment input (I) and sediment export (E), against sediment storage (ΔS),

$$I - E = \Delta S. \tag{1}$$

Numerous studies have focused on quantifying either the flux side [*Singer and Dunne*, 2004; *Vericat and Batalla*, 2006] or the storage side of (1) [*Lane et al.*, 1995; *Martin and Church*, 1995; *Ashmore and Church*, 1998; *Ham and Church*, 2000; *Brasington et al.*, 2003; *Surian et al.*, 2009]. Few studies have computed both sides of the budget. In the absence of closing a budget, the unmeasured components of the budget cannot be separated from the errors associated with the measured terms in the budget [*Kondolf and Matthews*, 1991]. Closure of the budget, i.e. independently calculating the left and right sides of (1) and determining if the two quantities match, provides a rigorous means by which the accuracy and precision of the budget can be evaluated. Spatial partitioning of the right side of (1), i.e. determining the amount of change in sediment storage in different parts of the channel and/or floodplain, provides even more insight into how channels adjust to longitudinal changes in sediment transport.

One of the persistent problems with developing sediment budgets is that measurement error is typically large. Both transport and storage sides of the budget often involve the small difference between two large and uncertain numbers, such that even the sign of either side of (1) is uncertain. Sediment transport estimated from either formulas [*Gomez and Church*, 1989; *Martin*, 2003; *Kuhnle*, 2006] or direct measurement [*Ham and Church*, 2000; *Wilcock*, 2001] may not be sufficiently accurate to determine the sign of the net flux. Topographic monitoring may not be sufficient to determine the sign of ΔS, even with recent advances in measurement and analysis [*Heritage and Hetherington*, 2007; *Wheaton et al.*, 2010; *Milan et al.*, 2011]. The result of measurement uncertainty in either flux or topography change is that sediment budgets may be indeterminate, in the sense than one cannot explicitly demonstrate that aggradation or degradation has occurred [*Grams and Schmidt*, 2005]. In some cases, budgets are indeterminate even where measurement programs are extensive [*Topping et al.*, 2000].

The ability to calculate a sediment budget with a definitive balance is influenced by the spatial and temporal scale of the analysis. For example, budgets may be developed over sufficiently long reaches such that there is a significant difference in fluxes at the upstream and downstream boundaries or over sufficiently short temporal scales so one can accurately relate topographic measurements to a discrete flow event. Even under these circumstances, however, challenges remain. Detecting the changes in storage for short time spans may be difficult, because there may have been little net topographic change during the period for which the budget is calculated. It may be difficult to extrapolate the budget to longer time scales, because a longer time span introduces more

uncertainty about the stability of sediment transport relations. Additionally, investigations spanning multiple years, or decades, are often limited by the lack of historic data. Calculation of budgets over short spatial scales provides the advantage that changes in storage can be measured with relative ease. However, when budgets are calculated for a short reach of river, there may not be a significant difference between the measured influx and efflux of sediment. Conversely, larger spatial scales provide the advantage that there may be a more substantial difference between influx and efflux. Yet, changes in storage are more difficult to comprehensively measure over longer reaches.

Here, we present a sediment budget for a reconfigured 4-km segment of the middle Provo River, near Heber City, Utah, USA (Figure 3.1), for a single flood that lasted approximately 3 weeks. We highlight the challenges and uncertainties associated with construction and closure of a sediment budget in an unusually well-constrained situation - a discrete flood on a relatively short segment of a gravel bed river. The study area had been reconfigured approximately 3 years earlier, and qualitative evidence indicated that the channel was accumulating gravel, primarily in point bars. Preliminary measurements of transport rates at the upstream and downstream boundaries of the study area suggested that sediment influx exceeded efflux by an order of magnitude [*Olsen*, 2006]. In constructing a sediment budget, we sought to (1) confirm whether or not aggradation was occurring, (2) understand the magnitude of difference between upstream sediment delivery and downstream sediment export, and (3) evaluate whether the observed channel changes could be attributed to sediment accumulation in the reach. We evaluate both sides of (1) in order to rigorously evaluate error and to examine the

different conclusions that can be drawn from budgets based on only measurements of flux or morphologic change.

2. Study area

2.1. History of flow manipulation on the Provo River

The Provo River flows from its headwaters in the Uinta Mountains in northern Utah to its outlet in Utah Lake. The river system is subject to large-scale flow manipulation and augmentation, primarily caused by two water resource development projects: the Provo River Project (PRP) and the Central Utah Project (CUP). As part of the PRP, trans-basin diversions from the Weber and Duchesne Rivers into the Provo River were constructed in 1948 and 1952, respectively. These diversions nearly doubled the magnitude of peak flows on the Provo River and substantially increased base flows. Deer Creek Dam was constructed at the downstream end of Heber Valley to provide reservoir storage for the augmented flow (Figure 3.1). Deer Creek Reservoir was filled soon after completion of the dam in 1941. To accommodate the additional flow and to protect adjacent lands from flooding, the Provo River in Heber Valley was straightened, enlarged, and confined between dikes along the entire length of the valley between 1960 and 1965. The only exception was a 2.5-km reach, which we refer to as the Never Channelized Reach (NCR; see Figure 3.1). During the period between 1965 and 1994, upstream bed incision caused gravel to accumulate in the NCR.

Jordanelle Dam, at the upstream end of the Heber Valley, was completed in 1994 as part of the CUP. Operations of Jordanelle Dam reduced the magnitude of peak floods by 25% from those of the post-flow-augmentation period. Additionally, trans-basin

diversions maintain summer flows that are much higher than natural base flows. Within the study area, streamflow has been measured since 1938 at U.S. Geological Survey gaging station 10155500 (Provo River near Charleston). There are no significant tributaries.

2.2. The Provo River Restoration Project

The Provo River Restoration Project (PRRP) involved reconfiguration of 16 km of the middle Provo River to restore elements of the pre-channelization ecosystem that can be maintained by the regulated flow regime provided by Jordanelle Dam. Twelve km of the PRRP are upstream from the NCR and 4 km are downstream from the NCR. Project construction began in 1999 and consisted of removing dikes, creating a wandering, gravel bed channel, reconnecting the river to existing remnants of historic secondary channels, and constructing small side channels to recreate natural aquatic features and wetlands. The reconstructed channel morphology is intended to maximize diversity of habitat conditions and establish a complex template on which ecosystem processes will thrive [*Utah Reclamation, Mitigation, and Conservation Commission*, 1997] .

Jordanelle Dam eliminated the sediment supply once delivered to the Heber Valley; thus, the upstream 12 km of the PRRP has no sediment input. Previous transport observations [*Olsen*, 2006] indicated that the NCR is now a source of gravel for the reconfigured 4-km segment downstream. Air photo observations in this segment indicated that point bars had grown since completion of channel reconfiguration in 2004 (Figure 3.2), suggesting a trend of sediment accumulation.

This study focuses on the 4-km segment immediately downstream from the NCR where qualitative observations suggested sediment is actively accumulating. The substantial influx of gravel into the study area (Figure 3.3) has the potential to augment channel dynamics, and perhaps aid in achieving restoration goals, but these channel changes also have the potential to be detrimental to the original restoration objectives. Thus, it is useful to determine the sediment balance in order to better understand the impact of sediment influx on channel morphology and dynamics. The PRRP upstream from the NCR has no sediment supply and gravel augmentation will be considered as a tool for promoting channel dynamics. Studies of the segment downstream from the NCR will inform plans for gravel augmentation plans upstream.

3. Methods

We quantified both net flux and change in storage, quantified their uncertainty, and evaluated the mass balance in terms of uncertainty in all terms. Here, we divide our discussion of methods into the quantification of bed load flux (section 3.1) and quantifying the change in storage through measurement of topographic change (section 3.2).

3.1. Determining bed load flux

3.1.1. Bed load transport measurements

In spring 2009, we worked with the U.S. Bureau of Reclamation (USBR) and the Central Utah Water Conservancy District (CUWCD) to design a controlled flood that allowed for an effective bed-load sampling program. On both rising and falling limbs,

discharge was changed in intervals of approximately 5.7 m^3s^{-1} each day and then held steady for at least 8 hours (Figure 3.4), allowing us to collect bed load measurements at the same constant flow rate at two sites. We collected transport samples at discharges ranging from 22.7 to 53.5 m^3s^{-1}. The peak of the 2009 flood had a recurrence interval of 4 years for the 17-year record following closure of Jordanelle Dam.

We established bed load transport measurement sites at the upstream and downstream boundaries of our study area, which we refer to as Midway and Charleston, respectively. At each bed load sampling site (Figure 3.3), we used a raft-based sampling platform [*Graham Matthews and Associates*, 2010] and a Toutle River 2 (TR-2) bed-load sampler [*Childers*, 1999]. The TR-2 sampler is well suited for measurements of the large grain sizes in transport during Provo River floods and the sampler has been used successfully on other large rivers [*Gaeuman et al.*, 2009; *Wallick et al.*, 2009; see Chapter 2]. We used a modified version of the Equal Width Interval [*Edwards and Glysson*, 1988] sampling method; one sample consisted of a single pass across the channel, during which data were collected at 8 – 10 points along the cross-section. The sampler remained on the bed for five minutes at each sampling station. We sieved and weighed all samples in 1/2-ϕ size classes.

Discharge at the time of each measurement was taken to be that measured at the USGS gage Provo River near Charleston. We also installed stage plates upstream and downstream of both bed load sampling sites. We measured the water surface slope over a distance of approximately 5 channel widths at the two sampling sites during each measurement. When flows receded after the flood, we conducted bed material point

counts of the submerged bed in the vicinity of each sampling site to determine the grain size distribution of the bed surface.

3.1.2. Computation of sediment flux

The bed load measurements from each site conform closely to a power function and showed no hysteresis. Transport rates were characterized using sediment rating curves,

$$Q_s = aQ^b, \quad (2)$$

where Q_s is sediment flux and Q is discharge. For each site, we calculated cumulative sediment transport for the 2009 flood using mean daily discharge data provided by the USGS gaging station.

We used a bootstrap approach to calculate the uncertainty associated with our estimates of the annual sediment load. For each data set, we generated 1000 random samples with replacement from the transport data. We fit a rating curve to each random sample and used the function to calculate total sediment load over the flood hydrograph. From the 1000 samples, we generated a distribution of estimated influx, efflux, and net storage, and we calculated the 95 and 5 percentiles of these distribution. We used a bulk density of 1,855 kg/m^3 to convert sediment mass to volume [*Bunte and Abt*, 2001].

3.2. Determining change in storage

We divided the study area into seven reaches for the purpose of calculating change in sediment storage (Figure 3.3). Reach boundaries were defined to provide consistent within-reach properties based on channel planform and measurement

technique. Reaches 1 and 2 are confined by a levee along the right bank protecting a wastewater treatment plant and, as a result, are relatively straight. In these reaches, the channel is steep and there is little space in the channel to accommodate new deposits. In Reaches 3 through 7, the river is relatively unconstrained, and the channel was constructed with a meandering planform.

Three reaches (1, 4, and 6), accounting for nearly one-third of the study area, were surveyed before the flood using total stations and rtkGPS systems. It was not possible to survey channel topography in the remaining four reaches prior to the flood. Pre-flood bathymetery for Reaches 2, 3, 5, and 7 was determined from a combination of aerial LiDAR and multispectral aerial imagery. We surveyed the entire study area after the flood using total station and rtkGPS surveys. We used the topographic data to construct pre- and post-flood digital elevation models (DEMs). We computed changes in bed material storage using geomorphic change detection techniques [*Milan et al.*, 2011], which we describe below.

3.2.1. Direct measurement of topography via ground surveys

In Reaches 1, 4, and 6, we surveyed pre-flood topography during low flows in September – October 2008 and post-flood topography during October – November 2009. All survey data were collected in WGS84, using a Topcon Hiper-Pro rtkGPS, Leica GS15 rtkGPS, and Leica TCRA 1203+ total station. The total station was used in portions of the channel that were too deep to safely survey with rtkGPS. Average point density of pre- and post-flood surveys was approximately 0.32 points m^{-2}. Point densities were greater in areas with steeper or more complex topography and less dense in parts of

the channel with little relief [*McCullagh*, 1981; *Brasington et al.*, 2000; *Valle and Pasternack*, 2006].

3.2.2. Remotely sensed topography

In Reaches 2, 3, 5, and 7, we mapped 2008 topography using a combination of remotely sensed data: LiDAR and multispectral (RGB) imagery. These data were acquired by Sanborn Mapping, Inc., on 23 September 2008. We used the data to create a composite terrain model for each reach, using LiDAR for above-water locations and estimating submerged elevations by subtracting estimated channel depth from the water surface elevation [*Legleiter*, 2012]. Channel depth was estimated using a statistical relation between flow depth and spectral intensity of the RGB imagery [e.g. *Winterbottom and Gilvear*, 1997; *Marcus and Fonstad*, 2008; *Legleiter et al.*, 2009]. Although this approach is inherently less accurate than ground-based surveys, it provides useful information and an interesting comparison in a study concerned with sediment budget accuracy. The Provo River provided ideal conditions to apply this technique; the flow is relatively shallow with very low turbidity, aquatic vegetation is minimal, and there is little overhanging riparian vegetation.

We calibrated relations between RGB intensity and measured flow depth using the pre-flood survey data in Reach 4. We collected these ground survey data within two weeks of the time when the air photos were acquired, and discharges during this time varied little (Table 3.1). We selected Reach 4 because the ground survey was conducted within two weeks of aerial photographs and discharge and stage were nearly identical on both dates.

For Reach 4, we developed a multiple linear regression between depth and reflectance intensity of the three bands [*Winterbottom and Gilvear*, 1997]:

$$h = -0.08672 - 0.000374\,R + 0.000311\,G + 0.0000777\,B \qquad (3)$$

where h is depth of the water column, R is the reflectance of the red band, G of the green band, and B of the blue band. We evaluated a variety of relations between reflectance and depth, including ratios of bands [*Legleiter and Roberts*, 2005] and found equation (3) to be the best predictor of depth ($R^2 = 0.94$; Figure 3.5). We validated the relation using survey data from Reaches 1 and 6, and found that the relations were a good predictor of depths in these reaches as well ($R^2 = 0.89$ and 0.92, respectively).

We surveyed a longitudinal profile of water surface elevation along the channel centerline on 12 October 2008, and used these data to convert estimates of depth to absolute elevations. Discharges recorded at gage 10155500 for the day of the air photo flight and the day of the water surface survey were 6.43 m^3s^{-1} and 6.60 m^3s^{-1}, respectively. This difference in flow corresponds to a difference in stage of 8 mm at the Charleston gage. We neglected this stage difference, because it is small relative to the magnitude of the uncertainty inherent in computation of depths using the RGB imagery (on the order of 20 cm). GPS points on the longitudinal profile were collected every 5 – 10 m, with an effort to survey points at locations where there was a change in water surface slope. We linearly interpolated the water surface between survey points to develop a continuous water surface profile. We then subtracted the estimated depths from

the interpolated water surface profile to compute elevations. We merged the spectrally based bathymetry with the bare-earth topography generated from the LiDAR to create a composite DEM [*Legleiter*, 2012].

In developing the relation between observed and predicted depth for the wetted channel, we first used a 3x3 averaging window to smooth the raster, which improved the quality of our predictions. Additionally, we manually digitized and removed areas of the wetted channel where i) shadows from overhanging riparian vegetation and ii) surface turbulence obscured visibility of the bed. These discontinuous areas accounted for approximately 4% of the wetted channel, and we excluded these areas from our analysis.

In addition to evaluating the quality of the statistical relations developed for computing bathymetry from depth-intensity relations, we visually inspected the DEMs developed using multispectral imagery to ensure that the DEMs were a reasonable depiction of channel form. The spectral bathymetry approach produced DEMs that accurately captured topographic features that were observed in the field, such as pools on the outside of bends and shallow areas of deposition on point bars.

3.2.3. Computing change in storage

With the hybrid mix of topographic survey data described above, we derived 1-m DEMs for the 7 reaches for pre-flood and post-flood conditions based on either ground survey or LiDAR and spectrally derived bathymetry. We selected a 1-m resolution because it adequately represents the topography of mapped geomorphic units and was supported by the point density available. We calculated the difference between DEMs for the pre- and post-flood periods on a cell-by-cell basis to calculate a DEM of Difference

(DoD) using the Geomorphic Change Detection Software [*Wheaton et al.*, 2010]. The change detection software was used to i) independently estimate the errors in the input DEMs; ii) propagate those errors into the DoD change calculation; iii) estimate the probability that calculated DoD changes are real; iv) and use the probability estimates to exclude areas of change that were not above a selected confidence interval from the volumetric estimates of erosion and deposition.

We used two techniques to estimate errors in the individual DEMs. In Reaches 1, 4, and 6, where ground survey data were available before and after the flood, we used a spatially variable fuzzy inference system calibrated to rtkGPS and total station surveys to estimate DEM errors [*Wheaton et al.*, 2010]. The fuzzy inference system is based on the idea that construction of a DEM from survey data is a tradeoff between sampling intensity and the topographic complexity of the surface being surveyed. In Reaches 2, 3, 5, and 7, where the spectral bathymetry technique was used to generate pre-flood DEMs, we used a more conservative spatially uniform estimate of DEM error. We assigned a 20-cm error to the pre-flood DEMs derived from the multispectral imagery (20 cm is the standard deviation of observed minus predicted elevations for Reach 4) and a 6-cm uniform error for the post flood surveys.

We calculated the combined error for the individual DEMs on a cell-by-cell basis using:

$$E = \sqrt{e_{dem1}^2 + e_{dem2}^2} \tag{4}$$

where E is the combined, or propagated, error, and e_{dem1} and e_{dem2} are the errors associated with the 2008 and 2009 DEMs [*Brasington et al.*, 2003]. We compared the propagated errors to the DoD to calculate a T-Score and estimate a probability that the calculated change was real, as described by *Lane et al.* [2003]. We used a more conservative 95% confidence interval in Reaches 2, 3, 5, and 7, where we were less confident in the topographic surfaces generated from the multispectral imagery. In reaches where topography was directly measured with rtkGPS both pre- and post-flood, we used a less conservative 80% confidence interval.

We calculated change in storage by comparing net volume differences between erosion and deposition (i.e. deposition minus erosion). We calculated volumetric errors (± volume) for the estimates of scour and fill volumes by multiplying the estimated propagated DEM error on a cell-by-cell basis by the area of the cell. Those individual volumetric errors were used to estimate the total uncertainty in the net volumetric change in storage calculated for each reach. Additionally, to facilitate comparison of the magnitudes of change in each reach, we calculated the relative change in storage (a volume to surface area ratio) by dividing the net volumetric change by the total area of the reach.

4. Results

4.1. Bed load flux

Bed load measurements were made on the rising and receding limbs of the flood at both sites. Sampling began at the onset of detectable gravel transport. We collected 32 samples at Midway and 31 samples at Charleston. Measured transport rates ranged from

0.01 – 57 g $m^{-1}s^{-1}$ at Midway and 0.2 – 27 g $m^{-1}s^{-1}$ at Charleston (Figure 3.6). At both sampling sites, measured bed load transport rates showed a strongly nonlinear relation with discharge and did not display any hysteresis.

Total sediment loads computed from the sediment rating curves demonstrate that there was net accumulation during 2009 (Figure 3.7). Approximately $5.84 \cdot 10^5$ kg (95% fall between $3.85 \cdot 10^5$ and $9.16 \cdot 10^5$ kg) entered at Midway and $5.95 \cdot 10^4$ kg (95% fall between $5.20 \cdot 10^4$ and $6.82 \cdot 10^4$ kg) exited at Charleston. These estimates correspond to sediment volumes of 286 m^3 (189 – 449 m^3) and 29 m^3 (26 - 33 m^3) at Midway and Charleston, respectively. Thus, despite the uncertainty associated with these estimates, these calculations demonstrate that bed load influx exceeded bed load efflux by nearly an order of magnitude. The estimated net sediment accumulation based on these transport measurements ranges from 163 - 416 m^3.

4.2. Change in storage

Both scour and fill are small in Reaches 1 and 2, where the channel is confined along the right bank by a levee (Table 3.2; Figures 3.8 and 3.9). Both scour and fill increase in Reaches 3 and 4, where the channel is more able to adjust. Scour and fill are both larger in Reach 4 than in any other reach. Deposition remains large in Reaches 5, 6, and 7 and deposition exceeds erosion in all reaches except 1 and 3. The only reaches in which the net storage exceeds the uncertainty in erosion and deposition estimates are Reaches 1 and 5 (Table 3.2). If minimum and maximum error values are propagated in the alongstream accumulation of scour, fill, and storage, the net reach storage of 472 m^3 is dwarfed by the accumulated error of ±1344 m^3 (Figure 3.9). This error estimate is

likely too large, however, because it assumes that the minimum and maximum errors consistently propagate from one reach to the next. In contrast to the net storage, both scour and fill estimates exceed the error bounds in all reaches except for erosion in Reach 6. The cumulative scour and fill for the entire study reach is roughly twice that of the cumulative error in each term (Table 3.2), even using the simple and conservative accumulation of minimum and maximum errors. Both cumulative scour (1454 m^3) and fill (1926 m^3) are significantly larger than the measured sediment flux at the upstream (286 m^3) and downstream (29 m^3) ends of the study reach.

The calculated change in storage computed from the analysis of pre- and post-flood topography is consistent with the imbalance in bed load transport described above. Based on the volumes of sediment scour and fill calculated from DoDs developed for each reach (Figures 3.8), we computed approximately 472 m^3 (± 1344 m^3) of net sediment deposition, resulting from approximately 1454 m^3 (± 796 m^3) of scour and 1926 m^3 (± 1043 m^3) of fill (Table 3.2).

Figure 3.10 depicts the DoDs and associated histograms from Reach 4. To better illustrate the influence that our strategy for quantifying uncertainty has on the detection of topographic change, we used the same topographic inputs to calculate two different DoDs. One DoD – the gross DoD – does not consider uncertainty (Figure 3.10C). The other DoD incorporates the spatially variable uncertainty threshold (Figure 3.10D), that was used to calculate changes in storage in this study. The computed volumes of scour, fill, and net channel change differ substantially between the two DoDs, highlighting the significant effect of uncertainty on the budget calculations. The DoDs shown in (C) and

(D) correspond to histograms (A) and (B), respectively, illustrating the large proportion of the channel where the magnitude of the topographic change did not exceed the defined uncertainty threshold. Areas not included in the budget calculations are primarily those with small elevation change. The impact of the uncertainty analysis on our estimates of change in storage is apparent in the histograms of channel change derived for the DoDs from all seven reaches (Figure 3.10). Distributions from Reaches 2, 3, 5, and 7 are truncated, because small changes were excluded from the analysis due to the more conservative uncertainty threshold applied to the DEMs derived from LiDAR and multispectral imagery.

The error bars bracketing our estimated net change in storage are relatively large (± 1344 m^3; Figures 3.9 and 3.10) because the propagated error estimates are large relative to the modest magnitudes of change that actually occurred (Table 3.2). It should be noted that even though the estimated DEM errors are much larger in the reaches where pre-flood topography was derived from multispectral imagery (Reaches 2, 3, 5 and 7), these errors do not necessarily result in larger estimates of volumetric uncertainty (Table 3.2, column 4). This is because the volumetric error is based only on the areas in the DoDs where the magnitude of channel change exceeded the calculated uncertainty threshold.

4.3 Closure of the sediment budget

With a flux estimate of approximately 260 m^3 of net aggradation and an estimate of change in storage of approximately 470 m^3 of net aggradation, both the change in

storage as determined from bed load transport and from topographic data demonstrate that sediment accumulation occurred during the 2009 flood (Figure 3.11).

5. Discussion

5.1. The Provo River sediment budget

Despite the inevitable uncertainties associated with calculation of each term in a sediment budget, our measurements are consistent with earlier observations that suggest aggradation is occurring. Both estimates of change in storage – as calculated from flux inputs minus export and from topographic measurements of deposition and erosion - show that the study area accumulated sediment during the 2009 flood. The change in storage determined from the direct measurements of sediment flux provides clear evidence of sediment accumulation within the study area. However, had we just constructed a morphological budget, our conclusions would have been indeterminate because the topographic changes that occurred in our system were relatively subtle. *Grams and Schmidt* [2005] pointed out that without faithful accounting of uncertainty, a budget may be considered closed, when in fact, it is indeterminate. Our findings provide a reminder that treatment of uncertainty that is overly conservative may suggest indeterminacy, when in fact there has been net accumulation or evacuation.

The sediment budget presented here also highlights the difference between net change and total change. Although our flux measurements provide a better-constrained estimate of change in storage for the system, they only capture net change in storage, whereas direct measurements of change in storage provide an estimate of both net channel change and total channel change (or channel activity). Calculation of all terms in

the budget reveals that the magnitude of the scour and fill terms is significantly larger than the magnitude of the measured influx and efflux (Figure 3.11). Thus, erosion within the study area (a local supply or input) was a larger contributor of sediment to deposition than sediment influx (an external supply or input). Total change greatly exceeded the magnitude of the net change, indicating that there was significant local reorganization of sediment within each of the reaches.

5.2. Uncertainties and implications for fluvial sediment budgeting

Development of sediment budgets is an essential exercise in geomorphology, used across the discipline in theoretical and applied studies. This study provides some general insights into the challenges and uncertainties associated with developing a reach-scale budget in a fluvial setting. Closing a sediment budget - matching measured changes in storage with calculated differences between inputs and outputs - is a difficult task even in well-constrained settings. Although we attempted to quantify all components of the sediment budget for the Provo River, in some cases the uncertainties associated with different budget terms exceeded the measured value.

Quantification of inputs and outputs is inevitably subject to the uncertainty associated with estimating transport rates. The magnitude of uncertainty that is associated with our estimates of sediment flux is a reflection of the fact that bed load transport rates exhibit great spatial and temporal variability [*Ashmore and Church*, 1998; *Hicks and Gomez*, 2003]. Even under steady flow conditions, bed load transport rates are highly variable [*Davies*, 1987; *Gomez*, 1991]. Bed load transport is also difficult to measure.

The bed load transport predictions we developed for the Provo River represented a significant effort to constrain the estimates of influx and efflux by directly measuring transport rates during a controlled flood, in a system without any supply limitation or hysteresis. Yet despite these efforts and despite the unique sampling opportunity, there is still unavoidable imprecision in our estimates of sediment flux.

In settings where morphologic adjustment is small relative to grain size and widely distributed, the magnitude of erosion and deposition may be detectable but the difference between the two, the net storage, may not be detectable. A standard approach to dealing with uncertainty when determining differences between two DEMs is to establish a minimum level of detection threshold, below which change in elevation is neglected [*Brasington et al.*, 2000]. The approach of *Wheaton et al.* [2010] is an attempt to improve upon this standard approach, by incorporating knowledge of data quality, density, and topographic complexity to refine estimates of uncertainty. Nevertheless, this approach does nothing to constrain or limit uncertainties, but is simply one approach for determining whether the "signal" of topographic change exceeds the associated "noise" [*Milan et al.*, 2011]. In systems where change is subtle and there is substantial uncertainty associated with the strategy used to measure topography, it may not be possible to accurately identify real morphologic adjustments

In the budget presented here, detection of topographic change was also limited by the need to use aerial imagery to generate topography for a portion of the pre-flood channel. The theoretical basis for and application of multispectral and hyperspectral imagery to quantify channel depths is well documented using both empirical and

theoretical approaches [*Winterbottom and Gilvear*, 1997; *Wright et al.*, 2000; *Whited et al.*, 2002; *Legleiter et al.*, 2004; 2009]. The technique performs best in systems where the water is relatively clear, shallow, and free of aquatic vegetation, such as in our study area. However, the DEMs derived from spectral bathymetry provide less accurate representations of channel topography than are the DEMs derived from high-density ground surveys. This increased the threshold of detection in Reaches 2, 3, 5 and 7. Additionally, as demonstrated in Figure 3.10, even in reaches where both the pre- and post-flood DEMs were derived from ground survey data, the uncertainty analysis excluded substantial areas of small deposition and erosion.

Closure of a sediment budget is challenging, because, even when sampling is 'event-based', there are inherent inconsistencies between the time domain of the flux measurements and the time when change in storage can be measured. Morphological sediment budgets are often integrated over many bed-mobilizing floods. We sought to minimize these inconsistencies by calculating a sediment mass balance for a discrete flood event. Although topographic data were collected over the course of more than a year and sediment flux data were only collected over a 3-week period, the dam-controlled hydrology limited bed-mobilizing flows to a single period between the topographic measurements. The controlled dam release presented a relatively unique field opportunity to isolate the erosion and deposition associated with a discrete flood; when integrating over multiple bed-mobilizing flows, the occurrence of compensating scour and fill make it probable that measurements of channel change are underestimates of total channel activity [*Lindsay and Ashmore*, 2002].

In the context of the Provo River sediment budget, we suspect that more accurate measurements would likely amplify the difference between the total volumetric change in storage and the total volume of sediment flux. With higher resolution topographic measurements, smaller topographic changes could be captured in the change-detection algorithm. This would improve our ability to document both total and net channel change. Because compensating scour and fill cannot be measured from before-and-after topography, measured volumetric change will inevitably be an underestimate of total volumetric change. These factors suggest that the magnitude of the erosion and deposition terms may be even larger relative to the influx and efflux terms in the Provo River sediment budget.

The difference between the magnitude of the flux terms and the topographic change terms of the budget has implications for development of sediment budgets in settings elsewhere. In a system in which a simple prediction of net storage is desired, measurement of sediment inputs and export may provide more reliable results. Not only were the erosion and deposition terms in the sediment budget much larger than the flux terms, but their error was much larger than that associated with our measurements of sediment flux. Thus, even when considering the significant uncertainties in estimates of sediment transport, this approach may be a more reliable estimate of net aggradation or degradation. However, in settings in which documenting the spatial distribution of erosion and deposition or the extent of channel activity is important, developing a morphological sediment budget is clearly the preferred approach.

6. Conclusions

We measured all components of a sediment mass balance for a single, dam-controlled flood on a reconfigured gravel bed river. Flow was released from Jordanelle Dam on the Provo River in a fashion that allowed measurements of bed load transport during steady flow at sections above and below the study reach. Detailed topographic data were collected before and after the dam release. Based on transport rate measurements, sediment input to the reach exceeded outputs, producing a net accumulation of sediment of approximately 260 m^3. Based on topographic differencing, the magnitude of total erosion (1454 m^3) and deposition (1926 m^3) was considerably larger than the sediment flux terms, indicating that internal sources and sinks were larger than flux at either upstream and downstream sections. Because the channel had been rebuilt 17 years before the dam release, it is not surprising that internal sources and sinks could exceed the net accumulation from input and output flux. Like the net flux, the difference between the erosion and deposition was positive (470 m^3), although uncertainty in the topographic differencing was larger than the observed net storage.

The findings suggest that when developing sediment budgets for which the primary interest is to quantify net accumulation or evacuation of sediment, measuring sediment flux may provide a useful strategy if appropriate sampling locations can be found. However, calculation of change in storage by subtracting sediment outputs from inputs only provides a measure of net change, not total channel change. The sediment budget developed here demonstrates that the total amount of erosion and deposition can far exceed the influx and efflux from the reach, such that the degree of channel dynamics

may be substantially underestimated by the net input and output to the reach. Although the reach studied here had been rebuilt, such that extensive reworking is not surprising, our work nonetheless suggests that an inference of total channel change from net sediment flux should be verified by observations of channel change within the reach. Direct measurement of changes in storage is necessary in order to accurately determine the total channel change and to describe spatial patterns of morphologic adjustment within a reach.

References

Ashmore, P. E., and M. A. Church (1998), Sediment transport and river morphology: A paradigm for study, in *Gravel-bed Rivers in the Environment*, edited by P. C. Kingman, et al., pp. 115-148, Water Resources Publications, Highlands Ranch, Colo.

Brasington, J., B. T. Rumsby, and R. A. McVey (2000), Monitoring and modelling morphological change in a braided gravel bed river using high resolution GPS based survey, *Earth Surf. Process. Landforms*, *25*(9), 973-990.

Brasington, J., J. Langham, and B. Rumsby (2003), Methodological sensitivity of morphometric estimates of coarse fluvial sediment transport, *Geomorphology*, *53*(3-4), 299-316, doi: 10.1016/S0169-555X(02)00320-3.

Bunte, K., and S. R. Abt (2001), Sampling surface and subsurface particle-size distributions in wadable gravel-and cobble-bed streams for analyses in sediment transport, hydraulics, and streambed monitoring, *Rep. RMRS-GTR-74*, 428 pp, General Technical Report, U.S. Department of Agriculture, Forest Service Rocky Mountain Research Station, Fort Collins, Colo.

Childers, D. (1999), Field comparisons of six pressure-difference bedload samplers in high-energy flow, *Rep. 92-4068*, 59 pp, Water Resource Investigations Report, U.S. Geological Survey Vancouver, Wash.

Davies, T. R. H. (1987), Problems of bed load transport in braided gravel-bed rivers, in *Sediment Transport in Gravel-bed Rivers*, edited by C. R. Thorne, et al., pp. 793-811, Wiley, Chichester.

Edwards, T. K., and G. D. Glysson (1988), Field methods for measurement of fluvial sediment, *Rep. TWRI 3-C2*, Techniques of Water-Resource Investigations U.S. Geological Survey, Reston, VA.

Gaeuman, D., E. D. Andrews, A. Krause, and W. Smith (2009), Predicting fractional bed load transport rates: Application of the Wilcock-Crowe equations to a regulated gravel bed river, *Water Resour. Res.*, *45*(6), W06409, doi: 10.1029/2008WR007320.

Gomez, B. (1991), Bedload transport, *Earth-Science Reviews*, *31*(2), 89-132.

Gomez, B., and M. Church (1989), An assessment of bed load sediment transport formulae for gravel bed rivers, *Water Resour. Res.*, *25*(6), 1161-1186.

Graham Matthews and Associates (2010), Trinity River WY2009 Sediment Transport Monitoring Report, *Rep.*, prepared for Trinity River Restoration Project, prepared for Trinity River Restoration Project, Weaverville, Calif.

Grams, P. E., and J. C. Schmidt (2005), Equilibrium of indeterminate? Where sediment budgets fail: sediment mass balance and adjustment of channel form, Green River downstream from Flaming Gorge Dam, Utah and Colorado, *Geomorphology*, *71*(1-2), 156-181, doi: 10.1016/j.geomorph.2004.10.012.

Ham, D. G., and M. Church (2000), Bed-material transport estimated from channel morphodynamics: Chilliwack River, British Columbia, *Earth Surf. Process. Landforms*, *25*(10), 1123-1142.

Heritage, G., and D. Hetherington (2007), Towards a protocol for laser scanning in fluvial geomorphology, *Earth Surf. Process. Landforms*, *32*(1), 66-74, doi: 10.1002/esp.1375.

Hicks, D. G., and B. Gomez (2003), Sediment transport, in *Tools in Fluvial Geomorphology*, edited by G. M. Kondolf, et al., pp. 425-461, John Wiley and Sons Ltd, Chichester, England.

Kondolf, G. M., and W. V. G. Matthews (1991), Unmeasured residuals in sediment budgets: A cautionary note, *Water Resour. Res.*, *27*(9), 2483-2486.

Kuhnle, R. A. (2006), Prediction of bed load transport on small gravel-bed streams, in *The 7th Int. Conf. on Hydroscience and Engineering*, edited, Philadelphia.

Lane, S. N., K. S. Richards, and J. H. Chandler (1995), Morphological estimation of the time-integrated bed load transport rate, *Water Resour. Res.*, *31*(3), 761-772.

Lane, S. N., R. M. Westaway, and D. M. Hicks (2003), Estimation of erosion and deposition volumes in a large, gravel-bed, braided river using synoptic remote

sensing, *Earth Surf. Process. Landforms*, *28*(3), 249-271, doi: DOI: 10.1002/esp.483.

Legleiter, C. J. (2012), Remote measurement of river morphology via fusion of LiDAR topography and spectrally based bathymetry, *Earth Surf. Process. Landforms*, *37*(5), 499-518, doi: DOI:10.1002/esp.2262.

Legleiter, C. J., and D. A. Roberts (2005), Effects of channel morphology and sensor spatial resolution on image-derived depth estimates, *Remote Sensing of Environment*, *95*(2), 231-247.

Legleiter, C. J., D. A. Roberts, and R. L. Lawrence (2009), Spectrally based remote sensing of river bathymetry, *Earth Surf. Process. Landforms*, *34*(8), 1039-1059, doi: 10.1002/esp.1787.

Legleiter, C. J., D. A. Roberts, W. A. Marcus, and M. A. Fonstad (2004), Passive optical remote sensing of river channel morphology and in-stream habitat: Physical basis and feasibility, *Remote Sensing of Environment*, *93*(4), 493-510.

Lindsay, J. B., and P. E. Ashmore (2002), The effects of survey frequency on estimates of scour and fill in a braided river model, *Earth Surf. Process. Landforms*, *27*(1), 27-43, doi: 10.1002/esp.282.

Marcus, W. A., and M. A. Fonstad (2008), Optical remote mapping of rivers at sub meter resolutions and watershed extents, *Earth Surf. Process. Landforms*, *33*(1), 4-24, doi: 10.1002/esp.1637.

Martin, Y. (2003), Evaluation of bed load transport formulae using field evidence from the Vedder River, British Columbia, *Geomorphology*, *53*(1-2), 75-95.

Martin, Y., and M. Church (1995), Bed-material transport estimated from channel surveys - Vedder River, British-Columbia, *Earth Surf. Process. Landforms*, *20*(4), 347-361.

McCullagh, M. J. (1981), Creation of smooth contours over irregularly distributed data using local surface patches, *Geophysical Analysis*, *13*, 51-63, doi: 10.1111/j.1538-4632.1981.tb00714.x.

Milan, D. J., G. L. Heritage, A. R. G. Large, and I. C. Fuller (2011), Filtering spatial error from DEMs: Implications for morphological change estimation, *Geomorphology*, *125*(1), 160-171, doi: 10.1016/j.geomorph.2010.09.012.

Olsen, D. (2006), Middle Provo River 2005 Monitoring Report, *Rep.* Bio-West, Inc., Logan, Utah.

Reid, L. M., and T. Dunne (2003), Sediment budgets as an organizing framework in geomorphology, in *Tools in Geomorphology*, edited by G. M. Kondolf, et al., pp. 463-500, John Wiley & Sons Ltd., Chichester, England.

Singer, M. B., and T. Dunne (2004), Modeling decadal bed material sediment flux based on stochastic hydrology, *Water Resour. Res.*, *40*(3), doi: 10.1029/2003WR002723.

Surian, N., L. Mao, M. Giacomin, and L. Ziliani (2009), Morphological effects of different channel-forming discharges in a gravel-bed river, *Earth Surf. Process. Landforms*, *10*, doi: 10.1002/esp.1798.

Topping, D. J., D. M. Rubin, and L. E. Vierra Jr. (2000), Colorado River sediment transport 1. Natural sediment supply limitation and the influence of Glen Canyon Dam, *Water Resour. Res.*, *36*(2), 515-542.

Trimble, S. W. (1983), A sediment budget for Coon Creek basin in the Driftless Area, Wisconsin, 1853-1977, *American Journal of Science*, *283*(5), 454.

Utah Reclamation, Mitigation, and Conservation Commission (1997), Provo River Restoration Project Final Environmental Impact Statement, *Rep.* U.S. Department of the Interior, Salt Lake City, Utah.

Valle, B. L., and G. B. Pasternack (2006), Field mapping and digital elevation modelling of submerged and unsubmerged hydraulic jump regions in a bedrock step-pool channel, *Earth Surf. Process. Landforms*, *31*(6), 646-664.

Vericat, D., and R. J. Batalla (2006), Sediment transport in a large impounded river: The lower Ebro, NE Iberian Peninsula, *Geomorphology*, *79*(1-2), 72-92, doi: 10.1016/j.geomorph.2005.09.017.

Wallick, J. R., S. W. Anderson, C. Cannon, and J. E. O'Connor (2009), Channel change and bed-material transport in the lower Chetco River, Oregon, *Rep. 2010-5065*, 83 pp, Scientific Investigations Report, U.S. Geological Survey, Reston, Va.

Wathen, S. J., and T. B. Hoey (1998), Morphological controls on the downstream passage of a sediment wave in a gravel bed stream, *Earth Surf. Process. Landforms*, *23*(8), 715-730.

Wheaton, J. M., J. Brasington, S. E. Darby, and D. A. Sear (2010), Accounting for uncertainty in DEMs from repeat topographic surveys: Improved sediment budgets, *Earth Surf. Process. Landforms*, *35*(2), 136-156, doi: 10.1002/esp.1886.

Whited, D., J. A. Stanford, and J. S. Kimball (2002), Application of airborne multispectral digital imagery to quantify riverine habitats at different base flows, *River Res. and Applications*, *18*(6), 583-594.

Wilcock, P. R. (2001), Toward a practical method for estimating sediment-transport rates in gravel-bed rivers, *Earth Surf. Process. Landforms*, *26*, 1395-1408.

Winterbottom, S. J., and D. J. Gilvear (1997), Quantification of channel bed morphology in gravel-bed rivers using airborne multispectral imagery and aerial photography, *Regulated Rivers: Res. & Management*, *13*(6), 489-499.

Wright, A., W. A. Marcus, and R. Aspinall (2000), Evaluation of multispectral, fine scale digital imagery as a tool for mapping stream morphology, *Geomorphology*, *33*(1-2), 107-120.

Table 3.1. Mean daily discharge and stage for USGS Gage 10155500, Provo River near Charleston for days with aerial photography or ground surveys. The absolute difference in the stage on the date of the air photo flight and the date of the ground surveys ranges from 0.5 to 5.4 cm.

	Date	Q (m^3s^{-1})	Stage (m)	Difference in stage (m)
Aerial photography flight	9/23/2008	6.43	1.173	--
Ground surveys				
Longitudinal profile	10/12/2008	6.60	1.181	-0.008
Reach 1	9/12/2008	7.65	1.227	-0.054
Reach 1	9/17/2008	6.12	1.158	0.015
Reach 4	10/6/2008	6.31	1.167	0.005
Reach 4	10/7/2008	6.23	1.163	0.009
Reach 6	9/26/2008	6.09	1.156	0.016
Reach 6	9/27/2008	6.03	1.155	0.019
Reach 6	9/28/2008	6.06	1.155	0.018
Reach 6	10/3/2008	5.58	1.131	0.042
Reach 6	10/4/2008	5.86	1.145	0.028
Reach 6	10/5/2008	6.31	1.167	0.005

Table 3.2. Calculated change in storage for all seven reaches. Scour, fill, net change in storage, and cumulative downstream change in storage were determined from the DEMs of Difference (DoDs). Relative change in storage is net volumetric change divided by reach area.

Reach	Scour (m^3)	Fill (m^3)	Net Storage (m^3)	Cumulative Storage (m^3)	Reach Area (m^2)	Relative Change in Storage (m^3/m^2)
1	122 (± 22)	51 (± 43)	-71 (± 49)	-71 (± 49)	4376	-0.016
2*	172 (± 51)	208 (± 87)	36 (± 100)	-35 (± 149)	10170	0.004
3*	303 (± 200)	283 (± 126)	-20 (± 237)	-55 (± 386)	19573	-0.001
4	311 (± 190)	440 (±293)	129 (± 349)	74 (± 735)	10972	0.012
5*	106 (± 30)	306 (± 135)	200 (± 139)	274 (± 874)	16752	0.012
6	183 (± 223)	348 (± 255)	165 (± 339)	439 (± 1213)	10692	0.015
7*	257 (± 80)	290 (± 104)	33 (± 131)	472 (± 1344)	13514	0.002
1+4+6	616 (± 435)	839 (± 591)	223 (± 737)	NA	26040	NA
∑1-7	**1454 (± 796)**	**1926 (± 1043)**	**472 (± 1344)**	**NA**	**86059**	**NA**

* pre-flood topography determined using surveyed water surface elevation and water depth estimated from aerial photography

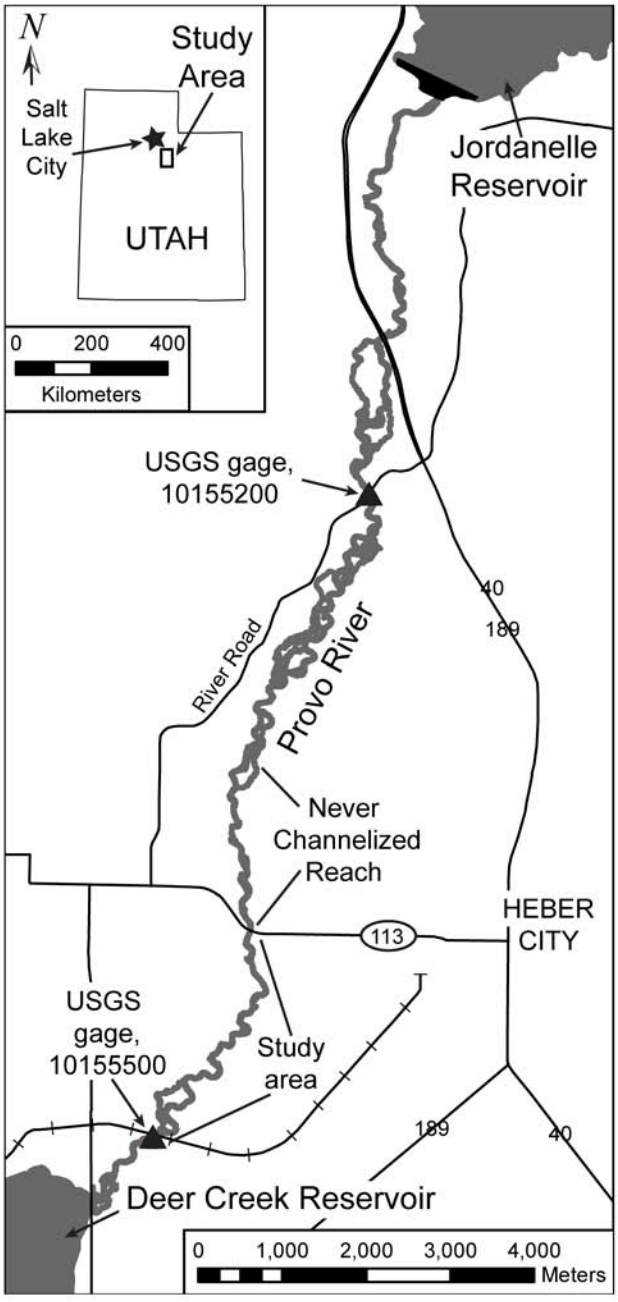

Figure 3.1. The middle Provo River, located in Heber Valley, Utah. The river flows approximately 19 km from the outlet of Jordanelle Dam (upper right) to Deer Creek Reservoir (lower left). The entire channel was reconfigured as part of the Provo River Restoration Project, with the exception of the Never Channelized Reach (NCR). Today, the NCR provides a local source of sediment to the study area.

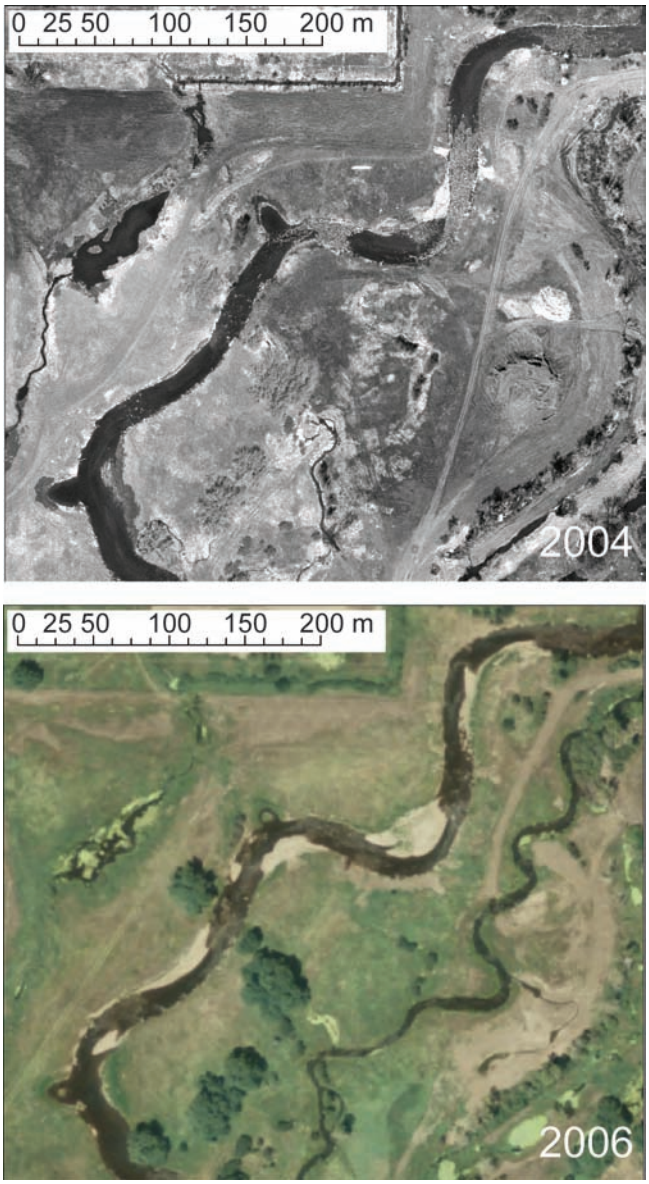

Figure 3.2. Aerial photos of Reach 4 taken in (A) 2004 and (B) 2006. The 2004 image, (A), was taken shortly after reconfiguration of this reach. Image (B) depicts point bars that grew during floods in 2005 and 2006. The location of the reach is shown in Figure 3.3.

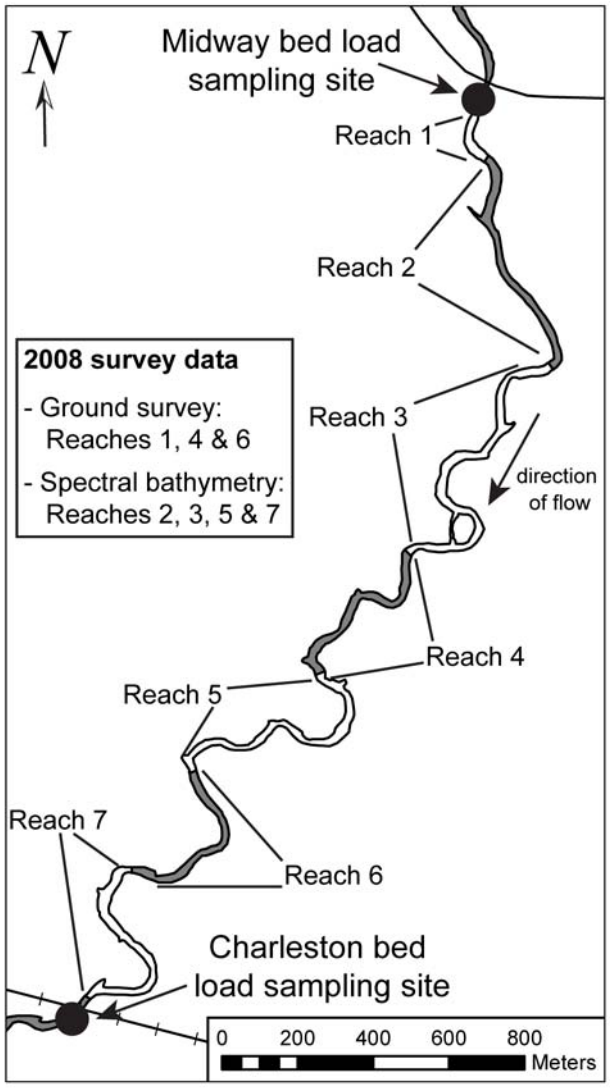

Figure 3.3. The study area: the lower 4-km of the Provo River Restoration Project (PRRP). A local sediment source, provided by the Never Channelized Reach (NCR), is located immediately upstream of the Midway sampling site (Figure 1). In 2009, we measured bed load transport at the upstream (Midway) and downstream (Charleston) sampling sites. Morphologic change associated with the 2009 flood was measured in each of the study reaches.

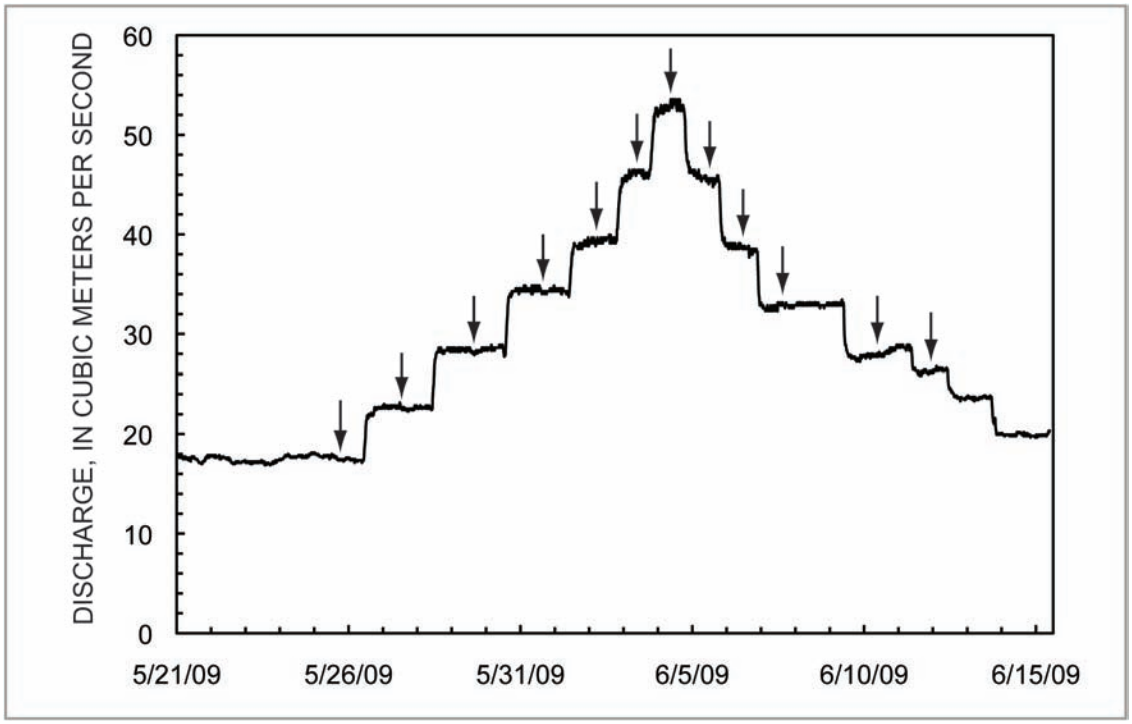

Figure 3.4. The 2009 flood hydrograph measured at USGS gage 10155500, Provo River near Charleston. We selected the stair-step pattern to facilitate measurement of bed load transport rates. The flow was increased or decreased by approximately 5.7 m^3s^{-1} increments, and was held constant for 1 – 2 days at each discharge. Arrows indicate days when we sampled bed load transport.

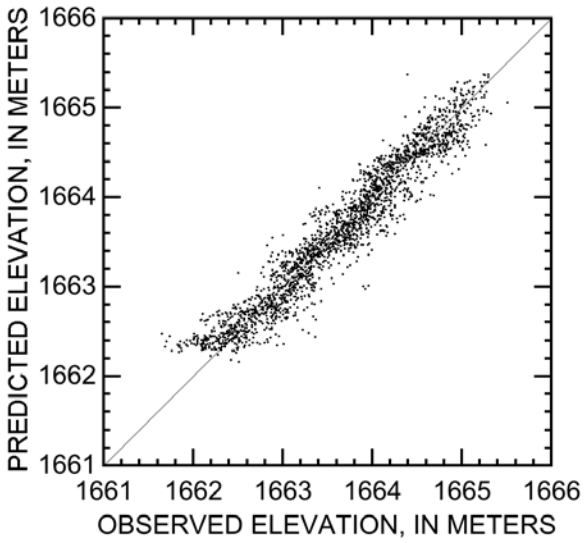

Figure 3.5. Relation between measured bed elevations and elevations derived from spectrally based bathymetry. Data is from Reach 4, the reach used to develop the multivariate regression (equation (3)). The multivariate regression was used to model flow depths. Bed elevations were obtained by subtracting the spectrally derived depths from the water surface profile.

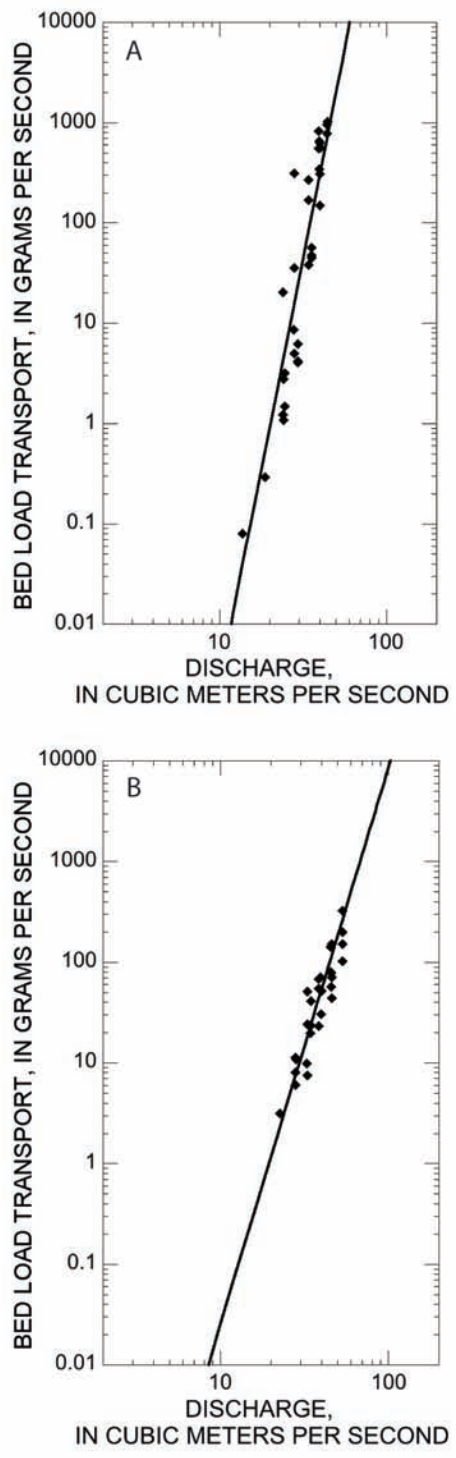

Figure 3.6. Bed load transport rates at Midway (A) and Charleston (B). Diamonds indicate field measurements of bed load transport collected during the flood in 2009. The lines represent the sediment rating curves.

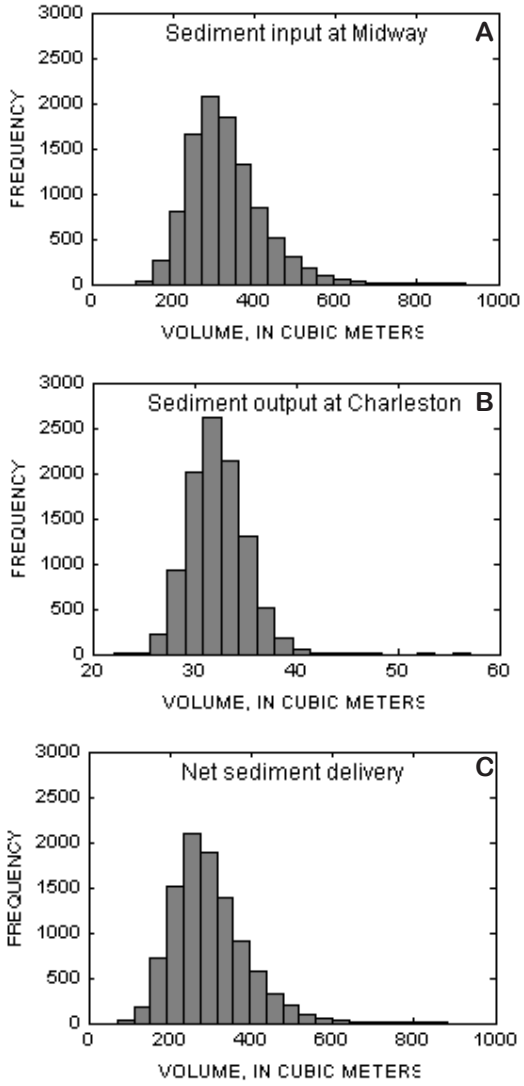

Figure 3.7. Estimated sediment influx (A), efflux (B), and net sediment accumulation (C). The median value of each distribution represents our best estimate of sediment flux or net accumulation.

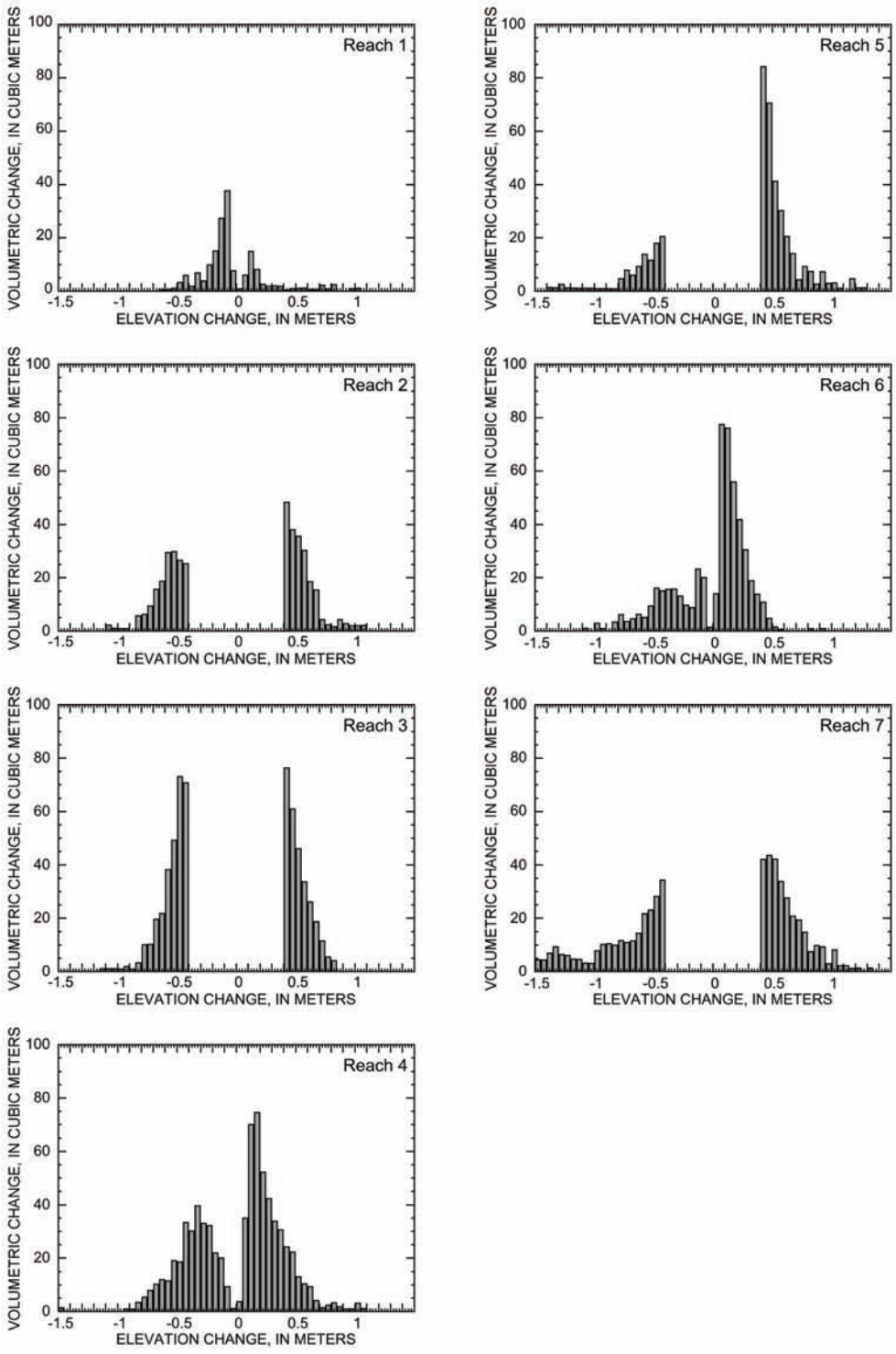

Figure 3.8. Volumetric change in storage for each reach calculated from the DEMs of difference (DoDs).

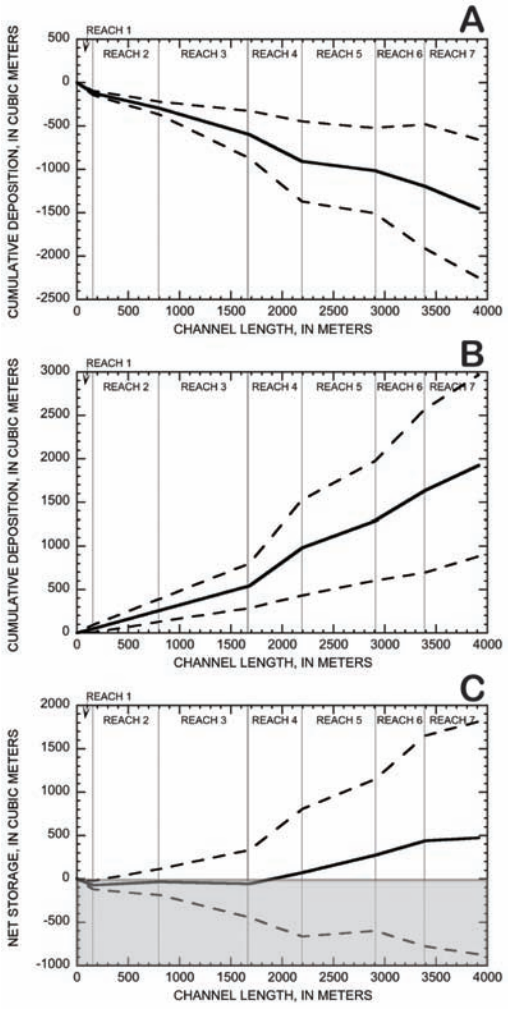

Figure 3.9. Cumulative scour (A), fill (B), and net sediment storage (C) in the study area, based on the analysis of the topographic data. The dashed lines represent the cumulative uncertainty.

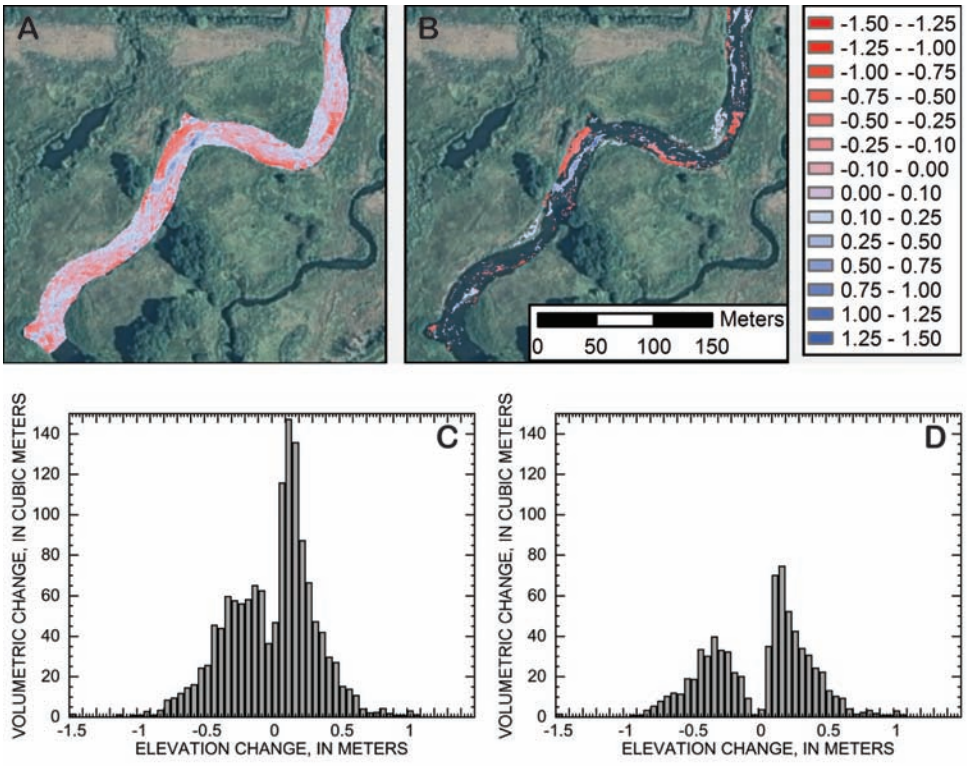

Figure 3.10. Volumetric change in storage for Reach 4 computed from (A) the gross DoD and (B) the DoD calculated using the spatially variable approach for quantifying uncertainty, as described in the methods. Image (C) depicts a histogram computed from the gross DoD, corresponding to (A); (D) depicts a histogram computed from the DoD calculated using the spatially variable uncertainty threshold (B).

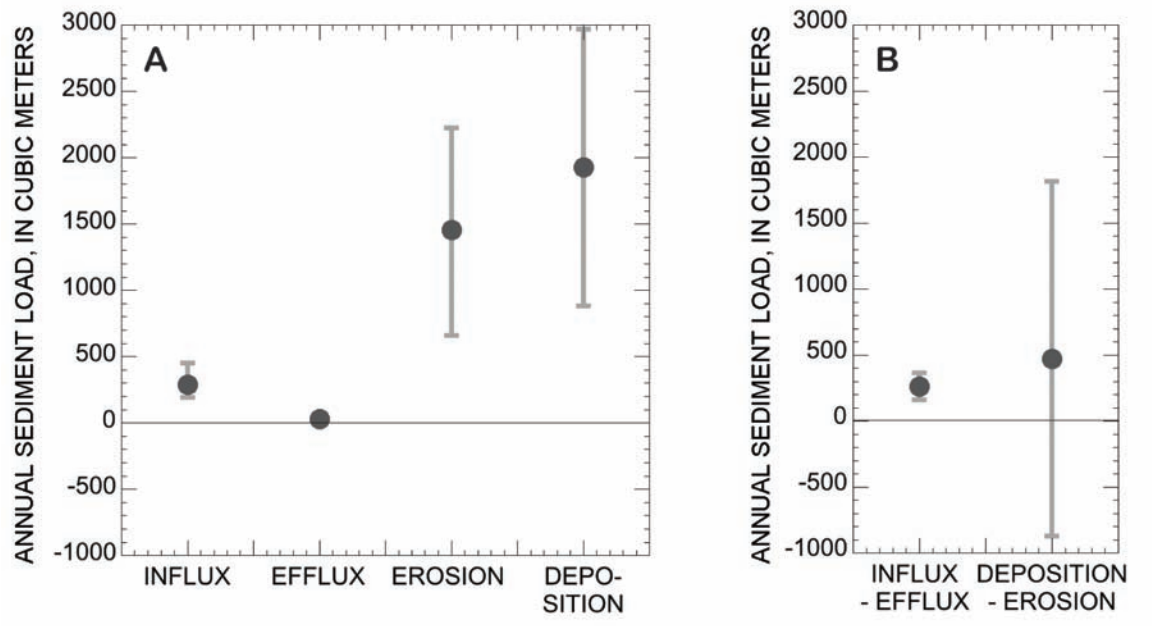

Figure 3.11. The sediment budget for the 2009 flood. (A) presents the four measured components of the budget: estimated influx and efflux (calculated from the sediment rating curves), and deposition and erosion (determined from topographic measurements). (B) depicts the change in storage computed from each of these components of the budget.

CHAPTER 4

INFLUENCE OF SEDIMENT SUPPLY ON POINT BAR MORPHOLOGY IN A LABORATORY

1. Introduction

Point bars, the bank-attached bars that occur on in the inside of a river bend, are a defining feature of meandering rivers. Although termed 'fixed' bars, because they do not migrate within the active channel, point bars are a dynamic component of sediment transport and storage within alluvial rivers. Point bar growth, and the accompanying erosion that occurs on the opposing outer bank, drives meander migration, floodplain formation, and determines the physical characteristics of aquatic habitat in meandering rivers.

Point bars develop via an adjustment amongst cross-section area, channel planform, bed topography, and bed grain size. Although patterns of flow and transport through bends have been long studied in both steady-state sand-bed [e.g. *Dietrich and Smith*, 1984] and steady-state gravel-bed channels [e.g. *Dietrich and Whiting*, 1989; *Julien and Anthony*, 2002; *Clayton and Pitlick*, 2007], there is far less known about the dynamic responses of point bars to changes in the driving factors of flow and sediment supply. This situation stems in part from the fact that, until recently, meandering channels have been difficult to create in flume settings [*Tal and Paola*, 2007; *Braudrick et al.*, 2009], which has limited experimental investigations of flow in bends. Field scale observations of point bar response to changes in sediment supply have largely been

limited to planform adjustment occurring over multiple bends [*Lewin*, 1976; *Nanson*, 1980].

When sediment supply to a point bar in steady-state is changed, the transport capacity of the river must adjust as the system evolves to a new steady state. The bed response can include changes in bed grain size [*Dietrich et al.*, 1989; *Buffington and Montgomery*, 1999; *Lisle et al.*, 2000; *Eaton and Church*, 2009] or changes in bed topography. For example, increased transport capacity may be achieved through a fining of the bed material, through deposition on the point bar or in the adjacent pool resulting in constriction and increased flow velocity, or through topographic adjustments that increase the variability in the boundary shear stress [*Paola*, 1996; *Ferguson*, 2003]. These changes may occur over relatively short time scales in flume experiments in which channel boundaries lack the cohesion of natural channels [*Eaton and Church*, 2004] or when alternate bars develop in straight flumes [*Lisle et al.*, 1997; *Madej et al.*, 2008]. Over longer time scales, channel planform or gradient can adjust to accommodate changes in sediment supply. Bank migration in rivers with cohesive banks can produce an increased transport capacity by adjusting channel slope. In this work, we use a channel with a constant planform and focus on shorter time-scale, in-channel adjustments.

We report here on the response of point bar topography to a change in sediment supply in a field-scale laboratory meander with a bed of gravelly sand. Following an initial run with a degraded bed with no sediment supply, we conducted two runs with a constant sediment supply and an intervening run with a sediment rate five times larger. We observed the adjustment of a full-scale point bar to different sediment supply rates as

well as the development of the point bar under both aggradational and degradational conditions. We collected high-resolution topography of the bed at the end of each run as well as cross-section topography during the transient response to changing sediment supply. This study is the first of which we are aware that documents point bar evolution in response to changing sediment supply in a field scale meander. Our results provide insight into the mechanisms of bar formation and suggest a conceptual model for bar response to changing sediment supply.

2.0. Experimental facility – the Outdoor Stream Lab

Our point bar experiment was conducted in the Outdoor StreamLab (OSL) of the St. Anthony Falls Laboratory at the University of Minnesota (Figure 4.1). The OSL is a unique facility, providing the opportunity to conduct field-scale experiments within a controlled setting [*Orr and Lightbody*, 2009]. It was constructed in an abandoned flood bypass channel along the Mississippi River, and occupies a 40 m by 20 m rectangular basin. The central feature of the OSL is a meandering channel approximately 2.5 m wide, 50 m long, and 0.3 m deep at bankfull flow. During channel construction, and at the time of the experiment presented here, the banks were reinforced with coconut-fiber matting to provide stability until riparian vegetation became well-established.

The experiment presented here focuses on the central bend of the channel, which has a meander wavelength of approximately 25 m and a sinuosity of 1.3. Cobble riffles are located upstream and downstream from the central meander bend. Bed material is more generally a mixture of sand and fine gravel. A constant feed rate is supplied by an auger system at the head of the channel and sediment is recirculated from a settling basin

at the downstream end of the channel. The median grain size of the material in transport during the experiment was 0.7 mm (Figure 4.2).

3.0. Methods

3.1. Experimental setup

The experiment consisted of three runs. Runs 1 and 3 used a feed rate of 4 kg min^{-1} and Run 2 used a sediment feed rate of 20 kg min^{-1}. The final bed geometry in each run provided the initial conditions for the next run. A preparatory run, which we refer to as Run 0, was conducted with no sediment feed, allowing the channel to evacuate most of the mobile sediment and erode the point bar. Thus, we could compare equilibrium point bars at a feed rate of 4 kg min^{-1} that had resulted from both aggradational (Run 1) and degradational (Run 3) processes.

Each run used a constant bankfull discharge of approximately 285 L s^{-1}. We held sediment feed constant during each run until quasi-steady-state conditions were reached. Because several days were required to reach steady-state, runs were divided into segments, with one segment per day. Between segments, we turned the sediment feed off and returned the discharge to base flow. The duration of a given run segment was limited by the feed rate during the run and the speed with which we could return sediment to the feed hopper. Thus, during the period of high feed in Run 2, segment durations were limited to approximately two hours, because sediment was fed out of the hopper much more rapidly than it could be replenished by the recirculation system.

3.2. Sediment input and export

Sediment delivery to the stream was controlled by adjusting the speed of an auger located in the sediment feed tank at the upstream end of the experimental basin (Figure 4.3a). We regularly sampled sediment feed rate by temporarily diverting the sediment feed into a bucket. We manually adjusted the auger speed to maintain constant delivery rates of sediment to the channel. A subset of the feed samples was returned to the lab for sieving to determine grain size distribution. Sediment from the settling basin at the downstream end of the channel (Figure 4.3b) was returned via suction hose directly to the sediment feed tank, and it was not possible to mix sediment from the settling basin. Because sediment in the settling basin was well-sorted, stratification of grains within the feed tank was influenced by the local grain size distribution of the location where sediment was being removed from the settling basin. Figure 4.2 provides some indication of the variability in the grain size of the sediment feed. Each input and output grain size distribution in Figure 4.2 presents the mean of 4 – 10 samples collected on a single day. Averaged over several days, the sediment had a grain size distribution that approximated the mean, but from hour to hour, there was significant variation in the grain size of the sediment feed.

Sediment output from the channel was computed by surveying the volume of sediment collected in the settling basin. The settling basin was partitioned into three bays, and we alternated which bay was collecting sediment in order to determine sediment efflux during a known period of time. Accumulated sediment was surveyed using a total station. To convert sediment volume to mass, we measured bulk density of the sediment

by oven drying and weighing sediment samples. We also sieved samples to determine the grain size distribution.

We calculated uncertainty for the rate of sediment feed of each run segment by calculating the 95 percent confidence interval of the distribution of mean transport rates each day. We used a bootstrap analysis to assess the uncertainty associated with measured sediment volumes in the settling basin, and thus, the calculated sediment output. For each survey of sediment that had accumulated in the settling basin, we calculated the volume from 100 random subsamples of the survey points, each of which contained 75% of the total number of survey points and included random horizontal and vertical uncertainties of up to 5 cm and 2 cm, respectively. The uncertainty for each surveyed volume was assumed to be equal to the standard deviation of the 100 simulated volumes.

Run 0 (no sediment feed) ran for 31 hours and was divided into over three segments. The run was terminated when sediment scour began to undermine the channel banks along the outside of the bend. Although mobile sediment remained in the channel bed, the bed elevation was deflated below the pre-existing topography.

Run 1, the low feed aggradational run, consisted of 11 segments and 95.5 total hrs of run time. Feed rate during Run 1 was 3.9 ± 1.6 kg min^{-1} (Table 4.1; Figures 4.4 and 4.5). The sediment feed rate was most variable during the first five segments of the run, with individual feed measurements varying by up to 500% of the mean feed rate. During six of the remaining seven days of the run, sediment feed was more consistent and was maintained within 25% of the specified feed rate. Sediment output during segments 1 – 9

of Run 1 averaged 1.0 kg min^{-1} (± 0.1). During segments 10 and 11, the sediment export rates were 4.5 ± 1.0 kg min^{-1} and 2.1 ± 1.3 kg min^{-1}, respectively. Thus, sediment efflux increased during the run, approaching the rate of sediment input, and confirmed our visual observations that the channel was approaching steady-state. The mass storage indicated by the difference between input and output is discussed below in the context of a mass balance.

Run 2 consisted of 7 segments of approximately 2 hours each with a total run duration of 14.2 hrs. The feed rate in Run 2 was 20 ± 2.0 kg min^{-1}, and sediment feed rate was maintained within 22% of the specified value. Sediment output rates increased consistently in segments 3 – 6. Sediment export during the last two segments of Run 2 were 13.3 ± 1.8 kg min^{-1} and 12.0 ± 1.4 kg min^{-1}, respectively, as compared with average sediment input rates of 20.2 ± 0.6 kg min^{-1} and 19.6 ± 0.6 kg min^{-1}.

Run 3 consisted of 8 segments with a total run duration of 63.2 hours. The sediment feed rate in Run 3 was 4.4 ± 0.5 kg min^{-1}, and sediment feed rate was maintained within 32% of the specified value. Although larger than the feed rate in Run 1, the measured difference between the mean feed rates in Run 1 and Run 3 was not statistically significant ($p > 0.05$, $n = 213$). Large sediment output rates corresponding to the aggraded state of Run 2 persisted during the first two run segments of Run 3 and then remained relatively stable at a value near the input rate for the remainder of the run.

3.3. Sediment mass balance

Sediment accumulation occurred not only in the study bend, but in the channel upstream and downstream from that bend, as well as in a short section between the channel and the stilling basin. We developed a sediment mass balance that accounted for the several sources and sinks of sediment within the channel (Table 4.2; Figure 4.6). The changes in storage determined from measured inputs minus outputs were 6.5 m^3, 5.5 m^3, and -1.4 m^3, during Runs 1, 2, and 3, respectively. The changes in storage determined from measured and estimated volumes of sediment deposition and erosion were 5.1 m^3, 4.2 m^3, and -3.0 m^3, for Runs 1, 2, and 3, respectively. Thus, estimated change in storage determined from deposition and erosion in the channel was consistently 1.5 m^3 smaller than the change in storage calculated from the known input and output, indicating that some deposition in parts of the channel beyond the center was must be underestimated. Changes in storage in the middle bend were precisely measured (described in section 3.4), and values were 0.7 m^3, 1.7 m^3, and -1.6 m^3, during Runs 1, 2, and 3, respectively. Thus, the middle bed accumulated substantially more sediment during the high feed run (Run 2) than the aggradational low feed run (Run 1). When we reduced the sediment feed in Run 3, approximately the same volume of sediment was evacuated from the bend as had been deposited during Run 2.

3.4. Topographic data

We collected high-resolution topographic data throughout the study meander bend at the end of each run. We used a data acquisition cart system that was equipped with instrumentation (laser and sonar) to measure channel topography, bathymetry, and water

surface elevation to within sub-centimeter accuracy to create a 1-cm by 1-cm grid over a 7.5-m by 2-m area. The cart was manually placed at a series of overlapping positions along the channel. We established the precise location of the cart at the beginning of each scan by surveying the location of four monumented benchmarks that were positioned under the cart. We filtered the data collected at each cart position to remove bank vegetation and erroneous data points. Data from each cart position was interpolated to a common grid.

For the purposes of calculating topographic metrics along the length of the bend, we converted topographic data from a Cartesian (x, y) to a channel-fitted (s, n) coordinate system using the methods of *Legleiter and Kyriakidis* [2006]. At 5-cm intervals along the channel centerline, we computed the maximum, minimum, and mean elevation in the cross-stream direction (n-coordinate). At each interval, we also calculated the channel relief, defined here as the difference between the maximum and minimum elevations along each cross section. When calculating each of these metrics, we excluded the banks from the analysis because the bank values were unchanging and our focus is within-channel topography.

Topographic data acquired using the cart system provided documentation of quasi-steady-state conditions at the end of runs. To capture transient adjustments as channel morphology evolved, we established five monumented cross-sections, along which topography and water surface were measured (Figure 4.7). The five cross-sections were evenly spaced approximately 1.5 m apart along the channel centerline, and metal framing remained in place at each cross-section through the experiment. Water surface

and bed elevation were measured at 20-cm intervals along the cross-sections using a manual point gage. We measured bed elevation 22 to 25 times during each run. Water surface elevations were measured 1 to 3 times.

Analysis of sediment output rate, as determined by the tailbox surveys, was not performed until the experiments were complete. Thus, it was not possible to assess whether steady-state conditions had been reached based on relative rates of sediment influx and efflux. Instead, we relied on cross-section topography to inform decisions regarding whether the channel had reached steady-state, because these data could be rapidly collected and analyzed. A run was concluded when several repeat cross-section surveys indicated that progressive topographic changes had ceased.

3.5. Velocity measurements and hydraulic modeling

Before ending the run, we collected point velocity measurements using an acoustic doppler velocimeter (ADV). The ADV was mounted on a horizontal metal traverse that spanned the channel, which allowed velocity to be measured at multiple locations across the channel. We measured velocity along the cross-sections at multiple vertical stations, including one near the bed and at least one higher in the water column. The number of vertical stations depended on the depth of the channel and the amount of time available during the run to measure velocity. In some locations, small dunes of 1-3 cm height migrated past a point with a period of two to five minutes. Thus, we measured velocity at each point for at least 5 minutes to ensure that our measurements were averaged over the passage of dunes.

It was not feasible to comprehensively measure and characterize the distribution of velocities throughout the bend at the end of each run. Thus, we used the measured data to calibrate a two-dimensional hydraulic model, which provided estimates of water surface elevation, flow depth, vertically average velocity, and boundary shear stress throughout the bend. We used the Flow and Sediment Transport for Morphological Evolution of Channels (FaSTMECH) numerical model [*Nelson et al.*, 2003]. Given inputs of channel topography, discharge, and roughness, FaSTMECH numerically solves the vertically-averaged and Reynolds-averaged momentum equations along a curvilinear grid. The model has been used previously in numerous field and experimental settings [e.g. *Lisle et al.*, 2000; *Kinzel et al.*, 2009; *May et al.*, 2009; *McDonald et al.*, 2010; *Harrison et al.*, 2011; *Legleiter et al.*, 2011].

We calibrated FaSTMECH to the observed water surface elevation by adjusting the roughness, as specified by a drag coefficient, and verified the simulations using the point velocity measurements. There were only negligible differences in the model results from Runs 1 and 3, because the topographic inputs were very similar. Thus, we only present the results from Runs 1 and 2 here. To calibrate Run 1, we used water surface elevations provided by the data acquisition cart (Figure 4.8a). For Run 2, the short duration of the run segments required that we use water surface elevations measured with a point gage along the cross-sections (Figure 4.8b). Point velocity data indicate that the calibrated model did a good job simulating depth-averaged flow through the bend (Figure 4.9).

4.0. Results

4.1. Topographic adjustments

Run 0 used no sediment feed and was stopped when the bed had deflated well below the steady state surface anticipated for Run 1. A deep pool occupied most of the bend upstream of the bend apex (Figure 4.10). The remnant point bar was submerged at bankfull flow and an inner bend chute was present between the inside of the bar and the floodplain. Lateral variability in topography occurred primarily through the bend apex, in association with the remnant point bar. The surface of the bar was covered with fine gravel and sand. Pea gravel was concentrated above its proportion in the bulk mix in the pool and along the outside of the bend downstream from the bar.

The increased sediment supply in Runs 1 and 2 took several hours to reach the bend. When the sediment supply arrived in the bend, channel adjustments proceeded rapidly as the morphology evolved to accommodate the increase in supply. Most of the topographic adjustment occurred over approximately 9 hrs in Run 1 and 4 hr in Run 2, periods corresponding to approximately 2200 kg of additional sediment supply in Run 1 and 4800 kg of additional sediment supply in Run 2. After the initial topographic adjustment, smaller topographic fluctuations persisted due to the migration of dunes and bed load sheets, but little progressive topographic adjustment occurred. Figure 4.11 depicts all cross-section topographic profiles, highlighting the initial and final profiles for comparison with Figure 4.10, as well as the transient adjustments.

In Run 1, the initial bed response was deposition in the pool (Figure 4.12). As the pool aggraded, small dunes developed and migrated up onto the bar. The dunes were one

cm to three cm in height, with spacing of 10 cm to 40 cm. The dunes were oriented in the alongstream direction and had a short wavelength (approximately 10 cm) when they initially appeared in the pool (Figure 4.13a). Dune orientation gradually shifted as the dunes climbed the bar until they were nearly perpendicular to the alongstream direction near the bar crest. The bar maintained approximately the same transverse slope angle as the pool filled, and the bar expanded laterally as sediment accreted onto the bar with passage of the dunes. After increasing in width, the bar began to extend longitudinally. Additionally, following the initial accumulation of sediment in the pool, deposition occurred along the outer bank downstream from the bend apex. This deposition diminished cross-stream topographic relief, resulting in a plane bed morphology through the downstream half of the bend (Figures 4.10 and 4.11). Dunes crests were oriented perpendicular to the alongstream direction through the plane bed portion of the channel.

Topographic adjustment during Run 1 involved initial inflation followed by deflation in the upstream half of the bend (Figures 4.11 and 4.12). Sediment deposition first occurred in the pool, followed by bar growth. Subsequent to these initial changes, some of the freshly deposited sediment in the pool and on the bar was evacuated. Comparison of the steady state topography from the ends of Run 0 and Run 1 (Figure 4.10) shows that the point bar expanded laterally and longitudinally, although the final elevations of the bar top and pool were lower than the maximum elevations observed during transient conditions (Figure 4.11). For example, there was 10 – 15 cm of deposition on the bar crest during segment 2 of Run 1, but the final maximum elevation of the bar surface was close to that at the beginning of the run. Similarly, the deepest

portion of the pool did not fill significantly. Deposition over the full course of Run 1 consisted of an expansion of the areal extent of high elevation portions of the bar and contraction of the deepest parts of the pool (Figure 4.10). Although the bar expanded laterally towards the inner bank, the chute at the inside of the bar persisted throughout Run 1 and never become fully attached to the bank. The downstream portion of the bend maintained little lateral topographic variation throughout Run 1 (Figure 4.11).

With an increase in sediment feed rate to 20 kg/min in Run 2, the initial topographic response was deposition in the pool, as observed in Run 1 (Figures 4.10 and 4.12). Again, pool deposition triggered dune migration from the pool on to the bar, producing lateral expansion of the bar. The migrating dunes were similar to those in Run 1, one cm to three cm in height, with spacing of 10 cm to 40 cm. Lateral expansion of the bar was particular pronounced in segment 3, approximately 2 hours after the increased sediment supply reached the bend. Lateral expansion of the bar was accompanied by an increase in maximum bar elevation and sediment deposition in the chute along the inner bank. As the chute filled, the bar extended longitudinally and the bar crest migrated towards the inner bank. Downstream from the bar apex, deposition occurred primarily along the inner bank, resulting in increased lateral relief through the downstream half of the bed (Figures 4.11 and 4.12). Unlike Run 1, aggradation in the upstream half of the bend during Run 2 persisted throughout the run, with no degradation following development of the maximum topography.

Comparison of steady state topography from Runs 1 and 2 (Figures 4.10 and 4.14) show that the larger sediment feed produced a longer, taller, and wider bar. The

maximum elevation of the bar grew approximately 10 – 15 cm, and the chute on the inside of the bend filled, attaching the point bar to the inside bank. The downstream portion of the bend, which was a plane bed during Run 1, developed more lateral topography due to downstream extension of the bar along the inner bank. Additionally, the pool filled substantially, with an increase in minimum bed elevation of 20 cm. The grain size of the bed surface through the outer portion of the bend also became finer (Figure 4.13). Visual observations indicated a decrease in the concentration of pea gravel such that the grain size distribution on the pool surface more closely matched that of the adjacent bar and the downstream part of the bend.

With a return to the lower sediment feed rate of 4 kg/min in Run 3, sediment evacuation began in the pool during the first run segment (Figure 4.12). As the pool scoured, sediment was progressively evacuated from the downstream portion of the channel, along the outer bank, and the outer flank of the bar. As the bar width decreased, we observed a reduction in the width of the flat bar top. This was followed by a shift outward in the location of the bar crest and the reemergence of the chute along the inner bank. The effect of chute scour was to detach the bar from the bank. These changes resulted in subsequent sediment evacuation at the bar head.

The steady state bar-pool morphology observed at the end of Run 3 was very similar to that of Run 1 (Figure 4.10). Reducing the sediment feed caused the bar to deflate, decreasing bar width, depth and length, and the inner bar chute reappeared. Pool depths and pool area also returned to a configuration like that of Run 1, and the downstream half of the bend resumed the low-relief plane bed configuration (Figure

4.11). Thus, the same bend topography was created for the same sediment feed rate under both aggradational and degradational conditions. Additionally, qualitative observations of the bed indicate that the coarse lag deposit present on the bed during Run 1 returned during Run 3. The primary difference between the topography of Runs 1 and 3 was that the bar extended further upstream by approximately 15 cm and was slightly narrower in Run 3 (Figures 4.10 and 4.14). Additionally, in Run 3 the deepest portion of the pool was located just downstream of the location of the deepest part of the pool in Run 1.

Topographic variability was smaller at the end of Run 2 (high sediment feed rate) relative to that at the end of Runs 1 and 3 (low sediment feed rate). Alongstream variation in maximum, minimum, and mean bed elevation was smaller in Run 2 than in Runs 1 and 3 (Figure 4.15). During Run 2, we observed a nearly uniform increase in maximum elevation along the length of the channel in response to the increased sediment supply (Figure 4.15a). In contrast, minimum elevation increased substantially upstream of the bend apex, due to pool filling, but did not increase in the downstream portion of the channel (Figure 4.15b). These topographic changes resulted in a somewhat smaller lateral relief through the upstream half of the bend in Run 2, where pool filling exceeded bar deposition (Figure 4.15d). Downstream of the bend apex, relief was consistently larger in Run 2, because the bar expanded downstream while there was little change in elevation along the outer bank.

4.2. Hydraulic adjustments

FaSTMECH predictions of water surface elevation, depth, flow speed, and boundary shear stress through the bend are depicted in Figure 4.16 and vector fields of velocity and boundary shear stress are given in Figure 4.17.

In Run 1, the simulated flow captures the water surface superelevation along the outside of the bend, beginning at the tail of the pool. At the upstream end of the bar, the water surface increased slightly as flow depths decreased at the bar head. This shoaling of the flow onto the bar resulted in a water surface elevation that was level in the cross-stream direction at the upstream end of the bar. Velocities in Run 1 were greatest at the entrance to the bend in the center of the channel (Figures 4.16 and 4.17). The presence of two zones of recirculation constrained the downstream flow to a narrow band in the center of the channel. One zone of recirculation was located upstream of the bar along the inner bank and the second was located in the pool along the outer bank. Shoaling of the flow at the bar head forced the flow to diverge and the high velocity core becomes less well organized. Through the downstream portion of the bend, velocity was relatively uniform across the width of the channel, with the exception of areas directly adjacent to the banks. Patterns in the boundary shear stress mirror those of the velocity. Boundary shear stress was greatest at the entrance to the bend, corresponding to the zone of high velocity in the center of the channel between the two areas of recirculation. Values of boundary shear stress decreased as flow diverged at the bar head and shear stress values through the remainder of the bend were low relative to those at the bend entrance.

The point bar expansion and pool filling in Run 2 did not substantially alter the water surface profile through the bend due, in part, to the hydraulic control provided by the cobble riffle at the downstream end of the meander. Thus, expansion of the point bar and deposition in the pool reduced mean flow depth across the channel, which constricted the cross-sectional area of the flow. The water surface super-elevation along the outer bank in Run 2 was comparable to that of Run 1 (Figure 4.16). The most pronounced difference in water surface elevation between the two runs occurred at the bar head, where the water surface was elevated during Run 1. As the bar expanded and the inner bend chute filled during Run 2, flow no longer diverged at the bar head, but instead flow was steered around the bar towards the outer bank.

As the bar expanded and flow was constricted, mean cross-sectional velocities increased (Figure 4.18). The maximum velocity increased from Run 1 to Run 2 (1.40 and 1.54 m/s in Runs 1 and 2, respectively), and there was a stronger and more well-defined high velocity core at the entrance to the bend in Run 2 (Figure 4.16). In addition, the size of the zones of recirculation were smaller in Run 2 (Figure 4.17). This was especially the case along the inside of the bend where bar expansion, deposition in the chute, and migration of the bar crest inward all worked to steer the high velocity core towards the outer bank. In contrast with Run 1, where the high velocity core dissipated by the bar apex, during Run 2 there was a coherent zone of high velocity through the entire length of the bend. There was a corresponding change in the boundary shear stress. Increased velocities result in an increase in the mean stress in the cross-stream direction through the bend. Maximum boundary shear stress was greater during the high feed run relative to the

low feed run (27.47 and 35.67 Pa, for Run 1 and 2, respectively), but perhaps more significant was the lateral expansion of the zone of high boundary shear stress through the bend during Run 2 (Figure 4.16). Additionally, in Run 2 the zone of concentrated high boundary shear stress was not restricted to the entrance to the bend, but it extended throughout the length of the meander.

5.0. Discussion

5.1. Bar response to an increase in sediment supply

When a meandering channel is at steady state, channel morphology is adjusted such that transport capacity matches the supply. If sediment supply increases, a larger stress is needed to maintain transport across the channel. In the absence of longer term adjustments that can alter planform and slope, a larger stress, and thus greater transport capacity, may be produced by two mechanisms: channel constriction, which increases mean velocity, and thus stress; or a change in topography that expands the range of the boundary shear stress. In the latter case, the nonlinear relation between stress and transport rate produces larger transport rates in locations with larger stress [*Paola*, 1996].

The flow structure through a meander bend that leads to the development of a point bar has received extensive attention [e.g. *Leopold and Wolman*, 1960; *Engelund*, 1974; *Ikeda et al.*, 1981; *Dietrich and Smith*, 1983; *Odgaard and Bergs*, 1988; *Bridge*, 1992; *Seminara*, 2006]. In sinuous channels there is a shift in the high velocity core from the inside to the outside bank through each meander [*Leopold and Wolman*, 1960; *Dietrich et al.*, 1979]. The outward flow at the surface, which is driven by centrifugal forces through the bend, causes superelevation of the water surface at the outer, concave

bank. This results in a cross-stream pressure gradient, which in turn drives near-bed, inward flow [*Dietrich and Smith*, 1984]. The shoaling of flow along the inner bank results in deposition, and thus point bar formation. These patterns of secondary circulation determine the pattern of sediment transport and deposition that govern the equilibrium form of the point bar. In the experiment presented here, the channel accommodated the increased sediment feed primarily through in-channel morphological changes that increased the mean velocity, thereby increasing boundary shear stress and transport capacity through the bend.

Bed load transport occurred largely via the migration of dunes, which allowed a qualitative observation of transport patterns. Dune migration, and thus the zone of maximum bed load transport, in the pool near the head of the bar was oriented approximately perpendicular to the alongstream direction (Figure 4.13). Further downstream, as sediment was routed around the bar, dune orientation shifted, such that dunes at the bend apex were climbing up the bar flank towards the bar crest. These changes in the migration direction of the dunes correspond to the location where flow became superelevated along the outside of the bend, indicating the development of secondary currents that would drive near-bed, inward flow.

As the rate of sediment delivery increased, but discharge remained constant, deposition occurred in the bend. Because flow and sediment are focused into the pool by the bend and the upstream part of the bar, the pool is the first place where we observed sediment deposition in each run. As dunes climbed out of the pool up the flank of the bar, sediment accreted onto the bar and bar width increased. Continued lateral expansion of

the bar resulted in deposition in the chute along the inner bank. This filling of the chute in conjunction with continued deposition at the bar head, worked as a positive feedback, further steering flow – and sediment – around the bar. Because there was minimal change in the water surface elevation, flow depths decreased throughout the bend, and constriction of the flow necessarily increased velocity through the bend. The channel reached a steady-state form when sufficient deposition in the pool and bar had occurred such that constriction of the flow had increased velocity, and thus shear stress, enough to route additional sediment through the meander.

Prior flume experiments have also documented the capability of a channel to adjust to an increase in sediment supply through morphological and textural changes. *Eaton and Church* [2004; 2009] conducted two experiments designed to evaluate response of point bar morphology to changes in sediment supply. In the first experiment the channel and floodplain were composed of unconsolidated sediment [*Eaton and Church*, 2004]. The primary adjustment to increased sediment supply occurred through bank erosion and a change in planform that increased channel slope. The second experiment was conducted with the same flow and sediment feed conditions in a sinuous channel with fixed walls [*Eaton and Church*, 2009]. With fixed sinuosity, the channel gradient remained constant and channel morphology was nearly identical after each run, and changes in sediment feed rate were nearly fully accommodated by textural changes of the bed [*Eaton and Church*, 2009]. However, although the flow and sediment feed rate were the same in the two experiments, the equilibrium channel slope was much less in the fixed-wall experiments, because the fixed-wall channel was able to attain a much greater

degree of cross-section asymmetry than was possible in unconsolidated sediment. This increase in cross-stream asymmetry increased sediment transport by broadening the distribution of shear stress.

Whereas *Eaton and Church* [2009] observed nearly identical geometry as they increased sediment feed, we observed both textural and morphologic changes with the increase in sediment feed. However, their increase in sediment feed was much more modest than relative change in sediment supply presented here: of those runs that reached equilibrium, the greatest increase in sediment feed was just 1.67 times the lowest feed rate [*Eaton and Church*, 2009]. These findings are supported by prior experiments [*Dietrich et al.*, 1989; *Lisle et al.*, 1993; *Buffington and Montgomery*, 1999] demonstrating that more modest adjustments in sediment feed rate may be fully accommodated by fining or coarsening of the bed. In the experiment we conducted in the OSL, the increase in sediment feed imposed on the channel clearly exceeded the ability of textural changes alone to achieve the necessary increase in transport capacity. Morphologic adjustments were necessary to produce the higher transport capacity required for the channel to reach steady-state.

Recent studies by *Harrison et al.* [2011] and *Legleiter et al.* [2011] provide field documentation of point bar evolution on a reconfigured reach of the Merced River. Over the course of a series of floods in the sinuous, constructed channel, they observed deposition on point bars and pool scour, thus increasing channel relief. However, the morphologic changes on the Merced represent the evolution of a constructed channel that had an "unnaturally low-amplitude cross-sectional asymmetry" following reconfiguration

[*Harrison et al.*, 2011]. In the experiment presented here, we documented response of a steady-state point bar to a change in sediment delivery to the channel. Whereas *Legleiter et al.* [2011] and *Harrison et al.* [2011] documented an increase in relief as the point bar evolved, we documented a reduction in cross-sectional relief in the portion of the channel with the greatest asymmetry, upstream of the bar apex. In both scenarios the bar expanded, but the difference in relief was driven by the response of the pool.

A decrease in relief has been observed elsewhere in rivers that are adjusting to changes in sediment supply. *Lisle* [1982] documented channel response to a period of aggradation resulting from a landslide. Although that study does not focus on meander point bars, it provides observations of channel response to a sudden increase in the sediment load. At the majority of the study sites, *Lisle* [1982] documented substantial filling of pools, a decrease in mean cross-sectional channel depth, and an increase in width and velocity. These observations suggest that increased transport capacity was achieved through a mechanism that is similar to coupled morphologic and hydraulic adjustments that we have described here.

5.2. Bar response to a decrease in sediment supply

The channel morphology observed at the end of Run 3 was very similar to the steady state channel configuration observed at the end of Run 1. With the exception of small differences at the bar head, the size, shape, and location of the bar were essentially identical following the two low-feed runs. This demonstration of equifinality - that the same bar was recovered via growth or shrinkage - indicates that the bar morphology is robust for a given discharge, sediment supply, and channel geometry.

5.3. Implications for meander migration

Although we did not observe planform adjustments during this experiment, our observations of bar response to changes in sediment supply suggest a mechanism for meander migration in which bar growth is the driver of erosion on the opposing bank, rather than bank erosion preceding and causing point bar growth, as has been asserted elsewhere [e.g. *Lewin*, 1976]. In the OSL, expansion of the bar constricted and focused the flow, leading to further development of the high velocity core that was present at the entrance to the bend in Run 1. The zone of high velocity not only extended through the length of the bend, but also shifted outward, towards the outer bank. As velocity along the outer bank increases, so does the potential for bank erosion and bankline migration. The sequence of adjustments described here follow a pattern in which point bar deposition precedes erosion of the opposing outer, concave bank.

6. Conclusions

We conducted a field-scale experiment to evaluate the influence of sediment supply on forced bar-pool morphology in a meander. In an effort to focus on in-channel processes, we used a channel with a fixed planform. Three experimental runs were conducted. In the first run, we introduced a low sediment feed and the nascent point bar aggraded. During Run 2, we increased the sediment feed by a factor of five. The bar width, height, and length increased, and substantial deposition occurred in the pool. In the final run, Run 3, we returned the sediment feed to the original low feed rate. The size, shape, and location of the bar were essentially identical for each low feed run even though the initial bar form differed.

When channels with resistant banks are subjected to a moderate increase in sediment supply, the increase in transport capacity may be achieved by textural changes and morphologic changes within the bend, and larger-scale adjustments in planform or gradient are not necessary to convey the additional sediment load. Prior research suggests that minor increases in sediment feed may be fully accommodated by changes in the grain size distribution of the bed. More substantial changes in sediment influx, such as was imposed here during Run 2, may require morphological adjustments in addition to changes in bed texture. Here, the steady-state channel adjusted to an increase in sediment feed through flow constriction, which increases mean cross-sectional velocity, and thus transport capacity. The expansion of the bar in absence of bank erosion suggests a mechanism for planform adjustments in which bar growth drives bank erosion, and subsequently meander migration.

References

Braudrick, C. A., W. E. Dietrich, G. T. Leverich, and L. S. Sklar (2009), Experimental evidence for the conditions necessary to sustain meandering in coarse-bedded rivers, *Proc. National Academy of Sciences*, *106*(40), 16936-16941.

Bridge, J. S. (1992), A revised model for water flow, sediment transport, bed topography and grain size sorting in natural river bends, *Water Resour. Res.*, *28*(4), 999-1013.

Buffington, J. M., and D. R. Montgomery (1999), Effects of sediment supply on surface textures of gravel-bed rivers, *Water Resour. Res.*, *35*(11), 3523-3530.

Clayton, J. A., and J. Pitlick (2007), Spatial and temporal variations in bed load transport intensity in a gravel bed river bend, *Water Resour. Res.*, *43*(2).

Dietrich, W. E., and J. D. Smith (1983), Influence of the point-bar on flow through curved channels, *Water Resour. Res.*, *19*(5), 1173-1192.

Dietrich, W. E., and J. D. Smith (1984), Bed-load transport in a river meander, *Water Resour. Res.*, *20*(10), 1355-1380.

Dietrich, W. E., and P. J. Whiting (1989), Boundary shear stress and sediment transport in rivers meanders of sand and gravel, in *River Meandering*, edited by S. Ikeda, et al., pp. 1-50, AGU, Washington, D.C.

Dietrich, W. E., J. D. Smith, and T. Dunne (1979), Flow and sediment transport in a sand bedded meander, *J. Geology*, *87*(3), 305-315.

Dietrich, W. E., J. W. Kirchner, H. Ikeda, and F. Iseya (1989), Sediment supply and the development of the coarse surface layer in gravel-bedded rivers, *Nature*, *340*(6230), 215-217.

Eaton, B. C., and M. Church (2004), A graded stream response relation for bed load-dominated streams, *J. Geophys. Res.*, *109*, F03011.

Eaton, B. C., and M. Church (2009), Channel stability in bed load dominated streams with nonerodible banks: Inferences from experiments in a sinuous flume, *J. Geophys. Res.*, *114*(F01024), F01024.

Engelund, F. (1974), Flow and bed topography in channel bends, *J. Hydraul. Div.*, *100*(11), 1631-1648.

Ferguson, R. I. (2003), The missing dimension: Effects of lateral variation on 1-D calculations of fluvial bedload transport, *Geomorphology*, *56*(1-2), 1-14.

Harrison, L. R., C. J. Legleiter, M. A. Wydzga, and T. Dunne (2011), Channel dynamics and habitat development in a meandering, gravel bed river, *Water Resour. Res.*, *47*(4), W04513, doi: 10.1029/2009WR008926.

Ikeda, S., G. Parker, and K. Sawai (1981), Bend theory of river meanders. Part 1. Linear development, *J. Fluid Mechanics*, *112*(1), 363-377.

Julien, P. Y., and D. J. Anthony (2002), Bed load motion and grain sorting in a meandering stream *J. Hydraul. Res.*, *40*(2), 125.

Kinzel, P. J., J. M. Nelson, and A. K. Heckman (2009), Response of sandhill crane (Grus canadensis) riverine roosting habitat to changes in stage and sandbar morphology, *River Res. Applications*, *25*(2), 135-152.

Legleiter, C. J., and P. C. Kyriakidis (2006), Forward and inverse transformations between Cartesian and channel-fitted coordinate systems for meandering rivers, *Mathematical geology*, *38*(8), 927-958.

Legleiter, C. J., L. R. Harrison, and T. Dunne (2011), Effect of point bar development on the local force balance governing flow in a simple, meandering gravel bed river, *J. Geophysical Res.*, *116*(F1), F01005, doi: 10.1029/2010JF001838.

Leopold, L. B., and M. G. Wolman (1960), River meanders, *Geol. Soc. Am. Bull.*, *71*(6), 769.

Lewin, J. (1976), Initiation of bed forms and meanders in coarse-grained sediment, *Geol. Soc. Am. Bull.*, *87*, 281-285.

Lisle, T. E. (1982), Effects of aggradation and degradation on riffle-pool morphology in natural gravel channels, northwestern California, *Water Resour. Res.*, *18*(6), 1643-1651.

Lisle, T. E., F. Iseya, and H. Ikeda (1993), Response of a channel with alternate bars to a decrease in supply of mixed-size bed load: A flume experiment, *Water Resour. Res.*, *29*(11), 3623-3629.

Lisle, T. E., J. E. Pizzuto, H. Ikeda, F. Iseya, and Y. Kodama (1997), Evolution of a sediment wave in an experimental channel, *Water Resour. Res.*, *33*(8), 1971-1981.

Lisle, T. E., J. M. Nelson, J. Pitlick, M. A. Madej, and B. L. Barkett (2000), Variability of bed mobility in natural, gravel-bed channels and adjustments to sediment load at local and reach scales, *Water Resour. Res.*, *36*(12), 3743-3755.

Madej, M. A., D. G. Sutherland, T. E. Lisle, and B. Pryor (2008), Channel responses to varying sediment input: A flume experiment modeled after Redwood Creek, California, *Geomorphology*, *103*(4), 507-519.

May, C. L., B. Pryor, T. E. Lisle, and M. Lang (2009), Coupling hydrodynamic modeling and empirical measures of bed mobility to predict the risk of scour and fill of salmon redds in a large regulated river, *Water Resour. Res.*, *45*(5), W05402.

McDonald, R., J. Nelson, V. Paragamian, and G. Barton (2010), Modeling the effect of flow and sediment transport on white sturgeon spawning habitat in the Kootenai River, Idaho, *J. Hydraul. Res.*, *136*, 1077.

Nanson, G. C. (1980), Point bar and floodplain formation of the meandering Beatton River, northeastern British Columbia, Canada, *Sedimentology*, *27*(1), 3-29.

Nelson, J. M., J. P. MBennett, and S. M. Wiele (2003), Flow and sediment transport modeling, in *Tools in Fluvial Geomorphology*, edited by G. M. Kondolf, et al., pp. 539-576, John Wiley, Chichester, U. K.

Odgaard, A. J., and M. A. Bergs (1988), Flow processes in a curved alluvial channel, *Water Resour. Res.*, *24*(1), 45-56.

Orr, C. H., and A. F. Lightbody (2009), Stream restoration research in the new Outdoor StreamLab (Minnesota), *Ecological Restoration*, *27*(4), 394-396, doi: DOI: 10.3368/er.27.4.394.

Paola, C. (1996), Incoherent structure: turbulence as a metaphor for stream braiding, *Coherent Flow Structures in Open Channels*, 705-723.

Seminara, G. (2006), Meanders, *J. Fluid Mechanics*, *554*(1), 271-297.

Tal, M., and C. Paola (2007), Dynamic single-thread channels maintained by the interaction of flow and vegetation, *Geology*, *35*(4), 347-350, doi: Doi 10.1130/G23260a.1.

	Duration (days)	Duration (hrs)	Flow rate (L/s)	Feed rate (kg/min)
Run 0: No feed, degradational	3	N/A	281 ± 4	0
Run 1: Low feed, aggradational	11	95.5	282 ± 6	3.5 ± 1.0
Run 2: High feed, aggradational	7	14.2	287 ± 4	20.0 ± 2.0
Run 3: Low feed, degradational	8	63.2	285 ± 7	4.4 ± 0.6

Table 4.1. Flow and sediment feed conditions during the experiment.

Table 4.2. Sediment mass balance.

	Run 1	Run 2	Run 3
Sediment feed (m^3)	11.6	8.6	7.4
Sediment output (m^3)	5.1	3.1	8.7
Input minus output (m^3)	6.5	5.5	-1.4
Upstream bend (m^3)	0.8	0.5	-0.5
Upstream riffle (m^3)	0.4	0.3	-0.3
Middle bend (m^3)	0.7	1.7	-1.6
Downstream riffle (m^3)	0.5	0.5	-0.5
Downstream bend (m^3)	1.0	0.6	-0.6
Exit reach (m^3)	3.2	1.9	2.2
Change in storage (m^3)	5.1	4.2	- 1.6

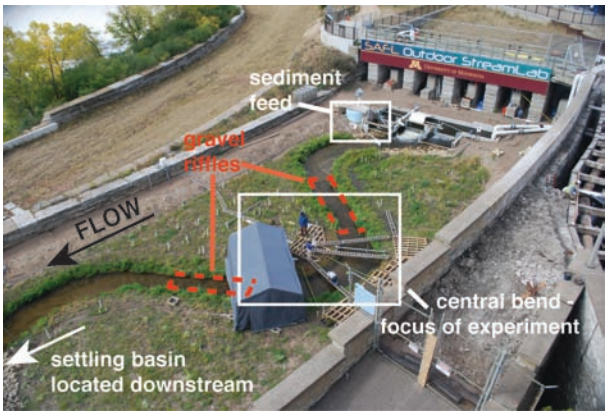

Figure 4.1. The Outdoor StreamLab at Saint Anthony Falls Laboratory at the University of Minnesota. Flow is from the upper left to the lower right of the figure.

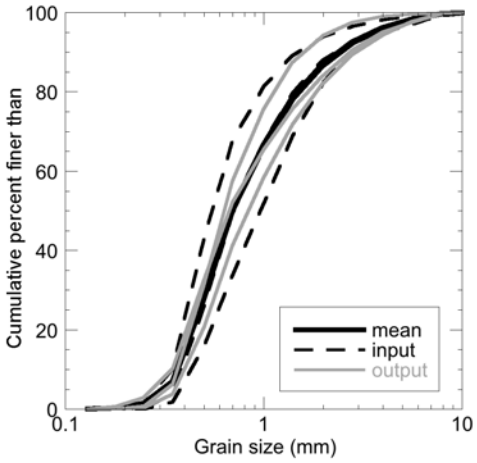

Figure 4.2. Grain size distribution of the sediment in transport in the OSL during the experiment. Each of the input and output distributions plotted here are composites of several samples collected on a single day, illustrating some variability in input grain size through time. The mean represents the mean grain size distribution of the sediment in transport.

Figure 4.3. The sediment feed system (a) and settling basin where exported sediment collects (b). In (a), the blue storage tank stores sediment, which is delivered by auger to the channel via the PVC pipe. Sediment exported from the system collects in the settling basin (b), where it was surveyed to determine volume of sediment exported from the system.

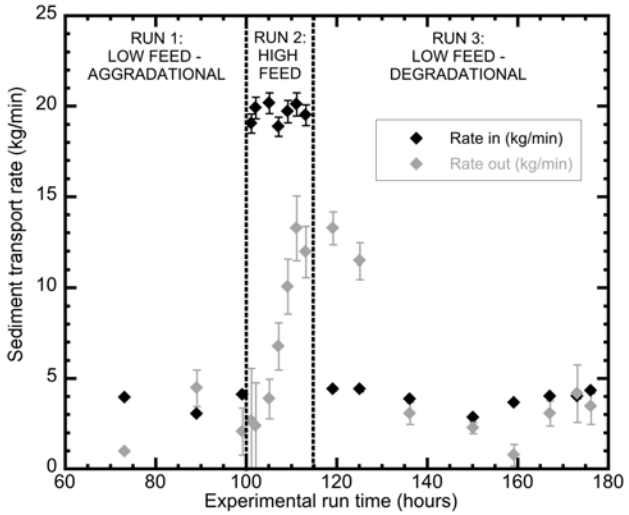

Figure 4.4. Sediment transport rate in to and out of the channel during Runs 1 – 3.

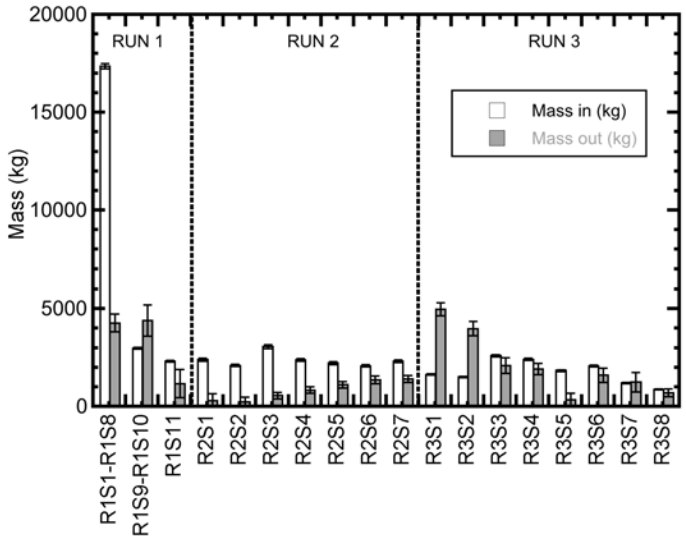

Figure 4.5. Mass of sediment input to and exported from the channel during Runs 1 – 3.

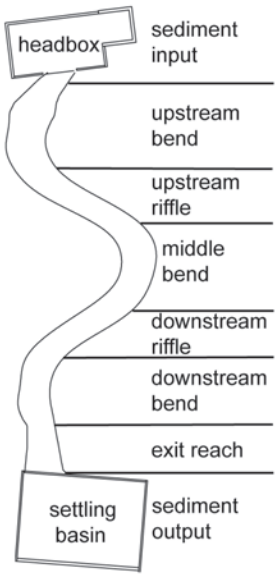

Figure 4.6. Zones of in-channel sediment storage corresponding to the sediment mass balance presented in Table 2.

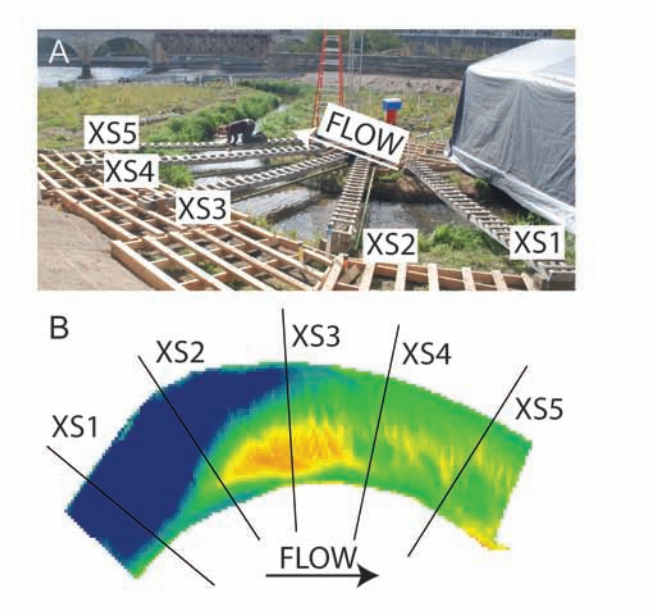

Figure 4.7. Locations of cross-sections used for documenting transient conditions in the bend. The topography in (b) is from the end of Run 1.

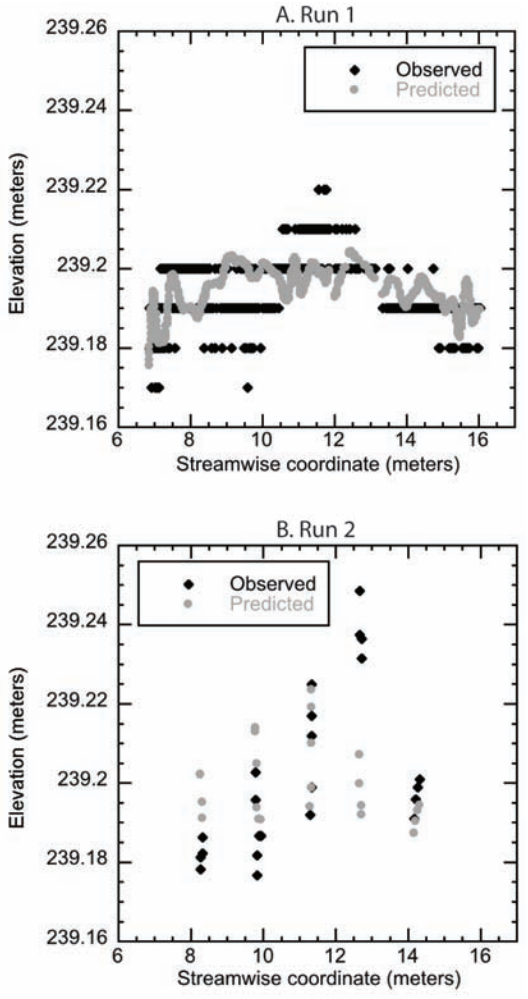

Figure 4.8. Measured and modeled water surface elevations from Run 1 (a) and Run 2 (b).

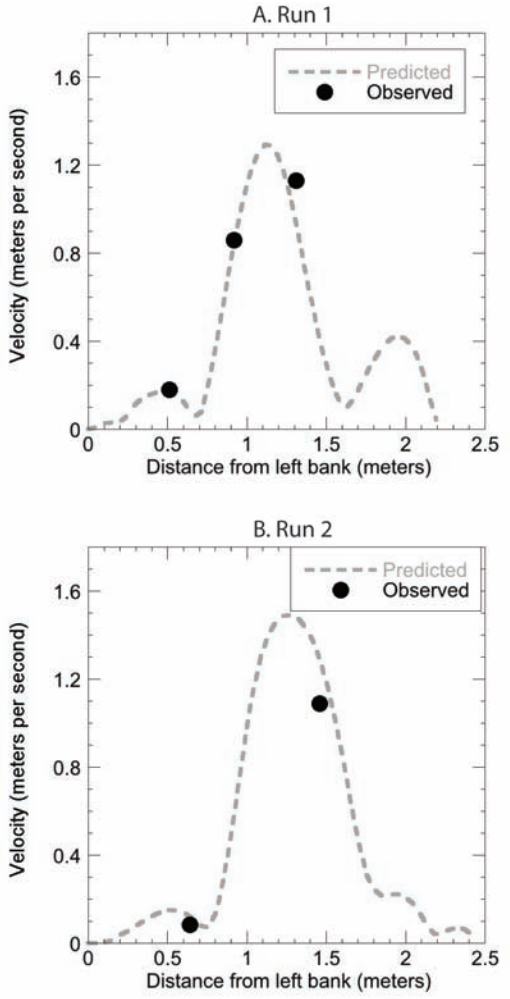

Figure 4.9. Measured and modeled depth-averaged velocity from Run 1 (a) and Run 2 (b). Data in both (a) and (b) are from cross-section 1.

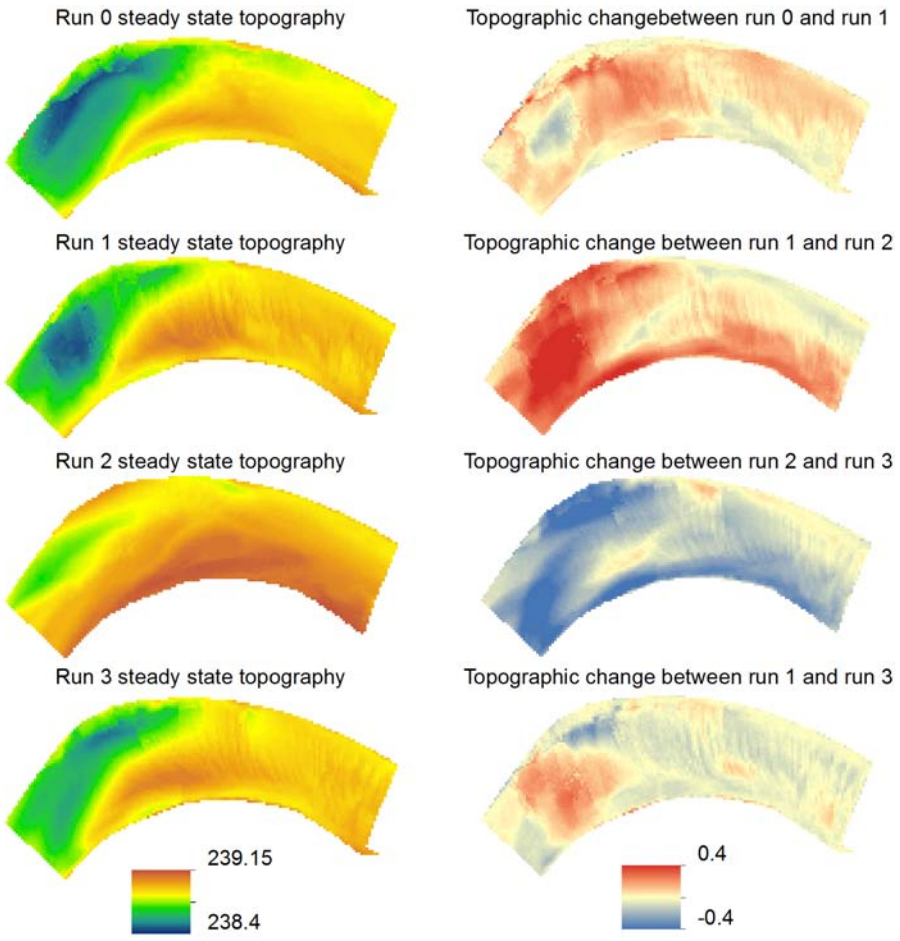

Figure 4.10. Steady-state channel topography collected at the end of Runs 0, 1, 2, and 3 (left column). Changes in elevation between the runs a presented in the right column.

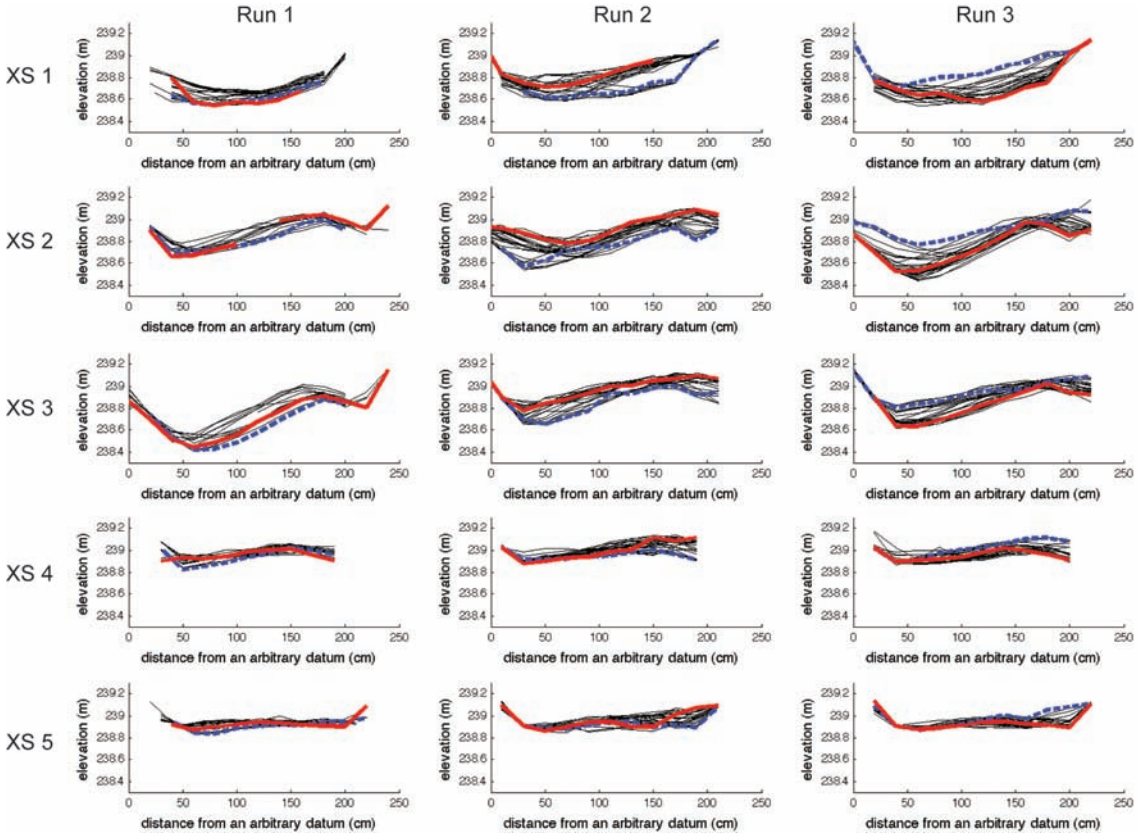

Figure 4.11. Cross-section measurements depicting transient conditions. The thick dashed blue line indicates topography at the beginning of the run. The thick solid red line indicates the cross section topography at the end of the run.

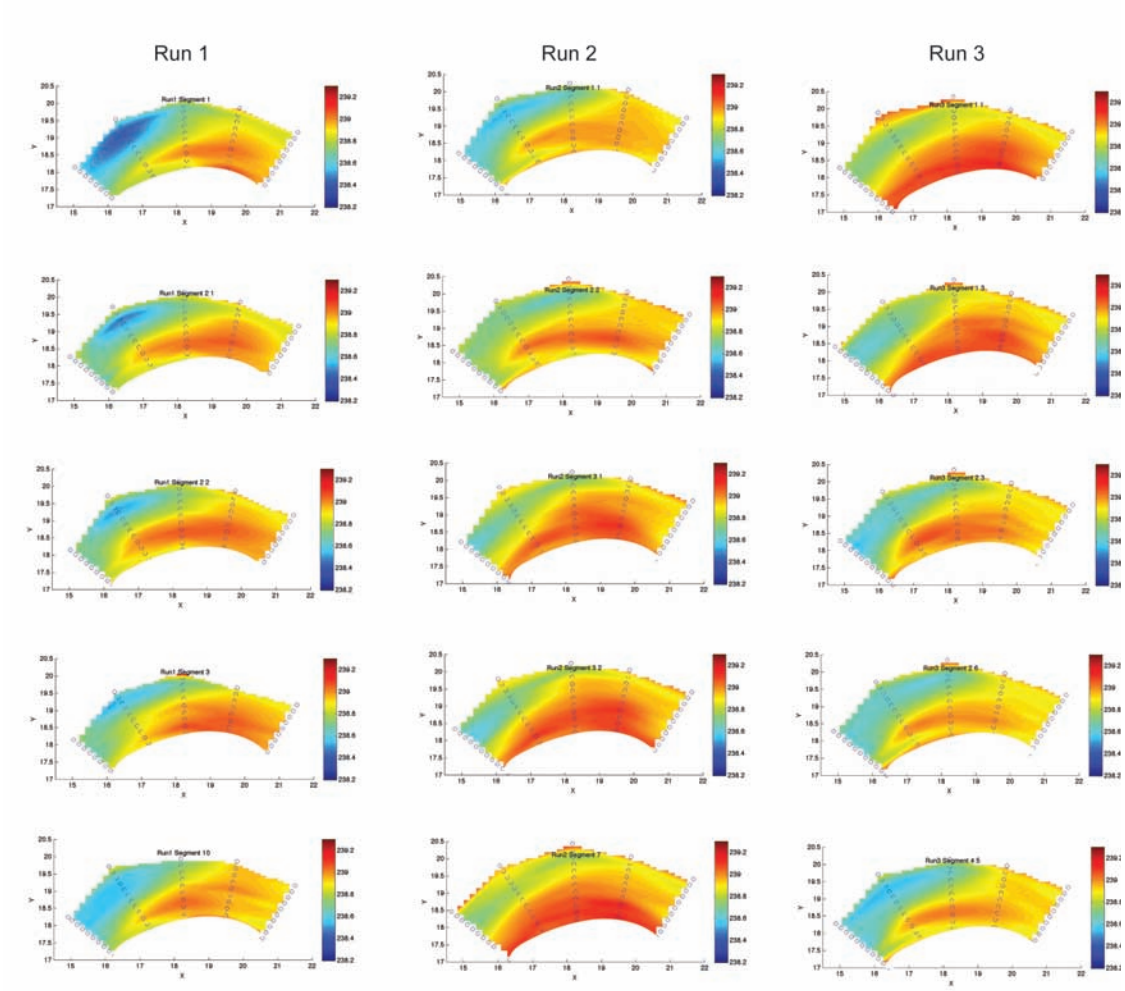

Figure 4.12. Linearly interpolated cross-section data. Panels do not show every single plot but depict a subset of the measurement data. Plots were selected which captured the sequence of events observed in the flume.

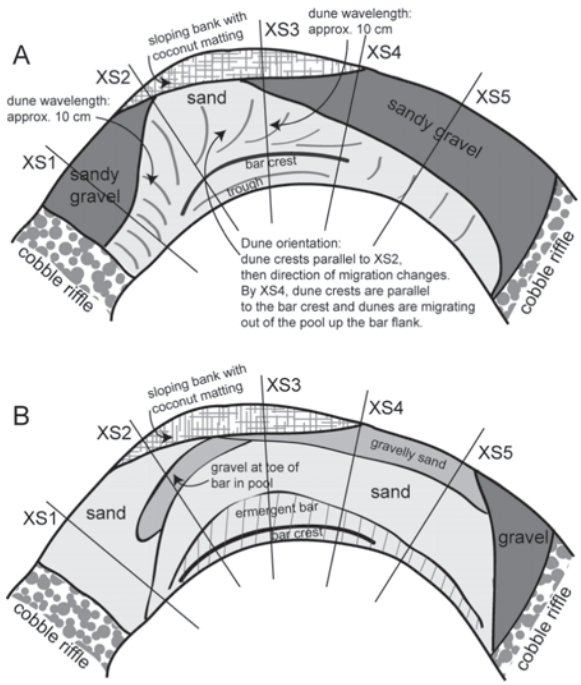

Figure 4.13. Facies maps from Run 1 (a) and Run 2 (2). Map (a) includes a sketch of the dune orientation. During Run 2, where a larger proportion of the bed was covered by sand, dunes extended across a greater portion of the channel, but their orientation and pattern of migration remained similar to that in Run 1. Dune mapping was not feasible in Run 2 due to time constraints. Map (b) depicts the portion of the bar that was emergent at base flow.

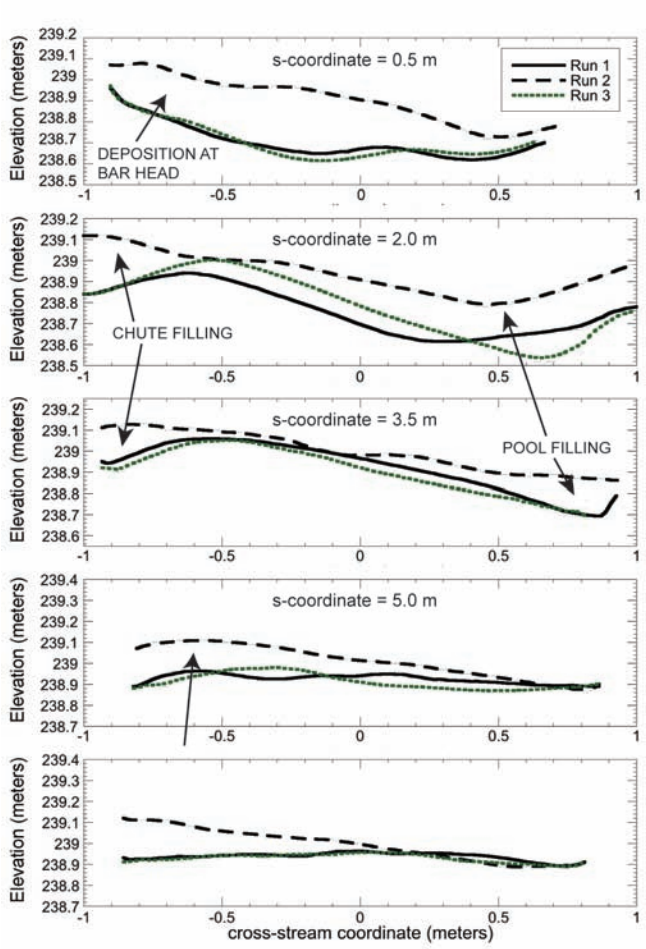

Figure 4.14: Sections depicting topography in the cross-stream direction, as measured in 1.5 m increments along the channel centerline, or streamwise coordinate (s-coordinate).

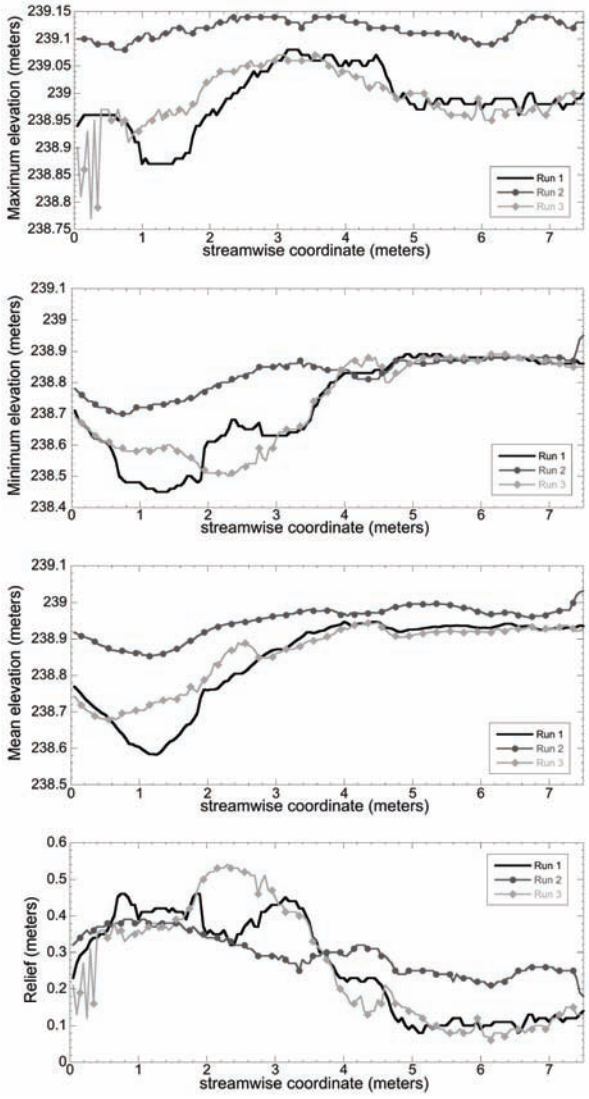

Figure 4.15: Topographic metrics - maximum elevation, minimum elevation, mean elevation, and channel relief - as computed in the cross-stream direction at 5 cm increments along the length of the channel.

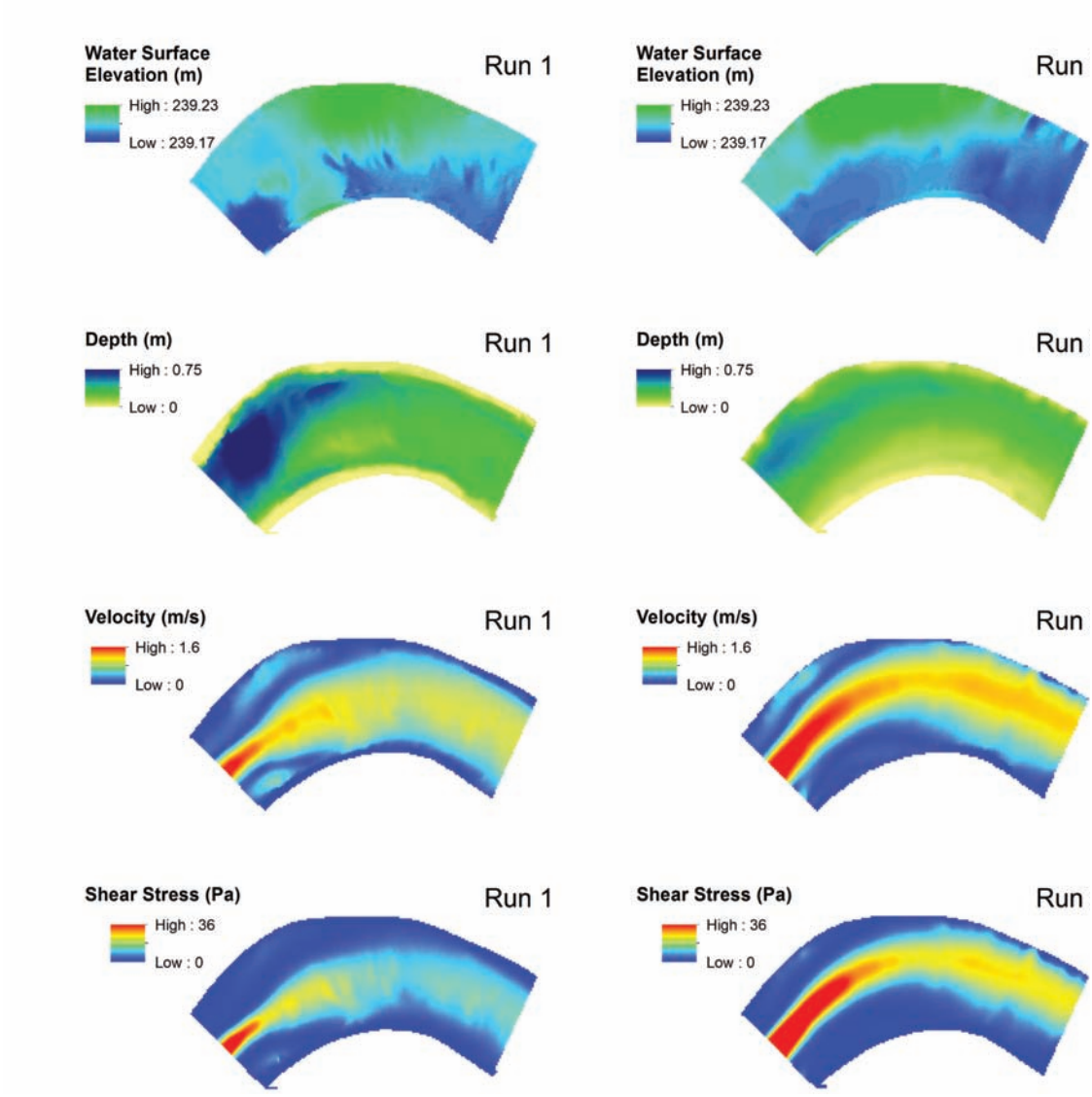

Figure 4.16. FaSTMECH scalar output: modeled water surface elevation, flow depth, depth-averaged velocity, and boundary shear stress for Run 1 and Run 2.

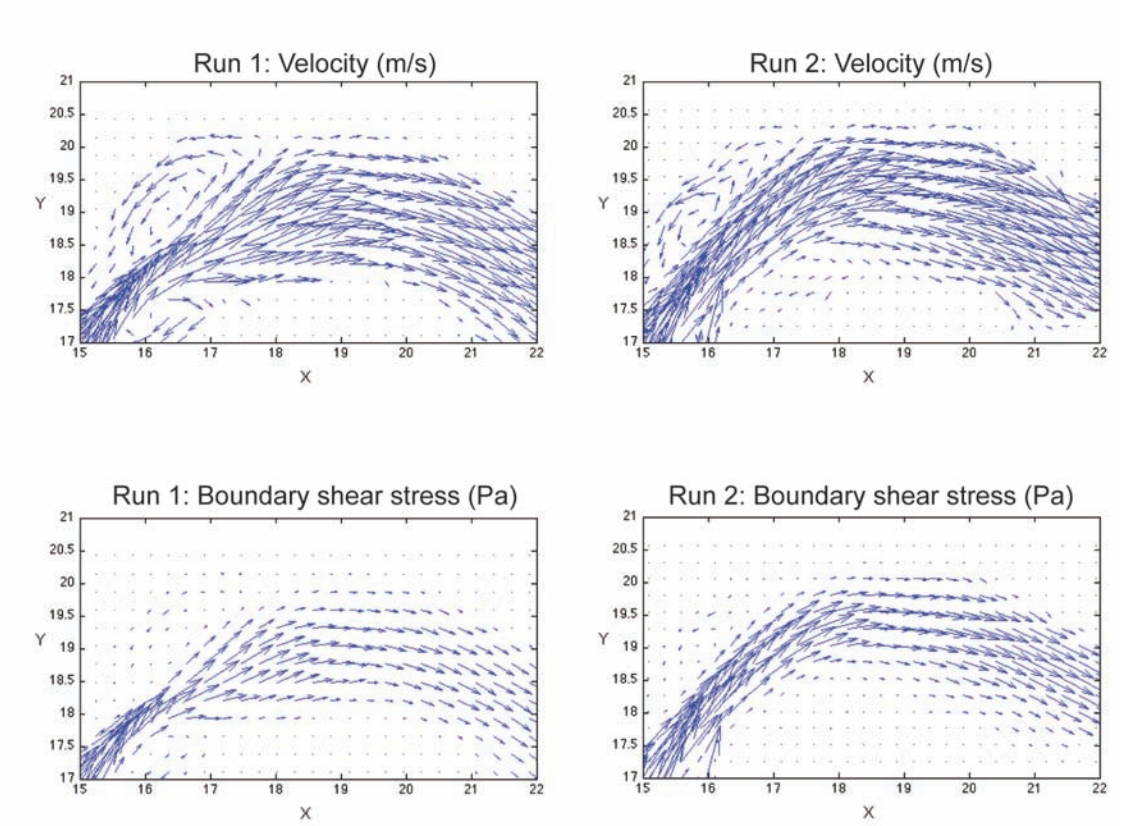

Figure 4.17. FaSTMECH vector output: depth-averaged velocity and boundary shear stress.

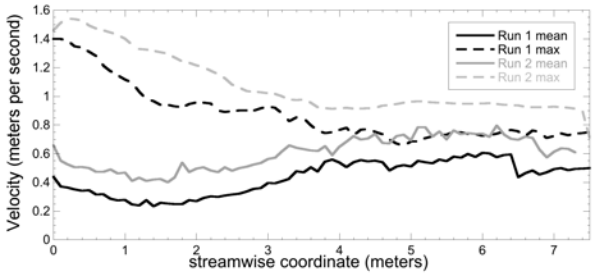

Figure 4.18. Mean cross-sectional velocity computed at 10-cm increments in the streamwise direction for Run 1 and Run 2.

CHAPTER 5

SUMMARY AND CONCLUSIONS

Channel morphology in alluvial rivers results from the interactions among the flow of water and sediment, the grain size distribution of the material in transport, and the characteristics of the materials making up the channel boundary. Many modern river management problems depend upon the ability to predict channel behavior in response to changes in the delivery of sediment. Sediment budgets provide a framework for explicitly evaluating the linkages between sediment delivery to and export from a river, and changes in storage [*Reid and Dunne*, 2003]. Here, I present three sediment budgets, developed at different spatial and temporal scales, for systems in which sediment is accumulating.

1.0 Summary

In Chapter 2, I present a bed load budget for the Snake River in Grand Teton National Park (GTNP), Wyoming. The analysis was designed to evaluate the effects of 50 years of flow regulation on net sediment flux and, thus, sediment storage for the Snake River below Jackson Lake Dam. Prior research [*Marston et al.*, 2005; *Schmidt and Wilcock*, 2008] suggested that the system was accumulating sediment due to reduction in the magnitude of annual floods. However, the analysis presented here reveals a subtlety about how JLD affects the downstream channel that had not been detected prior to the direct calculation of a sediment mass balance. The calculations indicate that more sediment exits the study reach than is being supplied by tributaries. The volume of sediment exported that was calculated using estimated unregulated hydrology indicates

that the magnitude of the naturally occurring sediment deficit would be greater in the absence of JLD. Thus, the calculations suggest that the Snake River was not in equilibrium prior to construction of JLD, but was naturally in sediment deficit.

In Chapter 3, I present a sediment budget for a single flood event on a reconfigured 4-km reach of the Provo River, Utah. Qualitative observations of channel adjustments in the period following channel construction indicated that the channel was accommodating upstream sediment largely through the growth of point bars. By quantifying all terms in the sediment mass balance for the study area, I show that both the change in storage as determined from bed load transport and from topographic data indicate that sediment accumulation occurred during the 2009 flood. However, calculation of both sediment fluxes and change in storage demonstrates that the magnitude of the deposition and erosion terms is substantially larger than the magnitude of the flux terms. Thus, local redistribution of sediment accounts for a larger portion of gravel accumulation during the flood than sediment influx.

In Chapter 4, I present the results from a physical experiment designed to evaluate the effect of changing sediment supply on point bar morphology in a single meander bend. The experiment was conducted in a field-scale flume, the Outdoor StreamLab (OSL) at the University of Minnesota. The findings indicate a mechanism for point bar adjustment to an increase in sediment supply. Because there was little change in water surface slope through the bend, aggradation of the bar and in the pool constricted flow. Channel constriction increased mean cross-sectional velocity, thereby increasing mean boundary shear stress and transport capacity through the bend. The morphologic changes were accompanied by textural changes of the bed (i.e. surface fining), but occurred in the

absence of adjustments in channel planform or gradient. When we reduced the feed rate and returned to the initial low feed rate, we recovered the same bar morphology via degradational processes that we had via aggradational processes. These findings suggest that bar morphology is robust for a given channel geometry, discharge, and sediment supply.

5.2. Synthesis

5.2.1. Point bar response to increase in sediment supply

The sediment budgets presented in Chapters 3 and 4 were both motivated, in part, by the desire to understand point bar response to an increase in sediment supply. The Provo River study took advantage of a unique field opportunity where point bars were rapidly growing in a constructed channel. The flume experiment in the OSL was conducted to investigate at the scale of a single bar the mechanisms controlling bar response to changes in sediment supply. Findings from the small-scale sediment budget developed for the OSL inform our understanding of processes operating at the scale of the Provo River.

Meander bends may adjust to an increase sediment supply through several mechanisms. Prior research has demonstrated that changes in surface grain size distribution alone may provide the adjustments necessary to accommodate an increase in sediment supply because a reduction in grain size increases sediment mobility [*Dietrich et al.*, 1989; *Buffington and Montgomery*, 1999; *Lisle et al.*, 2000]. More substantial increase in sediment influx may lead to adjustments in channel planform or slope. In the OSL, we observed a fining of the bed as we increased sediment supply. Because banks

were reinforced with coconut fiber, there were no changes in planform or gradient. There were, however, in-channel morphologic adjustments. The combination of these textural changes and the changes in morphology within the active channel were sufficient to alter flow and sediment transport capacity to accommodate the increased sediment load. These changes occurred in the absence of planform adjustments.

A fundamental difference between the channels of the OSL and Provo River is that in the OSL banks were reinforced, thus restricting bank erosion and channel migration. However, qualitative observations from the Provo River suggest that the processes observed in the flume may represent the first stages of bar growth in a system subjected to a moderate increase in sediment supply. On the Provo River, in the years immediately following construction, bars grew rapidly, yet bar expansion was accompanied by only a modest amount of bank erosion. Together the findings suggest that channel response may occur along a trajectory of increasing sediment loading. Relatively small increases in sediment supply may be accommodated through textural changes alone. More substantial increase in sediment supply may necessitate morphologic adjustments, which increases sediment transport capacity via changes in bend hydraulics. As velocity and shear stress continue to increase, at some point bank resistance provided by cohesion and root structure is overcome, and bank erosion ensues.

Another significant difference between the Provo River and the OSL is the caliber of the bed material. The Provo River channel is composed primarily of gravel and the OSL is a sand-bedded system. Although sediment transport in both systems occurs predominantly through bed load transport, the mechanisms differ because in the sand bed of the OSL, bed load transport occurs via dune migration. A change in sediment supply

may alter the size and structure of dunes, which in turn affect bed roughness, and thus the flow field. These changes in the flow field in turn affect transport capacity of the channel. This feedback loop was not addressed in Chapter 4 and warrants further exploration because the linkage between dunes, roughness, hydraulics, and transport provide a potentially significant mechanism for adjustment that is unique to sand-bed rivers.

An additional distinction between the Provo River and the OSL is that in the OSL, bend and bar morphology at the onset of the experiment was self-formed, whereas in the Provo River the channel had been constructed immediately prior to our initial observations of bar growth. These differences in channel history may have influenced the subsequent morphodynamic response. In OSL, although there were some fluctuations in bed topography, during the aggradational runs there was deposition throughout the bend during runs (i.e. there was both pool filling and bar growth). In the Provo, the bar growth and channel deposition was accompanied by zones of significant erosion.

A final distinction between the OSL and the Provo River is that the OSL was subject to the equivalent of a single flood even, whereas the research on the Provo River occurred several years after channel construction. Qualitative observations of the Provo River indicate that initially following construction, there was substantial redistribution of sediment in the meandering portions of the channel during the floods of 2005 and 2006, resulting in the rapid growth of point bars and associated scour on the outer banks. However, following the 2009 flood, sediment deposition was not restricted to bars, but was more uniformly distributed throughout the channel. It remains to be determined whether this shift in the style of channel adjustment was driven by the fact that the 2005

flood was larger than the 2009 flood, or whether the channel simply evolved most rapidly immediately following construction and subsequent topographic and hydraulic adjustments have been less pronounced.

These observations from the Provo are corroborated by the findings from a similar study on the Merced River, CA. *Harrison et al.* [2011] and *Legleiter et al.* [2011] documented point bar growth on a reconfigured reach of the Merced River where the channel was also built with a meandering planform, but the channel cross section geometry was simple and devoid of bars. Topographic evolution on the Merced River demonstrated that most of the topographic adjustment occurred during the first large flood, and relatively little adjustment occurred during a subsequent flood, despite the fact that the second flood was of larger magnitude and longer duration [*Harrison et al.*, 2011; *Legleiter et al.*, 2011]. The evidence from the Provo River, presented here, and from the Merced River suggests that pronounced adjustments in topography and hydraulics may occur during floods immediately following channel reconstruction. These rapid morphodynamic changes occur as channel morphology quickly adjusts to convey the imposed sediment load, and subsequent floods may lead to more subtle adjustments.

5.2.2. Developing fluvial sediment budgets

The research presented in Chapters 2 through 4 all involved changes in sediment supply and channel morphology in alluvial rivers. The distinct scale of each study influenced the scope of the analysis, the tools used to develop the budget, and the relative magnitude of the uncertainty associated with each term.

At the smallest scale, in the OSL, I was able to most precisely quantify terms in the budget. In the flume it was possible to explicitly connect cause and effect with a minimal number of assumptions. Laboratory settings provide precise experimental control and reduced degrees of freedom, so it is possible to isolate specific processes. In a field-scale flume such as the OSL, it was tractable to collect high-resolution measurements to a degree that is difficult in field settings. Thus, the flume was the only setting in which we were able to document transient adjustments as the bed evolved following a perturbation in the sediment regime. These observations of transient conditions are essential to gain insight into the mechanisms linking sediment supply and morphodynamic response, as was demonstrated in Chapter 4.

The experimental control and precision of measurements offered in experimental setting comes at a cost. The simplistic nature of a flume does not fully capture the complexity of natural systems, which can lead to difficulties scaling-up conceptual models developed from physical experiments. For example, as described above, the OSL is an imperfect analog for the Provo River because banks were not free to migrate.

As the scale of an investigation increases, in both the spatial and temporal domains, one often encounters with lower resolution information and the potential for unresolved controlling factors. At the large spatial and temporal scale of the Snake River, it was not possible to document changes in sediment storage due to lack of historical data. Thus, we measured modern rates of sediment flux and used these data to model sediment flux over the period of modern river management. Even if the time-frame of the study had been restricted to years during which we measured bed load transport, it would have been intractable to comprehensively measure morphologic adjustments for the entire

study reach. Yet although there were large uncertainties associated with both the bed load transport data and the modeled long-term estimates of sediment flux, the analysis provides important insights into the influence of dam operations on sediment flux.

On the Provo River, working at the scale of a single flood and a 4-km reach, we attempted to comprehensively document all terms of the sediment mass balance. At this intermediate scale, in addition to quantifying sediment flux in to and out of the study reach, we quantified changes in storage through a combination of direct measurement and remotely sensed data. Ultimately, our ability to close the budget was limited to some degree by our use of aerial imagery to model channel topography through a portion of the channel. Yet, even if were to comprehensively document topographic change, there remains an inherent inconsistency between the period of time over which flux measurements are made (i.e. during high flow) and the period when measurement of change in storage is feasible (i.e. intervening periods of low flow between floods).

The challenges of accurately measuring components of fluvial sediment budgets are not unique to the Provo and Snake Rivers. Indeed, even on river systems where there are extraordinary resources devoted to developing sediment budgets (e.g. the Colorado River downstream from Glen Canyon Dam), there are limits to the spatial and temporal extent of measurements and there remains unavoidable uncertainty associated with quantification of each term [*Grams et al.*, 2011]. Budgets constructed at larger spatial scale often rely on information collected in a subset of the study area, and then results are extrapolated to the entire study area. Budgets constructed over long-time frames often require extrapolation or modeling as well, because there is a paucity of information regarding sediment flux and morphodynamics, even for the most recent decades.

Despite these uncertainties, construction of a sediment budget is an essential tool for geomorphic research, because it provides insight into the sources and sinks of sediment within a watershed and may aid in the understanding of sediment transport pathways through the system. Additionally, a sediment budget is the necessary tool to explicitly document the linkages between sediment flux and channel morphodynamics. Even budgets in which the terms are only qualitatively evaluated serve a purpose, because the exercise of constructing a budget provides a framework for organizing thoughts and explicitly outlining linkages and processes operating within a fluvial system. For this dissertation I developed three sediment budgets, each conducted at a distinct spatial and temporal scale. The analyses highlighted the inherent challenges and uncertainties associated with each scale. Yet despite these inherent uncertainties, each sediment mass balance provided the opportunity to gain unique insights into the linkage between sediment supply and channel morphology.

References

Buffington, J. M., and D. R. Montgomery (1999), Effects of sediment supply on surface textures of gravel-bed rivers, *Water Resour. Res.*, *35*(11), 3523-3530.

Dietrich, W. E., J. W. Kirchner, H. Ikeda, and F. Iseya (1989), Sediment supply and the development of the coarse surface layer in gravel-bedded rivers, *Nature*, *340*(6230), 215-217.

Grams, P. E., D. J. Topping, J. C. Schmidt, M. A. Kaplinski, and J. E. Hazel (2011), Linking morphodynamic response with sediment mass balance: issues of scale, geomorphic setting, and sampling design, paper presented at American Geophysical Union Fall Conference 2011, American Geophysical Union, San Francisco, CA.

Harrison, L. R., C. J. Legleiter, M. A. Wydzga, and T. Dunne (2011), Channel dynamics and habitat development in a meandering, gravel bed river, *Water Resour. Res.*, *47*(4), W04513, doi: 10.1029/2009WR008926.

Legleiter, C. J., L. R. Harrison, and T. Dunne (2011), Effect of point bar development on the local force balance governing flow in a simple, meandering gravel bed river, *J. Geophysical Research*, *116*(F1), F01005, doi: 10.1029/2010JF001838.

Lisle, T. E., J. M. Nelson, J. Pitlick, M. A. Madej, and B. L. Barkett (2000), Variability of bed mobility in natural, gravel-bed channels and adjustments to sediment load at local and reach scales, *Water Resour. Res.*, *36*(12), 3743-3755.

Marston, R. A., J. D. Mills, D. R. Wrazien, B. Bassett, and D. K. Splinter (2005), Effects of Jackson Lake Dam on the Snake River and its floodplain, Grand Teton National Park, Wyoming, USA, *Geomorphology*, *71*(1-2), 79-98.

Reid, L. M., and T. Dunne (2003), Sediment budgets as an organizing framework in geomorphology, in *Tools in Geomorphology*, edited by G. M. Kondolf, et al., pp. 463-500, John Wiley & Sons Ltd., Chichester, England.

Schmidt, J. C., and P. R. Wilcock (2008), Metrics for assessing the downstream effects of dams, *Water Resour. Res.*, *44*(4), W04404, doi: 10.1029/2006WR005092.

APPENDIX

July 17, 2012

Nick Nelson
Interfluve, Inc.
220 Concord Ave., 2nd Floor
Cambridge, MA 02138

Dear Nick:

I am in the process of preparing my dissertation in the Watershed Sciences Department at Utah State University. I am requesting your permission to include the manuscript we coauthored, *Downstream effects of impounding natural lake: the Snake River downstream from Jackson Lake Dam, WY*, which was published in *Earth Surface Processes and Landforms* in 2011.

Please indicate your approval of this request by signing in the space provided below. If you have any questions, please call me at the number below.

Thank you for your cooperation,

Susannah

Susannah Erwin
Watershed Sciences Department
Utah State University
5210 Old Main Hill
Logan, UT 84322-5210
435-797-4016

I hereby give permission to Susannah Erwin to reprint the following material in her dissertation:

Erwin, S.O., Schmidt, J.C., and Nelson, N.C., 2011. Downstream effects of impounding a natural lake: the Snake River downstream from Jackson Lake Dam, WY, USA, *Earth Surface Processes and Landforms*, 36, pp. 1421-1434, DOI: 10.1002/esp.2159.

Signed _____ Date 7/24/12

JOHN WILEY AND SONS LICENSE TERMS AND CONDITIONS

Jul 17, 2012

This is a License Agreement between Susannah Erwin ("You") and John Wiley and Sons ("John Wiley and Sons") provided by Copyright Clearance Center ("CCC"). The license consists of your order details, the terms and conditions provided by John Wiley and Sons, and the payment terms and conditions.

All payments must be made in full to CCC. For payment instructions, please see information listed at the bottom of this form.

License Number	2951530954041
License date	Jul 17, 2012
Licensed content publisher	John Wiley and Sons
Licensed content publication	Earth Surface Processes and Landforms
Licensed content title	Downstream effects of impounding a natural lake: the Snake River downstream from Jackson Lake Dam, Wyoming, USA
Licensed content author	Susannah O. Erwin,John C. Schmidt,Nicholas C. Nelson
Licensed content date	Apr 11, 2011
Start page	1421
End page	1434
Type of use	Dissertation/Thesis
Requestor type	Author of this Wiley article
Format	Print and electronic
Portion	Full article
Will you be translating?	No
Order reference number	
Total	0.00 USD

VITA

Susannah O. Erwin
Watershed Sciences Department
Utah State University
5210 Old Main Hill, Logan, UT 84321
s.erwin@usu.edu
518-225-5683

EDUCATION

2012	**Utah State University**, Logan, UT Ph.D. in Watershed Sciences *Advisor:* John C. Schmidt; *Dissertation title:* Development of sediment budgets at multiple scales: investigations into the influence of sediment supply on channel morphology.
2010	**Utah State University**, Logan, UT M.E. in Civil Engineering, Water Engineering Graduate Program
2003	**Macalester College**, St. Paul, MN B.A. in Geography; B.A. in Environmental Studies

SCHOLARSHIPS AND AWARDS

2010	1st place, Student Poster Competition, 2010 Federal Interagency Sedimentation Conference, Las Vegas NV
2010	2nd place, Student Oral Presentation Competition, USU 2010 Spring Runoff Conference, Logan UT
2007-2011	S.J. and Jesse E. Quinney Ph.D. Fellowship
2007	National Park Service Rocky Mountain Cooperative Ecosystem Study Unit Student Award
2003	Cum Laude, Macalester College
2001	Macalester College Geography Department Merit Award
1998-2003	National Merit Scholarship Recipient

EMPLOYMENT HISTORY

Research Assistant, Utah State University, Logan, UT (2005-2012)
Directed the following research projects:

- **Provo River Restoration Project, Provo River, UT** (2008-2012)
  Major duties: Developed, implemented, and managed a geomorphic monitoring plan for a 16-km and $40,000,000 river restoration project; designed a controlled flood experiment from Jordanelle Dam to facilitate downstream measurements of bed load transport; comprehensively documented topographic changes associated with the controlled flood; extensive data collection using real time kinematic global positioning systems (rtkGPS); performed detailed analyses using

geographic information systems (GIS); supervised a field crew of six technicians; primary author of technical reports documenting findings for the Utah Reclamation, Mitigation, and Conservation Commission; currently developing recommendations for gravel augmentation to enhance aquatic habitat.

- **Outdoor StreamLab, Saint Anthony Falls Laboratory, MN** (2009)
  Major duties: Developed, implemented, and managed a field-scale experiment in an outdoor flume, designed to document effects of changes in sediment supply on channel morphology; measured velocity using hydroacoustic equipment (ADV); conducted hydraulic modeling to evaluate effect of changes in channel topography on flow; supervised a crew of five lab technicians.
- **Snake River, Grand Teton National Park, WY** (2005-2008)
  Major duties: Developed, implemented, and managed study to evaluate the effects of Jackson Lake Dam on the sediment transport and geomorphology of the Snake River in Grand Teton National Park; designed and implemented program to measure bed load transport rates on tributaries and the mainstem Snake River; conducted boat- and ground-based surveys to document channel change; supervised a field crew of five technicians; primary author of a technical report to document findings for the National Park Service.

Watershed Assessment Technician, Cornell Cooperative Extension*,* Kingston, NY (2004-2005); *Major duties:* Responsible for collection and analysis of geomorphic field data; developed watershed assessment protocol.

GIS Technician, Hudsonia Ltd*.,* Annandale, NY (2004-2005)
Major duties: Performed the geographic information system (GIS) analysis for a regional wildlife habitat study.

Stream Management Program Intern, New York City Department of Environmental Protection*,* Kingston (2004); *Major duties:* Performed a geographic information system (GIS) and field-based geomorphic assessment of the Esopus Creek watershed.

Forestry Technician, United States Forest Service Mesa, AZ (2003-2004)
Major duties: Construction of five miles of trail through rugged terrain in the Four Peaks Wilderness Area; removed wildfire debris; installed erosion control structures.

Forestry Technician, United States Forest Service*,* Ketchum, ID (2003)
Major duties: Assistant crew foreman leading trail maintenance crews; supervised installation of erosion control structures in wilderness settings in the Sawtooth National Forest; responsible for collection and processing of trail network data using a global positioning system (GPS).

TEACHING EXPERIENCE

Co-Instructor, *Geomorphic Change Detection Shortcourse*, Utah State University, (Spring 2011); Lectured on the collection of global positioning system data and performance of GIS analyses for use in investigations of fluvial geomorphology, river ecology, and river restoration.

Co-Instructor, *Stream Restoration Shortcourse*, Utah State University (Summer 2010)
Field demonstration of methods for sampling sediment transport; Lectured on use of two-dimensional hydrodynamic models to inform interdisciplinary restoration based on principles of fluvial geomorphology and river ecology.

Co-Instructor, *Fluvial Geomorphology*, Utah State University (Fall 2008)
Developed lectures in all areas of fluvial geomorphology, with an emphasis on sediment transport.

Teaching Assistant, *Fluvial Geomorphology*, Utah State University (Fall 2007)

Teaching Assistant, *Quantitative Methods in Geography*, Macalester College (Spring 2003)

Teaching Assistant, *Human Geography*, Macalester College (Spring 2003)

Teaching Assistant, *Physical Geography*, Macalester College (Spring 2002)

Teaching Assistant, *Physical Geography*, Macalester College (Spring 2000)

GRANTS AND FUNDING

2011 Development of a Comprehensive Monitoring Program and Recommendations for Ongoing Management of the Provo River Restoration Project. *Funded by* Utah Mitigation, Reclamation and Conservation Commission ($85,000), Co-PIs: J.C. Schmidt and S.O. Erwin.

2007-2011 S.J. and Jesse E. Quinney Ph.D. Fellowship.

2007 Development of a bed material budget for the regulated Snake River in Grand Teton National Park. *Funded by* the UW-NPS Research Center, Grand Teton National Park Wyoming ($5,000) Co-PIs: J.C. Schmidt and S.O. Erwin.

PEER-REVIEWED PUBLICATIONS

Erwin, S.O., Schmidt, J.C., and Nelson, N.C., 2011. Downstream effects of impounding a natural lake: the Snake River downstream from Jackson Lake Dam, WY, USA, *Earth Surface Processes and Landforms* 36, pp. 1421-1434, DOI: 10.1002/esp.2159.

Schmelter, M.L., **Erwin, S.O.,** Wilcock, P.R., 2012, Accounting for uncertainty in cumulative sediment transport using Bayesian statistics, *Geomorphology*, in press.

Submitted manuscripts:

Erwin, S.O., Schmidt, J.C., and Wheaton, J.M., Closing a sediment budget for the reconfigured Provo River, UT, in revision for *Water Resources Research*.

Manuscripts in preparation:

Nelson, N.C., **Erwin, S.O.*,** and Schmidt, J.C., Spatial and temporal patterns in channel change on the Snake River downstream from Jackson Lake Dam, Wyoming, in preparation for *Geomorphology.* (*corresponding author)

TECHNICAL REPORTS

Erwin, S.O., Majerova, M., Schmidt, J.C., 2010, *Water surface elevations during the 2010 flood*, submitted to the U.S. National Park Service, Moose, WY, p. 17.

Erwin, S.O. and Schmidt, J.C. 2009, *Development of a bed load budget for the Snake River in Grand Teton National Park, WY,* submitted to the U.S. National Park Service, Moose, WY and U.S. Geological Survey Northern Rocky Mountain Science Center, Bozeman, MT, p. 56.

Erwin, S.O. and Davis, D., 2005, *Phase I geomorphic assessment of Esopus Creek above Ashokan Reservoir*, submitted to New York City Department of Environmental Protection, Kingston, NY.

SELECTED ABSTRACTS

Erwin, S.O., Braudrick, C.A., Wilcock, P.R., *The influence of sediment supply on bar-pool morphology in a laboratory meander*, AGU Fall Meeting, San Francisco, CA, December 2011, poster presentation.

Khosronejad, A., **Erwin, S.O.,** Kozarek, J., Wilcock, P.R., Sotiropoulos, F., *Three-dimensional numerical simulation of point bar growth in a field-scale experimental meander bend*, AGU Fall Meeting, San Francisco, CA, December 2011, poster presentation.

Erwin, S.O., Schmidt, J.C., Wheaton, J.M., *Closure of sediment budgets: tractable task or elusive goal?* AGU Fall Meeting, San Francisco, CA, December 2010, poster presentation.

Schmidt, J.C., **Erwin, S.O.,** Wheaton, J.M., Wilcock, P.R., *Linking sediment flux and channel morphology in an aggrading gravel bed river,* Gravel Bed Rivers 7, Tadoussac, QU, August 2010, poster presentation.

Erwin, S.O., Braudrick, C.A., Wilcock, P.R., *The influence of sediment supply on bar-pool morphology in a laboratory meander,* Gravel Bed Rivers 7, Tadoussac, Quebec, August 2010, poster presentation.

Erwin, S.O., Schmidt, J.C., Wilcock, P.R., *Sediment transport and channel form in a reconfigured gravel bed river*, Joint Federal Interagency Conference, Las Vegas, NV, July 2010, poster presentation.

Erwin, S.O., Schmidt, J.C., *The Provo River Restoration Project: geomorphic monitoring to support creation and maintenance of fish habitat*, Western Division of the American Fisheries Society, Salt Lake City, UT, April 2010, oral presentation.

Erwin, S.O., Schmidt, J.C., *The Provo River Restoration Project: geomorphic monitoring to support creation and maintenance of fish habitat*, USU Spring Runoff Conference 2010, Logan UT, April 2010, oral presentation.

Erwin, S.O., Grams, P.E., Majerova, M.M., and Schmidt, J.C., *Calibrated transport relations, sediment budgets, and applications to river management,* AWRA Summer Specialty Conference, Snowbird, UT, July 2009, oral presentation.

Erwin, S.O., Schmidt, J.C., *Challenges and limitations of estimation sediment routing in a coarse bed braided river,* AGU Fall Meeting, San Francisco, CA, December 2008, oral presentation.

Erwin, S.O., Schmidt, J.C., *Development of a sediment budget to inform river management of the regulated Snake River in Grand Teton National Park,* GSA Fall Meeting, Denver, CO, October 2007, poster presentation.

Erwin, S.O., Schmidt, J.C., *Development of a sediment budget to inform river management of the Snake River in Grand Teton National Park,* Rocky Mountain Cooperative Ecosystem Study Unit Fall Meeting, Salt Lake City, UT, October 2007, oral presentation (invited).

Erwin, S.O., and Schmidt, J.C., *Development of a sediment budget for the Snake River in Grand Teton National Park,* Annual Grand Teton National Park River Guides Meeting, Moose, WY, May 2007, oral presentation (invited).

Davis, D., and **Erwin, S.O.**, *Stream and geomorphic watershed assessment for Espous Creek above Ashokan Reservoir*, 2005 New York City Watershed and Science and Technical Conference, Fishkill, NY, September 2005, oral presentation.

PROFESSIONAL SOCIETY AFFILIATIONS

American Geophysical Union
American Society of Civil Engineers
Geological Society of America